Description for MIROC6

2021 年 2 月 23 日

目 次

0.1 Basic Settings . . . 2
0.1.1 Coordinate System . . . 2
0.1.2 Physical Constants . . . 3
0.2 Computational flow of dynamical core . . . 9
0.2.1 Overview of dynamical core . . . 9

1 Mechanical Processes **10**
1.1 Basic Equations . . . 10
1.1.1 Basic Equations . . . 10
1.1.2 Boundary Conditions . . . 12
1.2 Vertical Discretization . . . 13
1.2.1 Model levels . . . 13
1.2.2 Vertical discretization . . . 14
1.2.3 Differences from σ-coordinate . . . 16
1.3 Horizontal discretization . . . 17
1.3.1 Spectral Expansion. . . . 17
1.3.2 Horizontal Diffusion Term . . . 19
1.3.3 Spectral representation of equations . . . 19
1.4 Time Integration `MODULE: [DYNSTP]` . . . 22
1.4.1 Time integration and time filtering with leap frog `MODULE: [DADVNC]` . . . 22
1.4.2 Semi-implicit time integration . . . 23
1.4.3 Applying semi-implicit time integration . . . 23
1.4.4 Time scheme properties and time step estimates . . . 26
1.4.5 Handling of the initiation of time integration . . . 27
1.5 Summary of the dynamical core . . . 28
1.5.1 Conversion of Horizontal Wind to Vorticity and Divergence `MODULE: [G2Wpush, G2Wtrans, G2Wshift, W2Gpush, W2Gtrans, W2Gshift]` . . . 28
1.5.2 Calculating a virtual temperature `MODULE: [VIRTMD]` . . . 28
1.5.3 Calculating the pressure gradient term `MODULE: [PSDOT]` . . . 28
1.5.4 Diagnosis of vertical flow. `MODULE: [PSDOT]` . . . 29
1.5.5 Tendency terms due to advection `MODULE: [GRTADV, GRUADV]` . . . 29

1.5.6 Transformation of prognostic variables to spectral space MODULE: [G2Wpush, G2Wtrans, G2Wshift] . . . 30
1.5.7 Transformation of tendency terms to spectral space MODULE: [G2Wpush, G2Wtrans, G2Wshift] . . . 31
1.5.8 Time integration in spectral space MODULE: [TINTGR] . . . 32
1.5.9 Transformation of prognostic variables to grid point Values MODULE: [W2Gpush, W2Gtrans, W2Gshift] . . . 32
1.5.10 Diffusion Correction along pressure level MODULE: [CORDIF] . . . 33
1.5.11 Frictional heat associated with diffusion. MODULE: [CORDIF] . . . 33
1.5.12 Horizontal Diffusion and Rayleigh Friction MODULE: [DSETDF] . . . 34
1.5.13 Time Filter MODULE: [DADVNC] . . . 34
1.5.14 Correction for conservation of mass MODULE: [FIXMAS, MASFIX] . . . 35
1.6 Cumulus scheme . . . 37
1.6.1 Outline of cumulus scheme . . . 37
1.6.2 Interaction between cumulus ensemble and large-scale environment . . . 38
1.6.3 Cloud base . . . 38
1.6.4 Updraft velocity and entrainment rate . . . 39
1.6.5 Normalized mass flux and updraft properties . . . 40
1.6.6 Spectral representation . . . 42
1.6.7 Cloud-base mass flux . . . 42
1.6.8 Microphysics . . . 42
1.6.9 Evaporation, sublimation and downdraft . . . 43
1.6.10 Cloudiness . . . 44
1.6.11 Cumulus Momentum Transport . . . 44

2 浅い積雲対流のパラメタリゼーション 45
2.1 1. 浅い積雲の概要 . . . 45
2.2 2. 雲モデルの基本 . . . 46
2.3 3. PSHCN での計算 . . . 46
2.3.1 3.1. 下部境界条件：雲底での質量フラックスの診断 . . . 47
2.3.2 3.2. 雲底高度の診断 . . . 47
2.3.3 3.3. 浅い積雲の有無の判定 . . . 48
2.3.4 3.4. 上昇流フラックスの鉛直プロファイルの診断 . . . 48
2.4 4. 実装に際しての補足 . . . 49
2.4.1 4.1. 質量フラックスのリミッター . . . 49
2.5 5. 参考文献 . . . 50

3 pmlsc: Large Scale Condensation 51
3.1 Physical basis for statistical PDF scheme . . . 51
3.2 Hybrid Prognostic Cloud (HPC) scheme . . . 52
3.3 PDF change through processes . . . 53
3.3.1 Cumulus convection . . . 53
3.3.2 Cloud Microphysics . . . 54
3.3.3 Turbulent mixing . . . 54

3.3.4 Subgrid-scale horizontal eddy . . . 55
3.3.5 Other processes . . . 55
3.4 Solving procedures . . . 55
3.4.1 PDF2CLD . . . 55
3.4.2 CLD2PDF . . . 57
3.4.3 Treatment of cloud ice and in-cloud water vapor . . . 58

4 pcldphys: Cloud Microphysics 60
4.1 Overview of Cloud Microphysics . . . 60
4.2 Microphysical Processes . . . 61
4.2.1 Ice Properties . . . 62
4.2.2 Evaporation of Rain and Snow . . . 62
4.2.3 Ice Fall . . . 63
4.2.4 Homogeneous nucleation . . . 63
4.2.5 Heterogeneous nucleation . . . 64
4.2.6 Deposition/Sublimation . . . 64
4.2.7 Cloud water collection by ice (riming) . . . 65
4.2.8 Ice melt . . . 65
4.2.9 Warm rain cloud microphysics . . . 66
4.2.10 Total precipitation . . . 66
4.3 Radiant Flux. . . . 67
4.3.1 Summary of Radiation Flux Calculations . . . 67
4.3.2 Wavelengths and Subchannels . . . 67
4.3.3 Calculating the Planck function [PLANKS] . . . 68
4.3.4 Calculating the optical thickness by gas absorption [PTFIT] . . . 69
4.3.5 Optical Thickness by Continuous Absorption and CFC Absorption [CNTCFC] 70
4.3.6 Scattering optical thickness and scattering moments [SCATMM] . . . 70
4.3.7 Albedo at Sea Level [SSRFC] . . . 71
4.3.8 Total Optical Thickness. . . . 72
4.3.9 Planck function expansion [PLKEXP] . . . 72
4.3.10 Transmission and reflection coefficients of each layer, the source function [TWST] . . . 72
4.3.11 Combinations of source functions for each layer . . . 74
4.3.12 Radiation flux at each layer boundary [ADDING] . . . 75
4.3.13 Add in the flux . . . 76
4.3.14 The temperature derivative of the flux . . . 77
4.3.15 Treatment of cloud cover . . . 77
4.3.16 Incidence flux and angle of incidence [SHTINS] . . . 78
4.3.17 Other Notes. . . . 80
4.4 Turbulence scheme . . . 81
4.4.1 Surface boundary layer . . . 82
4.4.2 Diagnosis of the buoyancy coefficients . . . 82
4.4.3 Stability functions in the Level 2 . . . 83
4.4.4 Master turbulent length scale . . . 85

4.4.5 Calculation of diffusion coefficients 86
4.4.6 Calculation of turbulent variables 89
4.4.7 Time integration with implicit scheme 92

5 1 Surface Flux **93**

6 1.1 Sea surface flux [OCNFLX] **94**
6.1 1.2 Sea Surface Conditions [OCNBCS] 95
6.1.1 1.2.1 Sea Surface Albedo for Visible [SEAALB] 98
6.1.2 1.2.2 Sea Surface Roughness [SEAZOF] 99
6.2 1.3 Sea Surface Flux [SFCFLX] 99
6.2.1 1.3.1 Bulk factor [BLKCOF] 101
6.3 1.4 Radiation Flux at Sea Surface [RADSFC] 102
6.4 1.5 Sea Surface Heat Balance [OCNSLV] 102

7 References (dynamics) **106**

Table of contents

- Basic Settings
  - Coordinate System (数式をハイブリッド化済)
  - Physical Constants (変更なし)

0.1 Basic Settings

Here we present the basic setup of the model.

0.1.1 Coordinate System

座標系は、基本的に、経度 λ、緯度 φ、正規化気圧 η (定義は後述) を用い、それぞれは直交するとして扱う。ただし、地中の鉛直座標は z を用いる。

Longitude is discretized at equal intervals `MODULE:[ASETL]`.

$$\lambda_i = 2\pi \frac{i-1}{I} \quad i = 1, \dots I-1 \tag{1}$$

The latitude is the Gauss latitude φ_j described in Mechanics, and it is derived from `MODULE:[ASETL]`, the Gauss-Legendre integral formula. This is the zero point of the Legendre polynomial of order J with $\mu = \sin\varphi$ as the argument, `MODULE:[GAUSS]`.

If J is large, we can approximate

$$\varphi_j = \pi(\frac{1}{2} - \frac{j-1/2}{J}) \quad j = 1, \dots J-1 \tag{2}$$

Usually, the grid spacing of longitude and latitude is taken to be approximately equal to $J = I/2$. This is based on the triangular truncation of the spectral method.

気圧 p は $k = 0 \dots K$ について、定数 $A_{k+1/2},\ B_{k+1/2}$ を用いて次の式で定義する。

$$p_{k+1/2} = A_{k+1/2} + B_{k+1/2}\, p_s \tag{3}$$

ただし、$A_{1/2} = A_{K+1/2} = 0,\ B_{1/2} = 1,\ B_{K+1/2} = 0$ であり、よって $p_{1/2} = p_s,\ p_{K+1/2} = 0$ である。また、$\sigma \equiv p/p_s$ は以下のように表せる。

$$\sigma_{k+1/2} = \frac{A_{k+1/2}}{p_s} + B_{k+1/2} \tag{4}$$

さらに、基準地表気圧 $p_0 = 1000$ hPa を用いて η を次の式で定義する。

$$\eta_{k+1/2} = \frac{A_{k+1/2}}{p_0} + B_{k+1/2} \tag{5}$$

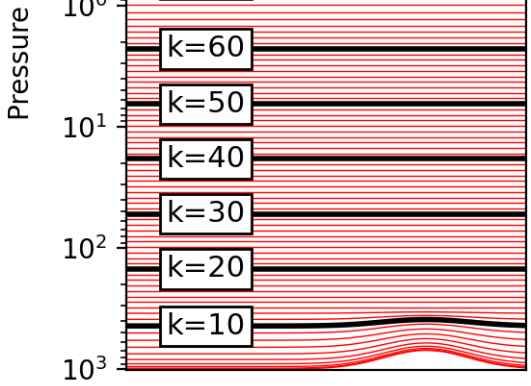

図 1: 鉛直 80 層とする場合のデフォルトの層配置

$A_{k+1/2}$, $B_{k+1/2}, p_0$ が定数であるため、$\eta_{k+1/2}$ も定数であり、これをモデルの鉛直座標とする。ただし、第二章で示すように、離散化を行った後の式は、$\eta_{k+1/2}$ が陽には現れず、$\sigma_{k+1/2}$ を多用する形になっている。これは、σ 座標とのソースコードの共通化を図るためである。

整数レベルにおける気圧 p_k $(k = 1, 2, \ldots K)$ は次の式で内挿する。

$$p_k = \left\{ \frac{1}{1+\kappa} \left(\frac{p_{k-1/2}^{\kappa+1} - p_{k+1/2}^{\kappa+1}}{p_{k-1/2} - p_{k+1/2}} \right) \right\}^{1/\kappa} \tag{6}$$

鉛直座標を 80 層にした場合の整数レベルの気圧を例示する。下層は地形に追従する一方で、上部の層は等圧になっており、両者が滑らかに接続されている。

Each predictor is entirely defined on a grid of $(\lambda_i, \varphi_j, \sigma_k)$ or $(\lambda_i, \varphi_j, z_l)$. (The underground level, z_l, is described in the section on physical processes.)

In the time direction, the predictive equations are discretized at evenly spaced Δt and time integration is performed. However, if the stability of the time integration may be impaired, the Δt may change.

0.1.2 Physical Constants

The basic physical constants are shown below `MODULE:[APCON]`.

))))
* * * *
0.25 Earth radius 3

)
*
0.25
))))
* * * *
0.25 Earth radius 6.37 ra- dius $\times 10^6$

))))
* * * *

0.25 0.25 ... Parameter1 Parameter2 Parameter3

)
*

0.25

))))
* * * *

0.25 0.25 0.25 0.25 acceleration of gravity 9.8

))))
* * * *

0.25 0.25 0.25 0.25 constant pressure specific heat 1004.6
kg^{-1}
K^{-1}

))))
* * * *

0.25 0.25 0.25 0.25 atmospheric gas constant 287.04
kg^{-1}
K^{-1}

))))
* * * *

0.25 0.25 0.25 0.25 latent heat of water evaporation 2.5
kg^{-1} $\times 10^6$

)
)
)
)
* * * *
0.25
)
)
)
)
* * * *
0.25
va-
por
con-
stant
pres-
sure
spe-
cific
heat
)
)
)
)
* * * *
0.25
con-
stant
of
wa-
ter
)
)
)
)
* * * *
0.25
of
liq-
uid
wa-
ter

	))))	
* * * *		
0.25		
	)	
*		
0.25		
	))))	
* * * *		
0.25		
Sat- u- rated va- por at 0 ◦		
	))))	
* * * *		
0.25		
Bolz- man Con- stant	$m^{-2} \times 10^{-8}$	K^{-4}
	))))	
* * * *		
0.25		
Con- stant		
	))))	
* * * *		
0.25		
heat of ice melt- ing	$kg^{-1} \times 10^{5}$	
	))))	
* * * *		
0.25		
Freez- ing Point		

)	)	)	)	
*	*	*	*	
0.25				
)	)	)	)	
*	*	*	*	
0.25				
)				
*				
0.25				
)	)	)	)	
*	*	*	*	
0.25				4,200.
pres-	kg^{-1}			
sure				
spe-				
cific				
heat				
of				
wa-				
ter				
)	)	)	)	
*	*	*	*	
0.25				271.35
freez-				
ing				
point				
of				
sea-				
wa-				
ter				
)	)	)	)	
*	*	*	*	
0.25				2397.
heat	$C_w -$			
ra-	L_M/T_M			
tio				
of				
ice				
at				
con-				
stant				
pres-				
sure				

))))
* * * *

0.25 0.25 Parameter 1 Parameter 2 Parameter 3

)
*

0.25

))))
* * * *

0.25 0.25 water 0.25 0.622
va- R/R_v
por
molec-
u-
lar
weight
ra-
tio

))))
* * * *

0.25 0.25 Coefficient 0.25 0.606
of $\epsilon^{-1}-$
pro-
vi-
sional
tem-
per-
a-
ture

))))
* * * *

0.25 0.25 Ratio 0.25 0.286
of R/C_p
spe-
cific
heat
to
gas
con-
stant

0.2 Computational flow of dynamical core

In this section, calculations of dynamical component based on coding are summarized. [module name(file name)]

0.2.1 Overview of dynamical core

1. calculate dynamical term [DYNTRM(dterm.F)]

   1.1 calculate volticity and divergence on wave space and get grid value. [G2W, W2G(xdsphe.F)]

   1.2 diagnose stream function and potential velocity [DYNTRM(dterm.F)]

   1.3 diagnose surface pressure advection, its tendency & vertical flow [PSDOT(dgdyn.F)]

   1.4 calculate factor for hydrostatic eq. & interporation of temprature on Hybrid coord. [CFACT(dcfct.F)]

   1.5 calculate vartual temprature [VIRTMD(dvtmp.F)]

   1.6 calculate temperature advection [GRTADV(dgdyn.F)]

   1.7 calculate momentum advection [GRUADV(dgdyn.F)]

   1.8 spectral transform of tendency terms [G2W(xdsphe.F)]

2. Time integration of equation DYNSTP(dstep.F)

   2.1 calculate tracer transport [TRACEG(dtrcr.F)]

   2.2 time integration on wave space [TINTGR(dintg.F)]

   2.3 time integration of tracer terms [GTRACE(dtrcr.F)]

   2.4 time filter [DADVNC(dadvn.F)]

   2.5 get horizontal wind of grid value from wave space [W2G(xdsphe.F)]

   2.6 correction of pressure-level diffusion [CORDIF(ddifc.F)]

   2.7 correction of horizontal friction heating [CORFRC(ddifc.F)]

Table of contents

- Mechanical Processes
  - Basic Equations
    - Basic Equations (数式をハイブリッド化済)
    - Boundary Conditions (数式をハイブリッド化済)

1 Mechanical Processes

1.1 Basic Equations

1.1.1 Basic Equations

The fundamental equations are a system of primitive equations at the spherical (λ, φ) and η coordinates, given as follows (Arakawa and Konor 1996).

1. Continuity equation

$$\frac{\partial m}{\partial t} + \nabla_\eta \cdot (m\mathbf{v}_H) + \frac{\partial (m\dot{\eta})}{\partial \eta} = 0 \tag{7}$$

2. Hydrostatic equation

$$\frac{\partial \Phi}{\partial \eta} = -\frac{RT_v}{p} m \tag{8}$$

3. Equation of motion

$$\frac{\partial \zeta}{\partial t} = \frac{1}{a\cos\varphi}\frac{\partial A_v}{\partial \lambda} - \frac{1}{a\cos\varphi}\frac{\partial}{\partial \varphi}(A_u \cos\varphi) - \mathcal{D}(\zeta) \tag{9}$$

$$\frac{\partial D}{\partial t} = \frac{1}{a\cos\varphi}\frac{\partial A_u}{\partial \lambda} + \frac{1}{a\cos\varphi}\frac{\partial}{\partial \varphi}(A_v \cos\varphi) - \nabla_\eta^2(\Phi + R\bar{T}\pi + E) - \mathcal{D}(D) \tag{10}$$

4. Thermodynamic equation

$$\frac{\partial T}{\partial t} = -\frac{1}{a\cos\varphi}\frac{\partial uT'}{\partial \lambda} - \frac{1}{a}\frac{\partial}{\partial \varphi}(vT'\cos\varphi) + T'D \tag{11}$$

$$-\dot{\eta}\frac{\partial T}{\partial \eta} + \frac{\kappa T}{\sigma}\left[B\left(\frac{\partial \pi}{\partial t} + \mathbf{v}_H \cdot \nabla_\eta \pi\right) + \frac{m\dot{\eta}}{p_s}\right] + \frac{Q}{C_p} + \frac{Q_{diff}}{C_p} - \mathcal{D}(T) \tag{12}$$

5. Tracers

ここでは水蒸気の移流方程式を示す。他のトレーサーも同様の方程式に従う。

$$\frac{\partial q}{\partial t} = -\frac{1}{a\cos\varphi}\frac{\partial uq}{\partial \lambda} - \frac{1}{a\cos\varphi}\frac{\partial}{\partial \varphi}(vq\cos\varphi) + qD \tag{13}$$

$$-\dot{\eta}\frac{\partial q}{\partial \eta} + S_q - \mathcal{D}(q) \tag{14}$$

Here,

$$m \equiv \left(\frac{\partial p}{\partial \eta}\right)_{p_s} \tag{15}$$

$$\theta \equiv T\,(p/p_0)^{-\kappa} \tag{16}$$

$$\kappa \equiv R/C_p \tag{17}$$

$$\Phi \equiv gz \tag{18}$$

$$\pi \equiv \ln p_S \tag{19}$$

$$\dot{\eta} \equiv \frac{d\eta}{dt} \tag{20}$$

$$T_v \equiv T(1+\epsilon_v q) \tag{21}$$

$$T \equiv \bar{T} + T' \tag{22}$$

$$\bar{T} \equiv 300\ \mathrm{K} \tag{23}$$

$$\zeta \equiv \frac{1}{a\cos\varphi}\frac{\partial v}{\partial \lambda} - \frac{1}{a\cos\varphi}\frac{\partial}{\partial \varphi}(u\cos\varphi) \tag{24}$$

$$D \equiv \frac{1}{a\cos\varphi}\frac{\partial u}{\partial \lambda} + \frac{1}{a\cos\varphi}\frac{\partial}{\partial \varphi}(v\cos\varphi) \tag{25}$$

$$A_u \equiv (\zeta+f)v - \dot{\eta}\frac{\partial u}{\partial \eta} - \frac{RT'}{a\cos\varphi}\frac{\partial \pi}{\partial \lambda} + \mathcal{F}_x \tag{26}$$

$$A_v \equiv -(\zeta+f)u - \dot{\eta}\frac{\partial v}{\partial \eta} - \frac{RT'}{a}\frac{\partial \pi}{\partial \varphi} + \mathcal{F}_y \tag{27}$$

$$E \equiv \frac{u^2 + v^2}{2} \tag{28}$$

$$\mathbf{v}_H \cdot \nabla \equiv \frac{u}{a\cos\varphi}\left(\frac{\partial}{\partial\lambda}\right)_\sigma + \frac{v}{a}\left(\frac{\partial}{\partial\varphi}\right)_\sigma \tag{29}$$

$$\nabla_\eta^2 \equiv \frac{1}{a^2\cos^2\varphi}\frac{\partial^2}{\partial\lambda^2} + \frac{1}{a^2\cos\varphi}\frac{\partial}{\partial\varphi}\left[\cos\varphi\frac{\partial}{\partial\varphi}\right]. \tag{30}$$

$\mathcal{D}(\zeta), \mathcal{D}(D), \mathcal{D}(T), \mathcal{D}(q)$ are horizontal diffusion terms, $\mathcal{F}_\lambda, \mathcal{F}_\varphi$ are forces due to small-scale kinetic processes (treated as 'physical processes'), Q are forces due to radiation, condensation, small-scale kinetic processes, etc. Heating and temperature change due to 'physical processes', and S_q is a water vapor source term due to 'physical processes' such as condensation and small-scale motion. Q_{diff} is the heat of friction and

$$Q_{diff} = -\mathbf{v} \cdot (\frac{\partial \mathbf{v}}{\partial t})_{diff}. \tag{31}$$

$(\frac{\partial \mathbf{v}}{\partial t})_{diff}$ is a time-varying term of u, v due to horizontal and vertical diffusion.

1.1.2 Boundary Conditions

鉛直流に関する上下端の境界条件は以下の通りである：

$$\dot{\eta} = 0 \quad at \;\; \eta = 0,\; 1. \tag{32}$$

これを用いて連続の式を鉛直積分することで、p_s の予報方程式と、鉛直流の診断方程式が導かれる。

Table of contents

- Vertical Discretization
  - Model levels (数式・説明をハイブリッド化済)
  - Vertical discretization (数式をハイブリッド化済)
  - Differences from σ-coordinate (新規追加)

1.2 Vertical Discretization

Following Arakawa and Konor (1996) but in the Lorentz grid, the basic equations are discretized vertically by differences. This scheme has the following characteristics.

- Save the total integrated mass
- Save the total integrated energy
- Preserving angular momentum for global integration
- Conservation of total mass-integrated potential temperature
- The hydrostatic pressure equation comes down to local (the altitude of the lower level is independent of the temperature of the upper level)
- For a given temperature distribution, constant in the horizontal direction, the hydrostatic pressure equation becomes accurate and the barometric gradient force becomes zero.
- Isothermal atmosphere stays isothermal forever

1.2.1 Model levels

下の層から上へと層の番号をつける。ζ, D, T, q の物理量は整数レベルで定義されるとし、鉛直速度 $\dot{\eta}$ は半整数レベルにおいて定義する。ただし、$\frac{1}{2}$ は下端 ($\eta = 1$)、$K + \frac{1}{2}$ は上端 ($\eta = 0$) である。さらに、半整数レベルにおける気圧 p を以下の式で定義する。

$$p_{k+1/2} = A_{k+1/2} + B_{k+1/2}\, p_s \tag{33}$$

よって、$\sigma \equiv p/p_s$ は以下のように表せる。

$$\sigma_{k+1/2} = \frac{A_{k+1/2}}{p_s} + B_{k+1/2} \tag{34}$$

また、基準地表気圧 $p_0 = 1000$ hPa を用いて η を次の式で定義する。

$$\eta_{k+1/2} = \frac{A_{k+1/2}}{p_0} + B_{k+1/2} \tag{35}$$

整数レベルにおける気圧 $p_k, (k = 1, 2, \ \ldots \ K)$ は次の式で内挿する。

$$p_k = \left\{ \frac{1}{1+\kappa} \left(\frac{p_{k-1/2}^{\kappa+1} - p_{k+1/2}^{\kappa+1}}{p_{k-1/2} - p_{k+1/2}} \right) \right\}^{1/\kappa} \tag{36}$$

さらに、

$$\Delta\sigma_k \equiv \sigma_{k-1/2} - \sigma_{k+1/2} \tag{37}$$

$$\Delta B_k \equiv B_{k-1/2} - B_{k+1/2} \tag{38}$$

を定義しておく。

1.2.2 Vertical discretization

各方程式のハイブリッド座標における離散化表現は次のようになる。

1. 連続の式、鉛直速度

$$\frac{\partial \pi}{\partial t} = -\sum_{k=1}^{K} \{ D_k \Delta\sigma_k + (\mathbf{v}_k \cdot \nabla\pi) \Delta B_k \} \tag{39}$$

MIROC6.0 では、以前のバージョンで用いられていた σ 座標系 (MIROC6.0 でも選択可能である) とできるだけ類似した表式で離散化を行ったため、鉛直速度は $\dot{\sigma} = m\dot{\eta}/p_s$ で表現している。また、鉛直移流 $\dot{\eta}(\partial/\partial\eta)$ は $m\dot{\eta}/p_s(\partial/\partial\sigma)$ と等価であり、プログラム中では後者を使用している。

$$(\dot{\sigma} =) \frac{(m\dot{\eta})_{k-1/2}}{p_s} = -B_{k-1/2} \frac{\partial \pi}{\partial t} - \sum_{l=k}^{K} \{ D_l \Delta\sigma_l + (\mathbf{v}_l \cdot \nabla\pi) \Delta B_l \} \tag{40}$$

$$\frac{(m\dot{\eta})_{1/2}}{p_s} = \frac{(m\dot{\eta})_{k+1/2}}{p_s} = 0 \tag{41}$$

2. 静水圧の式

$$\Phi_1 = \Phi_s + C_p(\sigma_1^{-\kappa} - 1) T_{v,1} \tag{42}$$

$$= \Phi_s + C_p \alpha_1 T_{v,1} \tag{43}$$

$$\Phi_k - \Phi_{k-1} = C_p \left[\left(\frac{p_{k-1/2}}{p_k} \right)^{\kappa} - 1 \right] T_{v,k} + C_p \left[1 - \left(\frac{p_{k-1/2}}{p_{k-1}} \right)^{\kappa} \right] T_{v,k-1} \tag{44}$$

$$= C_p\alpha_k T_{v,k} + C_p\beta_{k-1}T_{v,k-1} \tag{45}$$

ここで、

$$\alpha_k \equiv \left(\frac{p_{k-1/2}}{p_k}\right)^{\kappa} - 1 \tag{46}$$

$$\beta_k \equiv 1 - \left(\frac{p_{k+1/2}}{p_k}\right)^{\kappa}. \tag{47}$$

3. 運動方程式

$$\frac{\partial \zeta_k}{\partial t} = \frac{1}{a\cos\varphi}\frac{\partial (A_v)_k}{\partial \lambda} - \frac{1}{a\cos\varphi}\frac{\partial}{\partial \varphi}(A_u\cos\varphi)_k - \mathcal{D}(\zeta_k) \tag{48}$$

$$\frac{\partial D}{\partial t} = \frac{1}{a\cos\varphi}\frac{\partial (A_u)_k}{\partial \lambda} + \frac{1}{a\cos\varphi}\frac{\partial}{\partial \varphi}(A_v\cos\varphi)_k - \nabla_\sigma^2(\Phi_k + R\bar{T}\pi + (KE)_k) - \mathcal{D}(D_k) \tag{49}$$

$$(A_u)_k = (\zeta_k + f)v_k - \left[\frac{(m\dot{\eta})_{k-1/2}}{p_s}\frac{u_{k-1}-u_k}{\Delta\sigma_{k-1}+\Delta\sigma_k} + \frac{(m\dot{\eta})_{k+1/2}}{p_s}\frac{u_k - u_{k+1}}{\Delta\sigma_k + \Delta\sigma_{k+1}}\right] \tag{50}$$

$$-\frac{1}{a\cos\varphi}\frac{\partial \pi}{\partial \lambda}(C_p T_{v,k}\hat{\kappa} - R\bar{T}) + \mathcal{F}_x \tag{51}$$

$$(A_v)_k = -(\zeta_k + f)u_k - \left[\frac{(m\dot{\eta})_{k-1/2}}{p_s}\frac{v_{k-1}-v_k}{\Delta\sigma_{k-1}+\Delta\sigma_k} + \frac{(m\dot{\eta})_{k+1/2}}{p_s}\frac{v_k - v_{k+1}}{\Delta\sigma_k + \Delta\sigma_{k+1}}\right] \tag{52}$$

$$-\frac{1}{a}\frac{\partial \pi}{\partial \varphi}(C_p T_{v,k}\hat{\kappa} - R\bar{T}) + \mathcal{F}_y \tag{53}$$

$$\hat{\kappa}_k = \frac{B_{k-1/2}\alpha_k + B_{k+1/2}\beta_k}{\Delta\sigma_k} \tag{54}$$

4. 熱力学方程式

$$\frac{\partial T_k}{\partial t} = -\frac{1}{a\cos\varphi}\frac{\partial u_k T_k'}{\partial \lambda} - \frac{1}{a\cos\varphi}\frac{\partial}{\partial \varphi}(v_k T_k'\cos\varphi) + H_k \tag{55}$$

$$+\frac{Q_k}{C_p} + \frac{(Q_{diff})_k}{C_p} - \mathcal{D}(T_k) \tag{56}$$

ここで、

$$H_k \equiv T'_k D_k - \left[\frac{(m\dot{\eta})_{k-1/2}}{p_s} \frac{\hat{T}_{k-1/2} - T_k}{\Delta\sigma_k} + \frac{(m\dot{\eta})_{k+1/2}}{p_s} \frac{T_k - \hat{T}_{k+1/2}}{\Delta\sigma_k} \right] \tag{57}$$

$$+ \left\{ \alpha_k \left[B_{k-1/2} \mathbf{v}_k \cdot \nabla\pi - \sum_{l=k}^{K} (D_l \Delta\sigma_l + (\mathbf{v}_l \cdot \nabla\pi) \Delta B_l) \right] \right. \tag{58}$$

$$\left. + \beta_k \left[B_{k+1/2} \mathbf{v}_k \cdot \nabla\pi - \sum_{l=k+1}^{K} (D_l \Delta\sigma_l + (\mathbf{v}_l \cdot \nabla\pi) \Delta B_l) \right] \right\} \frac{1}{\Delta\sigma_k} T_{v,k} \tag{59}$$

$$= T'_k D_k - \left[\frac{(m\dot{\eta})_{k-1/2}}{p_s} \frac{\hat{T}_{k-1/2} - T_k}{\Delta\sigma_l} + \frac{(m\dot{\eta})_{k+1/2}}{p_s} \frac{T_k - \hat{T}_{k+1/2}}{\Delta\sigma_l} \right] \tag{60}$$

$$+ \hat{\kappa}_k \mathbf{v}_k \cdot \nabla\pi T_{v,k} \tag{61}$$

$$- \alpha_k \sum_{l=k}^{K} (D_l \Delta\sigma_l + (\mathbf{v}_l \cdot \nabla\pi) \Delta B_l) \frac{T_{v,k}}{\Delta\sigma_k} \tag{62}$$

$$- \beta_k \sum_{l=k+1}^{K} (D_l \Delta\sigma_l + (\mathbf{v}_l \cdot \nabla\pi) \Delta B_l) \frac{T_{v,k}}{\Delta\sigma_k} \tag{63}$$

$$\hat{T}_{k-1/2} = a_k T_k + b_{k-1} T_{k-1} \tag{64}$$

$$a_k = \alpha_k \left[1 - \left(\frac{p_k}{p_{k-1}} \right)^{\kappa} \right]^{-1} \tag{65}$$

$$b_k = \beta_k \left[\left(\frac{p_k}{p_{k+1}} \right)^{\kappa} - 1 \right]^{-1}. \tag{66}$$

5. 水蒸気の時間発展方程式

$$\frac{\partial q_k}{\partial t} = -\frac{1}{a\cos\varphi} \frac{\partial u_k q_k}{\partial \lambda} - \frac{1}{a\cos\varphi} \frac{\partial}{\partial \varphi} (v_k q_k \cos\varphi) + R_k + S_{q,k} - \mathcal{D}(q_k) \tag{67}$$

$$R_k = q_k D_k - \frac{1}{2} \left[\frac{(m\dot{\eta})_{k-1/2}}{p_s} \frac{q_{k-1} - q_k}{\Delta\sigma_k} + \frac{(m\dot{\eta})_{k+1/2}}{p_s} \frac{q_k - q_{k+1}}{\Delta\sigma_k} \right] \tag{68}$$

1.2.3 Differences from σ-coordinate

ここではハイブリッド座標を、できるだけ σ 座標に近い表式で離散化したため、両者の差は比較的少ない。両者の重要な対応関係を以下に挙げる。

- 全層で $A_{k+1/2} = 0$ とすれば、ハイブリッド座標は σ 座標に帰着する。
- ハイブリッド座標における ΔB_k と $\Delta\sigma$ は、σ 座標系においては両者とも $\Delta\sigma_k$ に対応する。

1.3 Horizontal discretization

The horizontal discretization is based on the spectral transformation method (Bourke, 1988). The differential terms for longitude and latitude are evaluated by the orthogonal function expansion, while the non-linear terms are calculated on the grid.

1.3.1 Spectral Expansion.

As an expansion function, the spherical harmonic functions $Y_n^m(\lambda, \mu)$, which are eigenfunction of Laplacian on a sphere, are used. However, $\mu \equiv \sin\varphi$ is used. Y_n^m satisfies the following equation,

$$\nabla_\sigma^2 Y_n^m(\lambda, \mu) = -\frac{n(n+1)}{a^2} Y_n^m(\lambda, \mu) \tag{69}$$

Using the Legendre jury function P_n^m it is written as follows.

$$Y_n^m(\lambda, \mu) = P_n^m(\mu) e^{\mathrm{i}m\lambda} \tag{70}$$

However, it is \$ n $\geq jmj$\$.
The expansion by spherical harmonic functions is ,

$$Y_n^m{}_{ij} \equiv Y_n^m(\lambda_i, \mu_j) \tag{71}$$

When I write ,

$$X_{ij} \equiv X(\lambda_i, \mu_j) = \mathcal{R}\rceil \sum_{m=-N}^{N} \sum_{n=|m|}^{N} X_n^m Y_n^m{}_{ij}, \tag{72}$$

The inverse of that is ,

$$X_n^m = \frac{1}{4\pi} \int_{-1}^{1} d\mu \int_0^{\pi} d\lambda X(\lambda, \mu) Y_n^{m*}(\lambda, \mu) \tag{73}$$

$$= \frac{1}{I} \sum_{i=1}^{I} \sum_{j=1}^{J} X_{ij} Y_n^{m*}{}_{ij} w_j \tag{74}$$

The formula is expressed as To evaluate by replacing the integral with a sum, we use the Gauss trapezoidal formula for the λ integral and the Gauss-Legendre integral formula for the μ integral. μ_j is the Gauss latitude and w_j is the Gauss load. Also, λ_i is a grid of evenly spaced Gauss loads.

Using spectral expansion, the grid point values of the terms containing the derivatives can be calculated as follows.

$$\left(\frac{\partial X}{\partial \lambda}\right)_{ij} = \mathcal{R}e \sum_{m=-N}^{N} \sum_{n=|m|}^{N} \mathrm{i}m X_n^m {Y_n^m}_{ij} \tag{75}$$

$$\left(\cos\varphi \frac{\partial X}{\partial \varphi}\right)_{ij} = \mathcal{R}e \sum_{m=-N}^{N} \sum_{n=|m|}^{N} X_n^m (1-\mu^2) \frac{\partial}{\partial \mu} {Y_n^m}_{ij} \tag{76}$$

Furthermore, the grid point values of u, v can be obtained from the spectral components of ζ and D as follows

$$u_{ij} = \frac{1}{\cos\varphi} \mathcal{R}e \sum_{m=-N}^{N} \sum_{\substack{n=|m| \\ n\neq 0}}^{N} \left\{ \frac{a}{n(n+1)} \zeta_n^m (1-\mu^2) \frac{\partial}{\partial \mu} {Y_n^m}_{ij} - \frac{\mathrm{i}ma}{n(n+1)} D_n^m {Y_n^m}_{ij} \right\} \tag{77}$$

$$v_{ij} = \frac{1}{\cos\varphi} \mathcal{R}e \sum_{m=-N}^{N} \sum_{\substack{n=|m| \\ n\neq 0}}^{N} \left\{ -\frac{\mathrm{i}ma}{n(n+1)} \zeta_n^m {Y_n^m}_{ij} - \frac{a}{n(n+1)} D_n^m (1-\mu^2) \frac{\partial}{\partial \mu} {Y_n^m}_{ij} \right\} \tag{78}$$

The derivative appearing in the advection term of the equation is calculated as

$$\left(\frac{1}{a\cos\varphi} \frac{\partial A}{\partial \lambda}\right)_n^m = \frac{1}{4\pi} \int_{-1}^{1} d\mu \int_0^{\pi} d\lambda \frac{1}{a\cos\varphi} \frac{\partial A}{\partial \lambda} Y_n^{m*} \tag{79}$$

$$= \frac{1}{4\pi} \int_{-1}^{1} d\mu \int_0^{\pi} d\lambda \, \mathrm{i}mA \cos\varphi \frac{1}{a(1-\mu^2)} Y_n^{m*} \tag{80}$$

$$= \frac{1}{I} \sum_{i=1}^{I} \sum_{j=1}^{J} \mathrm{i}m A_{ij} \cos\varphi_j {Y_n^{m*}}_{ij} \frac{w_j}{a(1-\mu_j^2)} \tag{81}$$

$$\left(\frac{1}{a\cos\varphi} \frac{\partial}{\partial \varphi}(A\cos\varphi)\right)_n^m = \frac{1}{4\pi a} \int_{-1}^{1} d\mu \int_0^{\pi} d\lambda \frac{\partial}{\partial \mu}(A\cos\varphi) Y_n^{m*} \tag{82}$$

$$= -\frac{1}{4\pi a} \int_{-1}^{1} d\mu \int_0^{\pi} d\lambda A\cos\varphi \frac{\partial}{\partial \mu} Y_n^{m*} \tag{83}$$

$$= -\frac{1}{I} \sum_{i=1}^{I} \sum_{j=1}^{J} A_{ij} \cos\varphi_j (1-\mu_j^2) \frac{\partial}{\partial \mu} {Y_n^{m*}}_{ij} \frac{w_j}{a(1-\mu_j^2)} \tag{84}$$

Furthermore,

$$\left(\nabla_\sigma^2 X\right)_n^m = -\frac{n(n+1)}{a^2} X_n^m \tag{85}$$

to be used for the evaluation of the ∇^2 section.

1.3.2 Horizontal Diffusion Term

The horizontal diffusion term is entered in the form ∇^{N_D} as follows.

$$\mathcal{D}(\zeta) = K_{MH}\left[(-1)^{N_D/2}\nabla^{N_D} - \left(\frac{2}{a^2}\right)^{N_D/2}\right]\zeta, \tag{86}$$

$$\mathcal{D}(D) = K_{MH}\left[(-1)^{N_D/2}\nabla^{N_D} - \left(\frac{2}{a^2}\right)^{N_D/2}\right]D, \tag{87}$$

$$\mathcal{D}(T) = (-1)^{N_D/2}K_{HH}\nabla^{N_D}T, \tag{88}$$

$$\mathcal{D}(q) = (-1)^{N_D/2}K_{EH}\nabla^{N_D}q. \tag{89}$$

This horizontal diffusion term has strong implications for computational stability. In order to represent selective horizontal diffusion on small scales, $4 \sim 16$ is used as N_D. Here, the extra term for vorticity and divergence diffusion indicates that the term of rigid body rotation in $n = 1$ does not decay.

1.3.3 Spectral representation of equations

1. a series of equations

$$\frac{\partial \pi_m^m}{\partial t} = -\sum_{k=1}^{K}(D_n^m)_k \Delta\sigma_k \tag{90}$$

$$+\frac{1}{I}\sum_{i=1}^{I}\sum_{j=1}^{J} Z_{ij}{Y_n^{m*}}_{ij}w_j, \tag{91}$$

Here,

$$Z \equiv -\sum_{k=1}^{K}\mathbf{v}_k \cdot \nabla\pi. \tag{92}$$

2. equation of motion

$$\frac{\partial \zeta_n^m}{\partial t} = \frac{1}{I}\sum_{i=1}^{I}\sum_{j=1}^{J} im(A_v)_{ij}\cos\varphi_j {Y_n^{m*}}_{ij}\frac{w_j}{a(1-\mu_j^2)} \tag{93}$$

$$+\frac{1}{I}\sum_{i=1}^{I}\sum_{j=1}^{J}(A_u)_{ij}\cos\varphi_j(1-\mu_j^2)\frac{\partial}{\partial\mu}{Y_n^{m*}}_{ij}\frac{w_j}{a(1-\mu_j^2)} \tag{94}$$

$$-(\mathcal{D}_M)_n^m\zeta_n^m\ , \tag{95}$$

$$\frac{\partial \tilde{D}_n^m}{\partial t} = \frac{1}{I}\sum_{i=1}^{I}\sum_{j=1}^{J} \mathrm{i}m(A_u)_{ij}\cos\varphi_j {Y_n^{m*}}_{ij}\frac{w_j}{a(1-\mu_j^2)} \tag{96}$$

$$-\frac{1}{I}\sum_{i=1}^{I}\sum_{j=1}^{J}(A_v)_{ij}\cos\varphi_j(1-\mu_j^2)\frac{\partial}{\partial\mu}{Y_n^{m*}}_{ij}\frac{w_j}{a(1-\mu_j^2)} \tag{97}$$

$$-\frac{n(n+1)}{a^2}\frac{1}{I}\sum_{i=1}^{I}\sum_{j=1}^{J}E_{ij}{Y_n^{m*}}_{ij}w_j \tag{98}$$

$$+\frac{n(n+1)}{a^2}(\Phi_n^m + C_p\hat{\kappa}_k\bar{T}_k\pi_n^m) - (\mathcal{D}_M)_n^m D_n^m, \tag{99}$$

However,

$$(\mathcal{D}_M)_n^m = K_{MH}\left[\left(\frac{n(n+1)}{a^2}\right)^{N_D/2} - \left(\frac{2}{a^2}\right)^{N_D/2}\right]. \tag{100}$$

3. thermodynamic equation

$$\frac{\partial T_n^m}{\partial t} = -\frac{1}{I}\sum_{i=1}^{I}\sum_{j=1}^{J}\mathrm{i}mu_{ij}T'_{ij}\cos\varphi_j {Y_n^{m*}}_{ij}\frac{w_j}{a(1-\mu_j^2)} \tag{101}$$

$$+\frac{1}{I}\sum_{i=1}^{I}\sum_{j=1}^{J}v_{ij}T'_{ij}\cos\varphi_j(1-\mu_j^2)\frac{\partial}{\partial\mu}{Y_n^{m*}}_{ij}\frac{w_j}{a(1-\mu_j^2)} \tag{102}$$

$$+\frac{1}{I}\sum_{i=1}^{I}\sum_{j=1}^{J}\left(H_{ij}+\frac{Q_{ij}+Q_{diff}}{C_p}\right){Y_n^{m*}}_{ij}w_j \tag{103}$$

$$-(\tilde{\mathcal{D}}_H)_n^m T_n^m\,, \tag{104}$$

However,

$$(\mathcal{D}_H)_n^m = K_{HH}\left(\frac{n(n+1)}{a^2}\right)^{N_D/2}. \tag{105}$$

4. water vapor formula

$$\frac{\partial q_n^m}{\partial t} = -\frac{1}{I}\sum_{i=1}^{I}\sum_{j=1}^{J}\mathrm{i}mu_{ij}q_{ij}\cos\varphi_j {Y_n^{m*}}_{ij}\frac{w_j}{a(1-\mu_j^2)} \tag{106}$$

$$+\frac{1}{I}\sum_{i=1}^{I}\sum_{j=1}^{J}v_{ij}q_{ij}\cos\varphi_j(1-\mu_j^2)\frac{\partial}{\partial\mu}{Y_n^{m*}}_{ij}\frac{w_j}{a(1-\mu_j^2)} \tag{107}$$

$$+\frac{1}{I}\sum_{i=1}^{I}\sum_{j=1}^{J}\left(\hat{R}_{ij}+S_{q,ij}\right){Y_n^{m*}}_{ij}w_j \tag{108}$$

$$+(\mathcal{D}_H)_n^m q_n^m \tag{109}$$

However,

$$(\mathcal{D}_E)_n^m = K_{EH}\left(\frac{n(n+1)}{a^2}\right)^{N_D/2}. \tag{110}$$

Table of contents

- Time Integration
  - Time integration and time filtering with leap frog (変更なし)
  - Semi-implicit time integration (変更なし)
  - Applying semi-implicit time integration (数式をハイブリッド化済)
  - Time scheme properties and time step estimates (変更なし)
  - Handling of the initiation of time integration (変更なし)

1.4 Time Integration `MODULE: [DYNSTP]`

The time difference scheme is essentially a leap frog. However, the diffusion terms and physical process terms are backward or forward differences. A time filter (Williams, 2009) is used to suppress the computational modes. A semi-implicit method is applied to the gravitational wave term to make the Δt larger (Bourke, 1988).

1.4.1 Time integration and time filtering with leap frog `MODULE: [DADVNC]`

We use leap frog as a time integration scheme for advection terms and so on. A backward difference of $2\Delta t$ is used for the horizontal diffusion term. The pseudo p surface correction of the diffusion term and the frictional heat due to horizontal diffusion term are treated as corrections, which are forward differences of $2\Delta t$. The physical process terms $(\mathcal{F}_\lambda, \mathcal{F}_\varphi, Q, S_q)$ still use the forward difference of $2\Delta t$ (except for the vertical diffusion term, which uses the forward difference of $\mathcal{F}_\lambda, \mathcal{F}_\varphi, Q, S_q$). (However, the calculation of the time-varying term of vertical diffusion is treated as a backward difference. Please refer to the chapter on physical processes for details.)

Expressed as X on behalf of each forecast variable,

$$\hat{X}^{t+\Delta t} = \bar{X}^{t-\Delta t} + 2\Delta t \dot{X}_{adv}\left(X^t\right) + 2\Delta t \dot{X}_{dif}\left(\hat{X}^{t+\Delta t}\right) \tag{111}$$

$\dot{X}_{adv}$ is the advection term etc., and $\dot{X}_{dif}$ is the horizontal diffusion term.

To $\hat{X}^{t+\Delta t}$, the term $X^{t+\Delta t}$ has been added with corrections for the heat of friction $(\dot{X}_{dis})$ and physical processes $(\dot{X}_{phy})$ for pseudo-equivalent p surface diffusion and horizontal diffusion.

$$X^{t+\Delta t} = \hat{X}^{t+\Delta t} + 2\Delta t \dot{X}_{dis}\left(\hat{X}^{t+\Delta t}\right) + 2\Delta t \dot{X}_{phy}\left(\hat{X}^{t+\Delta t}\right) \tag{112}$$

The time filter of Asselin (1972) is applied every step to remove computational modes in leap frog. I.e., the time filter of Asselin(1972) is applied every step of the way to remove the computation mode in

$$\bar{X}^t = (1 - 2\epsilon_f)X^t + \epsilon_f\left(\bar{X}^{t-\Delta t} + X^{t+\Delta t}\right) \tag{113}$$

and $\bar{X}$. Normally, 0.05 is used as the ϵ_f.

1.4.2 Semi-implicit time integration

Basically, the leap frog is used in mechanics calculations, but some terms are treated as implicit. Here, we consider the trapezoidal implicit as the implicit. For the vector quantity $\mathbf{q}$, the value of t is written as $\mathbf{q}$, the value of $t+\Delta t$ as $\mathbf{q}^+$, and the value of $t-\Delta t$ as $\mathbf{q}^-$, then the trapezoidal implicit means that the time change term evaluated by $(\mathbf{q}^+ + \mathbf{q}^-)/2$ is This is the solution of the problem by using the leap forg method. We now divide q into two time varying terms, one for the leap forg method and the other for the trapezoidal implicit method, B. We assume that A is nonlinear to q, while B is linear. In other words,

$$\mathbf{q}^+ = \mathbf{q}^- + 2\Delta t\mathcal{A}(\mathbf{q}) + 2\Delta t B(\mathbf{q}^+ + \mathbf{q}^-)/2 \tag{114}$$

However, B is a square matrix. Then write $\Delta\mathbf{q} \equiv \mathbf{q}^+ - \mathbf{q}$ and you will get

$$(I - \Delta t B)\Delta\mathbf{q} = 2\Delta t\left(\mathcal{A}(\mathbf{q}) + B\mathbf{q}\right) \tag{115}$$

This can be easily solved by matrix operations.

1.4.3 Applying semi-implicit time integration

Then, we apply this method and treat the term of linear gravity waves as implicit. This allows us to reduce the time step Δt.

In the system of equations, we divide the equation into a linear gravitational wave term ($T = \bar{T}_k$) with a stationary field as the basic field and other terms (with the indices NG). Using a vector representation of vertical direction ($\mathbf{D} = \{D_k\}$ and $\mathbf{T} = \{T_k\}$) ERR miura 122

$$\frac{\partial\pi}{\partial t} = \left(\frac{\partial\pi}{\partial t}\right)_{NG} - \mathbf{C}\cdot\mathbf{D}, \tag{116}$$

$$\frac{\partial\mathbf{D}}{\partial t} = \left(\frac{\partial\mathbf{D}}{\partial t}\right)_{NG} - \nabla_\eta^2(\mathbf{\Phi}_S + \underline{W}\mathbf{T} + \mathbf{G}\pi) - \mathcal{D}_M\mathbf{D}, \tag{117}$$

$$\frac{\partial\mathbf{T}}{\partial t} = \left(\frac{\partial\mathbf{T}}{\partial t}\right)_{NG} - \underline{h}\mathbf{D} - \mathcal{D}_H\mathbf{T}, \tag{118}$$

Here, the non-gravitational wave term is

$$\left(\frac{\partial\pi}{\partial t}\right)^{NG} = -\sum_{k=1}^{K}\mathbf{v}_k\cdot\nabla\pi\Delta B_k \tag{119}$$

$$\frac{(m\dot{\eta})^{NG}_{k-1/2}}{p_s} = -B_{k-1/2}\left(\frac{\partial\pi}{\partial t}\right)^{NG} - \sum_{l=k}^{K}\mathbf{v}_l\cdot\nabla\pi\Delta B_l \tag{120}$$

$$\left(\frac{\partial D}{\partial t}\right)^{NG} = \frac{1}{a\cos\varphi}\frac{\partial (A_u)_k}{\partial \lambda} + \frac{1}{a\cos\varphi}\frac{\partial}{\partial \varphi}(A_v \cos\varphi)_k - \nabla_\eta^2 \hat{E}_k - \mathcal{D}(D_k) \tag{121}$$

$$\left(\frac{\partial T_k}{\partial t}\right)^{NG} = -\frac{1}{a\cos\varphi}\frac{\partial u_k T_k'}{\partial \lambda} - \frac{1}{a\cos\varphi}\frac{\partial}{\partial \varphi}(v_k T_k' \cos\varphi) + \hat{H}_k - \mathcal{D}(T_k) \tag{122}$$

$$\hat{H}_k = T_k' D_k \tag{123}$$

$$-\left[\frac{(m\dot{\eta})_{k-1/2}}{p_s}\frac{\hat{T}_{k-1/2} - T_k}{\Delta\sigma_k} + \frac{(m\dot{\eta})_{k+1/2}}{p_s}\frac{T_k - \hat{T}_{k+1/2}}{\Delta\sigma_k}\right] \tag{124}$$

$$+\hat{\kappa}_k T_{v,k}\mathbf{v}_k \cdot \nabla\pi \tag{125}$$

$$-\frac{\alpha_k}{\Delta\sigma_k}T_{v,k}\sum_{l=k}^{K}\mathbf{v}_l \cdot \nabla\pi\Delta B_l - \frac{\beta_k}{\Delta\sigma_k}T_{v,k}\sum_{l=k+1}^{K}\mathbf{v}_l \cdot \nabla\pi\Delta B_l \tag{126}$$

$$-\frac{\alpha_k}{\Delta\sigma_k}T'_{v,k}\sum_{l=k}^{K}D_l\Delta\sigma_l - \frac{\beta_k}{\Delta\sigma_k}T'_{v,k}\sum_{l=k+1}^{K}D_l\Delta\sigma_l \tag{127}$$

$$+\frac{Q_k + (Q_{diff})_k}{C_p} \tag{128}$$

$$\hat{E}_k = E_k + \sum_{k=1}^{K} W_{kl}(T_{v,l} - T_l) \tag{129}$$

where the vector and matrix of the gravitational wave term (underlined) are

$$C_k = \Delta\sigma_k \tag{130}$$

$$W_{kl} = C_p\alpha_l\delta_{k\geq l} + C_p\beta_l\delta_{k-1\geq l} \tag{131}$$

$$G_k = R\bar{T} \tag{132}$$

$$h_{kl} = \frac{\bar{T}}{\Delta\sigma_k}\left[\alpha_k\Delta\sigma_l\delta_{k\geq l} + \beta_k\Delta\sigma_l\delta_{k+1\leq l}\right] \tag{133}$$

Here, for example, $\delta_{k\leq l}$ is 1 if $k \leq l$ is valid and 0 otherwise.
Using the following expression ,

$$\delta_t X \equiv \frac{1}{2\Delta t}\left(X^{t+\Delta t} - X^{t-\Delta t}\right) \tag{134}$$

$$\overline{X}^t \equiv \frac{1}{2}\left(X^{t+\Delta t} + X^{t-\Delta t}\right) \tag{135}$$

$$= X^{t-\Delta t} + \delta_t X \Delta t, \tag{136}$$

If we apply the semi-implicit method to the system of equations,

$$\delta_t \pi = \left(\frac{\partial \pi}{\partial t}\right)_{NG} - \mathbf{C}\cdot\overline{\mathbf{D}}^t \tag{137}$$

$$\delta_t \mathbf{D} = \left(\frac{\partial \mathbf{D}}{\partial t}\right)_{NG} - \nabla_\eta^2(\mathbf{\Phi}_S + \underline{W}\overline{\mathbf{T}}^t + \mathbf{G}\overline{\pi}^t) - \mathcal{D}_M(\mathbf{D}^{t-\Delta t} + 2\Delta t \delta_t \mathbf{D}) \tag{138}$$

$$\delta_t \mathbf{T} = \left(\frac{\partial \mathbf{T}}{\partial t}\right)_{NG} - \underline{h}\overline{\mathbf{D}}^t - \mathcal{D}_H(\mathbf{T}^{t-\Delta t} + 2\Delta t \delta_t \mathbf{T}) \tag{139}$$

So..,

$$\left\{(1+2\Delta t\mathcal{D}_H)(1+2\Delta t\mathcal{D}_M)\underline{I} - (\Delta t)^2(\underline{W}\ \underline{h} + (1+2\Delta t\mathcal{D}_M)\mathbf{G}\mathbf{C}^T)\nabla_\eta^2\right\}\overline{\mathbf{D}}^t \tag{140}$$

$$= (1+2\Delta t\mathcal{D}_H)(1+\Delta t\mathcal{D}_M)\mathbf{D}^{t-\Delta t} + \Delta t\left(\frac{\partial \mathbf{D}}{\partial t}\right)_{NG} \tag{141}$$

$$-\Delta t\nabla_\eta^2\left\{(1+2\Delta t\mathcal{D}_H)\mathbf{\Phi}_S + \underline{W}\left[(1+2\Delta t\mathcal{D}_H)\mathbf{T}^{t-\Delta t} + \Delta t\left(\frac{\partial \mathbf{T}}{\partial t}\right)_{NG}\right]\right. \tag{142}$$

$$\left. +(1+2\Delta t\mathcal{D}_H)\mathbf{G}\left[\pi^{t-\Delta t} + \Delta t\left(\frac{\partial \pi}{\partial t}\right)_{NG}\right]\right\}. \tag{143}$$

Since the spherical harmonic expansion is used, we can solve the above equation for $\overline{\mathbf{D}_n^m}^t$ with the result that it is in fact, a spherical harmonic expansion is used. After that,

$$D^{t+\Delta t} = 2\overline{\mathbf{D}}^t - D^{t-\Delta t} \tag{144}$$

and, (109), (111) to obtain the value $\hat{X}^{t+\Delta t}$ in $t+\Delta t$.

1.4.4 Time scheme properties and time step estimates

advectional equation

$$\frac{\partial X}{\partial t} = c\frac{\partial X}{\partial x} \tag{145}$$

Considering the stability of the discretization in the leap frog in Now,

$$X = X_0 \exp(ikx) \tag{146}$$

If we place the difference between

$$X^{n+1} = X^{n-1} + 2ik\Delta t X^n \tag{147}$$

That would be. Here,

$$\lambda = X^{n+1}/X^n = X^n/X^{n-1} \tag{148}$$

So,

$$\lambda^2 = 1 + 2ikc\Delta t\lambda\ . \tag{149}$$

The solution is called $kc\Delta t = p$,

$$\lambda = -ip \pm \sqrt{1-p^2} \tag{150}$$

This absolute value is

$$|\lambda| = \begin{cases} 1 & |p| \leq 1 \\ p \pm \sqrt{p^2-1} & |p| > 1 \end{cases} \tag{151}$$

and in the case of $|p| > 1$, we get $|\lambda| > 1$, and the absolute value of the solution increases exponentially with time. This indicates that the computation is unstable.

In the case of $|p| \leq 1$, however, the calculation is neutral since the value of $|\lambda| = 1$. However, there are two solutions to λ, one of which, when set to $\Delta t \to 1$, leads to $\lambda \to 1$, while the other leads to $\lambda \to -1$. This indicates a time-varying solution. This mode is called "computational mode" and is one of the problems of the leap frog method. This mode can be degraded by applying a time filter.

The condition for $|p| = kc\Delta t \leq 1$ is that given the horizontal discretization grid spacing Δx, it causes the maximum value of k to be

$$\max k = \frac{\pi}{\Delta x} \tag{152}$$

From becoming ,

$$\Delta t \leq \frac{\Delta x}{\pi c} \tag{153}$$

In the case of the spectral model, the In the case of the spectral model, the Earth's radius is defined as a by the maximum wavenumber, N,

$$\Delta t \leq \frac{a}{Nc} \tag{154}$$

This is a condition for stability.

In order to guarantee the stability of the integral, for c, the fastest advection and propagation speed can be adopted and a time step smaller than Δt, which is determined by this speed, can be used. When the semi-implicit method is not used, the propagation speed of the gravity wave ($c \sim 300m/s$) is the criterion for stability, but when the semi-implicit method is used, the advection caused by the easterly wind is usually a limiting factor. Therefore, Δt assumes that U_{max} is the maximum value of zonal wind,

$$\Delta t \leq \frac{a}{NU_{max}} \tag{155}$$

In practice, this is multiplied by a safety factor. In practice, this is multiplied by a safety factor.

1.4.5 Handling of the initiation of time integration

When starting from a suitable initial value that is not calculated by AGCM, it is not possible to give two physical quantities of time, t and $t-\Delta t$, that are consistent with the model. However, giving an inconsistent value for $t - \Delta t$ will result in a large computation mode.

So, firstly, as $X^{\Delta t/4} = X^0$, in the time step of 1/4

$$X^{\Delta t/2} = X^0 + \Delta t/2\dot{X}^{\Delta t/4} = X^0 + \Delta t/2\dot{X}^0 \tag{156}$$

and furthermore, in the time step of 1/2,

$$X^{\Delta t} = X^0 + \Delta t\dot{X}^{\Delta t/2} \tag{157}$$

And, in the original time step,

$$X^{2\Delta t} = X^0 + 2\Delta t\dot{X}^{\Delta t} \tag{158}$$

and use leap frog as usual, it prevents the occurrence of the calculation mode.

1.5 Summary of the dynamical core

In this section, we enumerate the calculations performed in the dynamical core, although they overlap with the previous descriptions.

1.5.1 Conversion of Horizontal Wind to Vorticity and Divergence `MODULE: [G2Wpush, G2Wtrans, G2Wshift, W2Gpush, W2Gtrans, W2Gshift]`

Obtain grid point values of vorticity and divergence from the grid point values of u_{ij}, v_{ij} for horizontal wind. First, we obtain the vorticity and divergence in spectral space, ζ_n^m, D_n^m,

$$\zeta_n^m = \frac{1}{I}\sum_{i=1}^{I}\sum_{j=1}^{J} \mathrm{i}m v_{ij}\cos\varphi_j {Y_n^{m*}}_{ij}\frac{w_j}{a(1-\mu_j^2)} + \frac{1}{I}\sum_{i=1}^{I}\sum_{j=1}^{J} u_{ij}\cos\varphi_j(1-\mu_j^2)\frac{\partial}{\partial\mu}{Y_n^{m*}}_{ij}\frac{w_j}{a(1-\mu_j^2)} \quad (159)$$

$$D_n^m = \frac{1}{I}\sum_{i=1}^{I}\sum_{j=1}^{J} \mathrm{i}m u_{ij}\cos\varphi_j {Y_n^{m*}}_{ij}\frac{w_j}{a(1-\mu_j^2)} - \frac{1}{I}\sum_{i=1}^{I}\sum_{j=1}^{J} v_{ij}\cos\varphi_j(1-\mu_j^2)\frac{\partial}{\partial\mu}{Y_n^{m*}}_{ij}\frac{w_j}{a(1-\mu_j^2)}; \quad (160)$$

The grid point value is calculated by

$$\zeta_{ij} = \mathcal{R}\mathbf{e}\sum_{m=-N}^{N}\sum_{n=|m|}^{N}\zeta_n^m {Y_n^m}_{ij}\ , \quad (161)$$

and so on.

1.5.2 Calculating a virtual temperature `MODULE: [VIRTMD]`

virtual Temperature T_v is ,

$$T_v = T(1+\epsilon_v q - l)\ , \quad (162)$$

However, it is $\epsilon_v = R_v/R - 1$ and R_v is the gas constant for water vapor (461 $\mathrm{Jkg^{-1}K^{-1}}$) and R is the gas constant for air (287.04 $\mathrm{Jkg^{-1}K^{-1}}$).

1.5.3 Calculating the pressure gradient term `MODULE: [PSDOT]`

The pressure gradient term $\nabla\pi = \frac{1}{p_S}\nabla p_S$ is first used to define the π_n^m

$$\pi_n^m = \frac{1}{I}\sum_{i=1}^{I}\sum_{j=1}^{J}(\ln p_S)_{ij}{Y_n^{m*}}_{ij}w_j\ , \quad (163)$$

to a spectral representation and then ,

$$\frac{1}{a\cos\varphi}\left(\frac{\partial\pi}{\partial\lambda}\right)_{ij} = \frac{1}{a\cos\varphi}\mathcal{R}\mathbf{e}\sum_{m=-N}^{N}\sum_{n=|m|}^{N} \mathrm{i}m\tilde{X}_n^m {Y_n^m}_{ij}\,, \tag{164}$$

$$\frac{1}{a}\left(\frac{\partial\pi}{\partial\varphi}\right)_{ij} = \frac{1}{a\cos\varphi}\mathcal{R}\mathbf{e}\sum_{m=-N}^{N}\sum_{n=|m|}^{N} \pi_n^m(1-\mu^2)\frac{\partial}{\partial\mu}{Y_n^m}_{ij}\,. \tag{165}$$

1.5.4 Diagnosis of vertical flow. `MODULE: [PSDOT]`

Pressure change term, and lead DC,

$$\frac{\partial\pi}{\partial t} = -\sum_{k=1}^{K}\{D_k\Delta\sigma_k + (\mathbf{v}_k\cdot\nabla\pi)\Delta B_k\} \tag{166}$$

$$\frac{(m\dot{\eta})_{k-1/2}}{p_s} = -B_{k-1/2}\frac{\partial\pi}{\partial t} - \sum_{l=k}^{K}\{D_l\Delta\sigma_l + (\mathbf{v}_l\cdot\nabla\pi)\Delta B_l\} \tag{167}$$

and its non-gravity components.

$$\left(\frac{\partial\pi}{\partial t}\right)^{NG} = -\sum_{k=1}^{K}\mathbf{v}_k\cdot\nabla\pi\Delta B_k \tag{168}$$

$$\frac{(m\dot{\eta})^{NG}_{k-1/2}}{p_s} = -B_{k-1/2}\left(\frac{\partial\pi}{\partial t}\right)^{NG} - \sum_{l=k}^{K}\mathbf{v}_l\cdot\nabla\pi\Delta B_l \tag{169}$$

1.5.5 Tendency terms due to advection `MODULE: [GRTADV, GRUADV]`

Momentum advection term `MODULE: [GRUADV]`:

$$(A_u)_k = (\zeta_k+f)v_k - \left[\frac{(m\dot{\eta})_{k-1/2}}{p_s}\frac{u_{k-1}-u_k}{\Delta\sigma_{k-1}+\Delta\sigma_k} + \frac{(m\dot{\eta})_{k+1/2}}{p_s}\frac{u_k-u_{k+1}}{\Delta\sigma_k+\Delta\sigma_{k+1}}\right] \tag{170}$$

$$-\frac{1}{a\cos\varphi}\frac{\partial\pi}{\partial\lambda}(C_pT_{v,k}\hat{\kappa} - R\bar{T}) + \mathcal{F}_x \tag{171}$$

$$(A_v)_k = -(\zeta_k+f)u_k - \left[\frac{(m\dot{\eta})_{k-1/2}}{p_s}\frac{v_{k-1}-v_k}{\Delta\sigma_{k-1}+\Delta\sigma_k} + \frac{(m\dot{\eta})_{k+1/2}}{p_s}\frac{v_k-v_{k+1}}{\Delta\sigma_k+\Delta\sigma_{k+1}}\right] \tag{172}$$

$$-\frac{1}{a}\frac{\partial\pi}{\partial\varphi}(C_pT_{v,k}\hat{\kappa} - R\bar{T}) + \mathcal{F}_y \tag{173}$$

Temperature advection term `MODULE: [GRTADV]`:

$$(uT')_k = u_k(T_k - \bar{T}) \tag{174}$$

$$(vT')_k = v_k(T_k - \bar{T}) \tag{175}$$

$$H_k = T'_k D_k - \left[\frac{(m\dot{\eta})_{k-1/2}}{p_s} \frac{\hat{T}_{k-1/2} - T_k}{\Delta\sigma_l} + \frac{(m\dot{\eta})_{k+1/2}}{p_s} \frac{T_k - \hat{T}_{k+1/2}}{\Delta\sigma_l} \right] \tag{176}$$

$$+\hat{\kappa}_k \mathbf{v}_k \cdot \nabla\pi T_{v,k} \tag{177}$$

$$-\alpha_k \sum_{l=k}^{K} (D_l \Delta\sigma_l + (\mathbf{v}_l \cdot \nabla\pi)\Delta B_l) \frac{T_{v,k}}{\Delta\sigma_k} \tag{178}$$

$$-\beta_k \sum_{l=k+1}^{K} (D_l \Delta\sigma_l + (\mathbf{v}_l \cdot \nabla\pi)\Delta B_l) \frac{T_{v,k}}{\Delta\sigma_k} \tag{179}$$

Water vapor advection term:

$$(uq)_k = u_k q_k \tag{180}$$

$$(vq)_k = v_k q_k \tag{181}$$

$$R_k = q_k D_k - \frac{1}{2} \left[\frac{(m\dot{\eta})_{k-1/2}}{p_s} \frac{q_{k-1} - q_k}{\Delta\sigma_k} + \frac{(m\dot{\eta})_{k+1/2}}{p_s} \frac{q_k - q_{k+1}}{\Delta\sigma_k} \right] \tag{182}$$

1.5.6 Transformation of prognostic variables to spectral space `MODULE: [G2Wpush, G2Wtrans, G2Wshift]`

(122) and (123).

Transform $u_{ij}^{t-\Delta t}, v_{ij}^{t-\Delta t}$ to a spectral representation of vorticity and divergence ζ_n^m, D_n^m. Furthermore, transforming the temperature $T^{t-\Delta t}$, specific humidity $q^{t-\Delta t}$, and $\pi = \ln p_S^{t-\Delta t}$ to

$$X_n^m = \frac{1}{I} \sum_{i=1}^{I} \sum_{j=1}^{J} X_{ij} {Y_n^m}^*_{ij} w_j \ , \tag{183}$$

to a spectral representation.

1.5.7 Transformation of tendency terms to spectral space `MODULE: [G2Wpush, G2Wtrans, G2Wshift]`

Tendency Term of Vorticity

$$\frac{\partial \zeta_n^m}{\partial t} = \frac{1}{I}\sum_{i=1}^{I}\sum_{j=1}^{J} \mathrm{i}m(A_v)_{ij}\cos\varphi_j {Y_n^{m*}}_{ij}\frac{w_j}{a(1-\mu_j^2)} \tag{184}$$

$$+\frac{1}{I}\sum_{i=1}^{I}\sum_{j=1}^{J}(A_u)_{ij}\cos\varphi_j(1-\mu_j^2)\frac{\partial}{\partial\mu}{Y_n^{m*}}_{ij}\frac{w_j}{a(1-\mu_j^2)} \tag{185}$$

The non-gravity wave component of the tendency term of the divergence

$$\left(\frac{\partial D_n^m}{\partial t}\right)^{NG} = \frac{1}{I}\sum_{i=1}^{I}\sum_{j=1}^{J} \mathrm{i}m(A_u)_{ij}\cos\varphi_j {Y_n^{m*}}_{ij}\frac{w_j}{a(1-\mu_j^2)} \tag{186}$$

$$-\frac{1}{I}\sum_{i=1}^{I}\sum_{j=1}^{J}(A_v)_{ij}\cos\varphi_j(1-\mu_j^2)\frac{\partial}{\partial\mu}{Y_n^{m*}}_{ij}\frac{w_j}{a(1-\mu_j^2)} \tag{187}$$

$$-\frac{n(n+1)}{a^2}\frac{1}{I}\sum_{i=1}^{I}\sum_{j=1}^{J}\hat{E}_{ij}{Y_n^{m*}}_{ij}w_j \tag{188}$$

$$\tag{189}$$

The non-gravity wave component of the tendency term of temperature

$$\left(\frac{\partial T_n^m}{\partial t}\right)^{NG} = -\frac{1}{I}\sum_{i=1}^{I}\sum_{j=1}^{J} \mathrm{i}m(uT')_{ij}\cos\varphi_j {Y_n^{m*}}_{ij}\frac{w_j}{a(1-\mu_j^2)} \tag{190}$$

$$+\frac{1}{I}\sum_{i=1}^{I}\sum_{j=1}^{J}(vT')_{ij}\cos\varphi_j(1-\mu_j^2)\frac{\partial}{\partial\mu}{Y_n^{m*}}_{ij}\frac{w_j}{a(1-\mu_j^2)} \tag{191}$$

$$+\frac{1}{I}\sum_{i=1}^{I}\sum_{j=1}^{J}\hat{H}_{ij}{Y_n^{m*}}_{ij}w_j \tag{192}$$

Tendency term of water vapor

$$\frac{\partial q_n^m}{\partial t} = -\frac{1}{I}\sum_{i=1}^{I}\sum_{j=1}^{J} \mathrm{i}m(uq)_{ij}\cos\varphi_j {Y_n^{m*}}_{ij}\frac{w_j}{a(1-\mu_j^2)} \tag{193}$$

$$+\frac{1}{I}\sum_{i=1}^{I}\sum_{j=1}^{J}(vq)_{ij}\cos\varphi_j(1-\mu_j^2)\frac{\partial}{\partial\mu}{Y_n^{m*}}_{ij}\frac{w_j}{a(1-\mu_j^2)} \tag{194}$$

$$+\frac{1}{I}\sum_{i=1}^{I}\sum_{j=1}^{J}R_{ij}{Y_n^{m*}}_{ij}w_j \tag{195}$$

1.5.8 Time integration in spectral space MODULE: [TINTGR]

Equations in matrix form

$$\left\{(1+2\Delta t\mathcal{D}_H)(1+2\Delta t\mathcal{D}_M)\underline{I}-(\Delta t)^2(\underline{W}\ \underline{h}+(1+2\Delta t\mathcal{D}_M)\mathbf{G}\mathbf{C}^T)\nabla_\sigma^2\right\}\overline{\mathbf{D}}^t \tag{196}$$

$$=(1+2\Delta t\mathcal{D}_H)(1-\Delta t\mathcal{D}_M)\mathbf{D}^{t-\Delta t}+\Delta t\left(\frac{\partial\mathbf{D}}{\partial t}\right)_{NG} \tag{197}$$

$$-\Delta t\nabla_\sigma^2\left\{(1+2\Delta t\mathcal{D}_H)\mathbf{\Phi}_S+\underline{W}\left[(1-2\Delta t\mathcal{D}_H)\mathbf{T}^{t-\Delta t}+\Delta t\left(\frac{\partial\mathbf{T}}{\partial t}\right)_{NG}\right]\right. \tag{198}$$

$$\left.+(1+2\Delta t\mathcal{D}_H)\mathbf{G}\left[\pi^{t-\Delta t}+\Delta t\left(\frac{\partial\pi}{\partial t}\right)_{NG}\right]\right\}. \tag{199}$$

Using LU decomposition, $\bar{D}$ is obtained by solving for

$$\frac{\partial\mathbf{T}}{\partial t}=\left(\frac{\partial\mathbf{T}}{\partial t}\right)_{NG}-\underline{h}\mathbf{D} \tag{200}$$

$$\frac{\partial\pi}{\partial t}=\left(\frac{\partial\pi}{\partial t}\right)_{NG}-\mathbf{C}\cdot\mathbf{D} \tag{201}$$

Calculate the value of the spectrum in $\partial\mathbf{T}/\partial t$, $\partial\pi/\partial t$ and then calculate the value of the spectrum in $t+\Delta t$ using

$$\zeta^{t+\Delta t}=\left(\zeta^{t-\Delta t}+2\Delta t\frac{\partial\zeta}{\partial t}\right)(1+2\Delta t\mathcal{D}_M)^{-1} \tag{202}$$

$$D^{t+\Delta t}=2\bar{D}-D^{t-\Delta t} \tag{203}$$

$$T^{t+\Delta t}=\left(T^{t-\Delta t}+2\Delta t\frac{\partial T}{\partial t}\right)(1+2\Delta t\mathcal{D}_H)^{-1} \tag{204}$$

$$q^{t+\Delta t}=\left(q^{t-\Delta t}+2\Delta t\frac{\partial q}{\partial t}\right)(1+2\Delta t\mathcal{D}_E)^{-1} \tag{205}$$

$$\pi^{t+\Delta t}=\pi^{t-\Delta t}+2\Delta t\frac{\partial\pi}{\partial t} \tag{206}$$

1.5.9 Transformation of prognostic variables to grid point Values MODULE: [W2Gpush, W2Gtrans, W2Gshift]

Obtain grid values of horizontal wind speed from the spectral values of vorticity and divergence (ζ_n^m, D_n^m) u_{ij}, v_{ij}.

$$u_{ij}=\frac{1}{\cos\varphi_j}\mathcal{R}\mathbf{e}\sum_{m=-N}^{N}\sum_{\substack{n=|m|\\ n\neq 0}}^{N}\left\{\frac{a}{n(n+1)}\zeta_n^m(1-\mu^2)\frac{\partial}{\partial\mu}Y_n^m{}_{ij}-\frac{\mathrm{i}ma}{n(n+1)}D_n^mY_n^m{}_{ij}\right\} \tag{207}$$

$$v_{ij} = \frac{1}{\cos\varphi_j}\mathcal{R}\mathbf{e}\sum_{m=-N}^{N}\sum_{\substack{n=|m|\\ n\neq 0}}^{N}\left\{-\frac{\mathrm{i}ma}{n(n+1)}\zeta_n^m Y_n^m{}_{ij} - \frac{a}{n(n+1)}\tilde{D}_n^m(1-\mu^2)\frac{\partial}{\partial\mu}Y_n^m{}_{ij}\right\} \tag{208}$$

Furthermore,

$$T_{ij} = \mathcal{R}\mathbf{e}\sum_{m=-N}^{N}\sum_{n=|m|}^{N} T_n^m Y_n^m{}_{ij}\ , \tag{209}$$

T_{ij}, π_{ij}, q_{ij}, and so on,

$$p_{S\,ij} = \exp\pi_{ij} \tag{210}$$

to calculate.

1.5.10 Diffusion Correction along pressure level `MODULE: [CORDIF]`

The horizontal diffusion is applied on the surface of $\eta-$plane, but it can cause problems in large slopes, such as transporting water vapor uphill and causing false precipitation at the top of a mountain. To mitigate this problem, corrections have been made for T, q, l to make the diffusion closer to that of the p surface, e.g., for T, q, l.

$$\mathcal{D}_p(T) = (-1)^{N_D/2}K\nabla_p^{N_D}T \simeq (-1)^{N_D/2}K\nabla_\eta^{N_D}T - \frac{\partial\sigma}{\partial p}(-1)^{N_D/2}K\nabla_\eta^{N_D}p\cdot\frac{\partial T}{\partial\sigma} \tag{211}$$

$$= (-1)^{N_D/2}K\nabla_\eta^{N_D}T - (-1)^{N_D/2}K\nabla_\eta^{N_D}\pi\cdot\sigma\frac{\partial T}{\partial\sigma} \tag{212}$$

$$= \mathcal{D}(T) - \mathcal{D}(\pi)\sigma\frac{\partial T}{\partial\sigma} \tag{213}$$

So,

$$T_k \leftarrow T_k - 2\Delta t\sigma_k\frac{T_{k+1}-T_{k-1}}{\sigma_{k+1}-\sigma_{k-1}}\mathcal{D}(\pi) \tag{214}$$

and so on. In $\mathcal{D}(\pi)$, the spectral value of π is converted to a grid by multiplying the spectral value of π_n^m by the spectral representation of the diffusion coefficient.

1.5.11 Frictional heat associated with diffusion. `MODULE: [CORDIF]`

Frictional heat from diffusion is ,

$$Q_{DIF} = -\left(u_{ij}\mathcal{D}(u)_{ij} + v_{ij}\mathcal{D}(v)_{ij}\right) \tag{215}$$

It is estimated that Therefore,

$$T_k \leftarrow T_k - \frac{2\Delta t}{C_p}\left(u_{ij}\mathcal{D}(u)_{ij} + v_{ij}\mathcal{D}(v)_{ij}\right) \tag{216}$$

1.5.12 Horizontal Diffusion and Rayleigh Friction `MODULE: [DSETDF]`

The coefficients of horizontal diffusion can be expressed spectrally,

$$\mathcal{D}_M{}_n^m = K_M \left[\left(\frac{n(n+1)}{a^2} \right)^{N_D/2} - \left(\frac{2}{a^2} \right)^{N_D/2} \right] + K_R \tag{217}$$

$$\mathcal{D}_H{}_n^m = K_M \left(\frac{n(n+1)}{a^2} \right)^{N_D/2} \tag{218}$$

$$\mathcal{D}_E{}_n^m = K_E \left(\frac{n(n+1)}{a^2} \right)^{N_D/2} \tag{219}$$

K_R is the Rayleigh coefficient of friction. The Rayleigh coefficient of friction is

$$K_R = K_R^0 \left[1 + \tanh \left(\frac{z - z_R}{H_R} \right) \right] \tag{220}$$

However, the profile is given in the same way as However,

$$z = -H \ln \sigma \tag{221}$$

The results are approximate to those of $K_R^0 = (30day)^{-1}$ and $z_R = -H \ln \sigma_{top}$. The standard values are $K_R^0 = (30day)^{-1}$, $z_R = -H \ln \sigma_{top}$ (σ_{top}: top level of the model), $H = 8000$ m, and $H_R = 7000$ m.

1.5.13 Time Filter `MODULE: [DADVNC]`

To reduce numerical mode associated with leap frog scheme, time filter is applied every time step. MIORC6 used modified Asselin time filter (Williams, 2009), which is updated version of Asselin(1972) used previous version of MIROC. Although Asselin time filter attenuate high frequency physical mode, bringing low accuracy of leap frog scheme, current time filter succeeded in suppressing it.

Modified Asselin filter is expressed as following equation

$$\bar{\bar{X}}^t = \bar{X}^t + \nu\alpha[\bar{\bar{X}}^{t-\Delta t} - 2\bar{X}^t + X^{t+\Delta t}] \tag{222}$$

$$\bar{X}^{t+\Delta t} = X^{t+\Delta t} + \nu(1-\alpha)[\bar{\bar{X}}^{t-\Delta t} - 2\bar{X}^t + X^{t+\Delta t}] \tag{223}$$

where bar indicates time filter. The parameters set to $\nu = 0.05$, $\alpha = 0.5$. Assuming $\alpha = 1$, modified Asselin filter is same as Asselin filter.

In the model,

$$\bar{\bar{X}}^{t*} = (1 - \nu\alpha)^{-1}[(1 - 2\nu\alpha)\bar{X}^t + \nu\alpha\bar{\bar{X}}^{t-\Delta t}] \tag{224}$$

is firstly calculated at `MODULE: [DADVNC]` where transformation of prognostic variableto grid point values. And then, $X^{t-\Delta t} - 2X^t$ is stored. When the $X^{t+\Delta t}$ is obtained later, time filter conduct at `MODULE [TFILT]`,

$$\bar{\bar{X}}^t = (1 - \nu\alpha)\bar{\bar{X}}^{t*} + \nu\alpha X^{t+\Delta t} \tag{225}$$

$$\bar{X}^{t+\Delta t} = X^{t+\Delta t} + \nu(1 - \alpha)[\bar{\bar{X}}^{t-\Delta t} - 2\bar{X}^t + X^{t+\Delta t}] \tag{226}$$

1.5.14 Correction for conservation of mass `MODULE: [FIXMAS, MASFIX]`

In the spectral method, the global integral of $\pi = \ln p_S$ is preserved with rounding errors removed, but the preservation of the mass, i.e. the global integral of p_S is not guaranteed. Moreover, a wavenumber break in the spectra sometimes results in negative values of the water vapor grid points. For this reason, we perform a correction to preserve the masses of dry air, water vapor, and cloud water, and to remove the regions with negative water vapor content.

Before entering dynamical calculations, `MODULE:[FIXMAS]`, the global integrals of water vapor and cloud water are calculated for M_q, M_l.

$$M_q^0 = \sum_{ijk} q p_S \Delta\lambda_i w_j \Delta\sigma_k \tag{227}$$

$$M_l^0 = \sum_{ijk} l p_S \Delta\lambda_i w_j \Delta\sigma_k \tag{228}$$

In the first step of the calculation, the dry mass M_d is calculated and stored.

$$M_d^0 = \sum_{ijk} (1 - q - l) p_S \Delta\lambda_i w_j \Delta\sigma_k \tag{229}$$

After exiting dynamical calculation, `MODULE:[MASFIX]`, the following procedure is followed.

First, negative water vapor is removed by dividing the water vapor from the grid points immediately below the grid points. Suppose that $q_k < 0$ is used,

$$q'_k = 0 \tag{230}$$

$$q'_{k-1} = q_{k-1} + \frac{\Delta p_k}{\Delta p_{k-1}} q_k \tag{231}$$

However, this should only be done if it is $q_{k-1}' \geq 0$.

Next, set the value to zero for the grid points not removed by the above procedure.

3. calculate the global integral value of M_q and multiply the global water vapor content by a fixed percentage so that it is the same as that of M_q^0.

$$q'' = \frac{M_q^0}{M_q} q' \tag{232}$$

4. correct for dry air mass Likewise calculate M_d,

$$p_S'' = \frac{M_d^0}{M_d} p_S \tag{233}$$

1.6 Cumulus scheme

1.6.1 Outline of cumulus scheme

The Chikira scheme (Chikira and Sugiyama 2010) has been adopted since version 5 of MIROC. It represents updrafts, downdrafts, their detrainment and compensating downward motion over the surrounding area as well as microphysical processes associated with updrafts and downdrafts.

The updraft is based on an entraining plume model, where the mass flux increases upward due to lateral entrainment. The detrainment occurs only at the cloud top which is defined as the neutral buoyancy level of the updraft air parcel. The lateral entrainment rate is formulated in terms of buoyancy and vertical velocity of the air parcel at each level following Gregory (2001). The momentum transport is formulated following Gregory et al. (1997).

The cloud base mass fluxes are determined by the prognostic convective kinetic energy closure proposed by Arakawa and Xu (1990) and Xu (1991, 1993), which was adopted in the prognostic Arakawa–Schubert scheme (Randall and Pan 1993; Pan 1995; Randall et al. 1997; Pan and Randall 1998). The convective kinetic energy increases by buoancy and decreases by dissipation.

The cloud types are spectrally represented according to the updraft vertical velocity at the cloud base. Larger (smaller) vertical velocities give smaller (larger) entrainment rates which result in higher (lower) cloud tops. The cloud base is diagnosed as the lifting condensation level of the air parcel at the lowest model layer.

The scheme has a simple downdraft model, where a part of the precipitation caused by the updrafts evaporates and forms the cold air which enters into the downdrafts. The detrainment of the downdraft mass fluxes occurs at the neutral buoyancy level and near the surface.

The interaction of the updrafs and downdrafts with the surrounding environment is formulated following Arakawa and Schubert (1974). The areal fractions of the updrafts and downdrafts are assumed to be sufficiently small and the grid-mean prognostic variables are supposed to be the same as those over the environmental area, which are changed by the detrainment of the updrafts and downdrafts, the compensating subsidence and the evaporation and sublimation of the precipitation associated with the updrafts.

The input variables to this scheme are temperature T, specific humidity q, cloud liquid water q_l, cloud ice q_i, zonal wind u, meridional wind v, all tracers including aerosols and greenhouse gases, height z, pressure p, and cloud cover C. The scheme gives the tendencies of T, q_v, q_l, q_i, u, v, C and all the tracers. The vertical profiles of the rainfall and snowfall fluxes, cloud liquid water, cloud ice and cloud fraction associated with the updrafts are also output as diagnostic variables.

The procedure of the calculations is given as follows along with the names of the subroutines.

1. calculation of cloud base `CUMBAS`.
2. calculation of in-cloud properties `CUMUP`.
3. calculation of cloud base mass flux `CUMBMX`.
4. calculation of cloud mass flux, detrainment, and precipitation `CUMFLX`.
5. diagnosis of cloud water and cloud cover by cumulus `CUMCLD`.
6. calculation of tendencies by detrainment `CLDDET`.
7. calculation of freezing, melting, evaporation, sublimation, and downdraft mass flux `CUMDWN`.

8. calculation of tendencies by compensating subsidence `CLDSBH`.
9. calculation of cumulus momentum transport `CUMCMT`.
10. calculation of tracer updraft `CUMUPR`.
11. calculation of tracer downdraft `CUMDNR`.
12. calculation of tracer subsidence `CUMSBR`.
13. fixing tracer mass `CUMFXR` .

1.6.2 Interaction between cumulus ensemble and large-scale environment

Following Arakawa and Schubert (1974), the equations for tendencies of the grid-mean variables are written as

$$\frac{\partial \bar{h}}{\partial t} = M\frac{\partial \bar{h}}{\partial z} + \sum_j D_j \left[h_j(z_{T,j}) - \bar{h}\right], \tag{234}$$

$$\frac{\partial \bar{q}}{\partial t} = M\frac{\partial \bar{q}}{\partial z} + \sum_j D_j \left[q_j(z_{T,j}) - \bar{q}\right], \tag{235}$$

where M, D, h denote total mass flux, detrainment mass flux and moist static energy. q is a substitute for q_v, q_l and q_i and any tracers which are calculated in the same way. z_T is the height of the updraft. The hats indicate in-cloud properties, the overbars grid-mean. The subscripts j are an index for the updraft types.

The total mass flux M and detrainment D are defined as

$$M(z) = \sum_j M_{u,j} + M_d\,, \tag{236}$$

$$D_j(z) = M_{u,j}(z_{T,j})\delta(z - z_{T,j}) \tag{237}$$

respectively, where M_u and M_d denote mass fluxes of updraft and downdraft respectively. The updraft mass flux is formulated as

$$M_{u,j}(z) = M_{B,j}\,\eta_j(z) \tag{238}$$

where M_B and η are the updraft mass flux at its cloud base and normalized mass flux.

1.6.3 Cloud base

The cloud base is determined as the lifting condensation level of the air at the lowest model layer. It is defined as the smallest z which satisfies

$$\bar{q}_t(z_1) \geq {\bar{q}_v}^* + \frac{\gamma}{L_v(1+\gamma)}\left[\bar{h}(z_1) - \bar{h}^*(z)\right], \tag{239}$$

where q_t denotes total water, L_v the latent heat of vaporization, z_1 the height of the lowest model layer at the full level and

$$\gamma \equiv \frac{L_v}{C_p}\left(\frac{\partial \bar{q}^*}{\partial \bar{T}}\right)_{\bar{p}}. \tag{240}$$

C_p denotes the specific heat of dry air at constant pressure and the stars indicate saturation values.

The normalized mass flux below the cloud base is given by $\eta = (z/z_B)^{1/2}$ for all of the updraft types where z_B denotes the cloud base height.

1.6.4 Updraft velocity and entrainment rate

The entrainment rate is defined by

$$\epsilon = \frac{1}{M_u}\frac{\partial M_u}{\partial z} \tag{241}$$

and allowed to vary vertically. Based on the formulation of Gregory (2001), the updraft velocity is calculated by

$$\frac{1}{2}\frac{\partial \hat{w}^2}{\partial z} = aB - \epsilon \hat{w}^2 \tag{242}$$

where w and B are the vertical velocity and the buoyancy of updraft air parcel respectively. a is a dimensionless constant parameter ranging from 0 to 1 and represents a ratio of buoyancy force used to accelerate the updraft velocity. The hats indicate the values of the updraft. The second term on the right-hand side represents reduction in the upward momentum of the air parcel through the entrainment. Here and hereafter, the equation number corresponds to that in Chikira and Sugiyama (2010).

Then it is assumed that

$$\epsilon \hat{w}^2 \simeq C_\epsilon aB, \tag{243}$$

where C_ϵ is a dimensionless constant parameter ranging from 0 to 1. This formulation denotes that a certain fraction of the buoyancy-generated energy is reduced by the entrainment, which is identical to the fraction used to accelerate the entrained air to the updraft velocity. Thus, the entrainment rate is written as

$$\epsilon = C_\epsilon \frac{aB}{\hat{w}^2}. \tag{244}$$

Eqs. (1) and (2) lead to

$$\frac{1}{2}\frac{\partial \hat{w}^2}{\partial z} = a(1 - C_\epsilon)B \tag{245}$$

which shows that $\hat{w}$ is continuously accelerated upward when buoyancy is positive. Many CRM and LES results show, however, that updraft velocity is often reduced if the parcel approaches its cloud top. For this reason, adding an additional term, we use

$$\frac{1}{2}\frac{\partial \hat{w}^2}{\partial z} = a(1 - C_\epsilon)B - \frac{1}{z_0}\frac{\hat{w}^2}{2} \tag{246}$$

where the last term denotes that the energy of the updraft velocity is relaxed to zero with a height scale z_0. Eq. (4) is discretized as

$$\frac{1}{2}\frac{\hat{w}^2_{k+1/2} - \hat{w}^2_{k-1/2}}{\Delta z_k} = a(1 - C_\epsilon)B_k - \frac{1}{z_0}\frac{\hat{w}^2_{k+1/2}}{2} \tag{247}$$

where k is an index of full levels and $k + 1/2$ and $k - 1/2$ indicate the upper and lower sides of the half levels. Δz is the depth of the model layer. Note that the equation is solved for $\hat{w}^2$ rather than $\hat{w}$.

The buoyancy of the cloud air parcel is determined by

$$B = \frac{g}{\bar{T}}(\hat{T}_v - \bar{T}_v) \tag{248}$$

$$\simeq g\left\{\frac{\hat{h} - \bar{h}^*}{C_p\bar{T}(1+\gamma)} + \varepsilon(\hat{q}_v - \bar{q}_v) - [(\hat{q}_l + \hat{q}_i) - (\bar{q}_l + \bar{q}_i)]\right\} \tag{249}$$

where g and T_v denote gravity and virtual temperature respectively. $\varepsilon = R_v/R_d - 1$ where R_v and R_d are the gas constants for water vapor and dry air respectively.

$\hat{w}$, B and ϵ are calculated for each of the updraft types separately, but we omit the subscript j for convenience.

1.6.5 Normalized mass flux and updraft properties

The properties of the updraft are determined by

$$\frac{\partial \eta \hat{h}}{\partial z} = \epsilon\eta\bar{h} + Q_i, \tag{250}$$

$$\frac{\partial \eta \hat{q}_t}{\partial z} = \epsilon\eta\bar{q}_t - P \tag{251}$$

and

$$\frac{\partial \eta}{\partial z} = \epsilon\eta, \tag{252}$$

where Q_i and P denote heating by liquid-ice transition and precipitation respectively. All the other variables such as temperature, specific humidity, and liquid and ice cloud water are computed from these quantities. Tracers are calculated by a method identical to that for $\hat{q}_t$.

Equation (7) leads to

$$\frac{\partial \ln \eta}{\partial z} = \epsilon. \tag{253}$$

Then, η and ϵ are discretized as

$$\frac{\ln \eta_{k+1/2} - \ln \eta_{k-1/2}}{\Delta z_k} = \epsilon_k. \tag{254}$$

Note that this discrete form leads to an exact solution if ϵ is vertically constant. Also, η is finite as far as ϵ is. For ϵ_k, a maximum value of $4 \times 10^{-3} m^{-1}$ is applied.

Equations (5) and (6) are written as

$$\frac{\partial \eta \hat{h}}{\partial z} = E\bar{h} + Q_i, \tag{255}$$

$$\frac{\partial \eta \hat{q}_t}{\partial z} = E\bar{q}_t - P \tag{256}$$

respectivuly, where $E = \epsilon\eta$. These equations are discretized as

$$\frac{\eta_{k+1/2}\hat{h}_{k+1/2} - \eta_{k-1/2}\hat{h}_{k-1/2}}{\Delta z_k} = E_k\bar{h}_k + Q_{i,k} \tag{257}$$

$$\frac{\eta_{k+1/2}\hat{q}_{t,k+1/2} - \eta_{k-1/2}\hat{q}_{t,k-1/2}}{\Delta z_k} = E_k\bar{q}_{t,k} - P_k \tag{258}$$

Considering the relation that $\partial\eta/\partial z = \epsilon\eta$, we descretize E_k as

$$E_k = \frac{\eta_{k+1/2} - \eta_{k-1/2}}{\Delta z_k} \tag{259}$$

Note that conservation of mass, energy, and water is guaranteed with Eqs. (A1)–(A4). This set of equations leads to exact solutions of $\hat{h}$ under the special case that ϵ and $\bar{h}$ are vertically constant and Q_i is zero. From Eqs. (A1), (A2), and (A4), assuming Q_i is zero,

$$\hat{h}_{k+1/2} = e^{-\epsilon_k \Delta z_k}\hat{h}_{k-1/2} + (1 - e^{-\epsilon_k \Delta z_k})\bar{h}_k, \tag{260}$$

which shows that $\hat{h}_{k+1/2}$ is a linear interpolation between $\hat{h}_{k-1/2}$ and $\bar{h}_k$. Thus, the stability of $\hat{h}$ is guaranteed. The same property applies to $\hat{q}_t$ as well, if P is zero.

These calculations are made for each of the updraft types separately, but we omit the subscript j for convenience.

1.6.6 Spectral representation

Following the spirit of the Arakawa–Schubert scheme, updraft types are spectrally represented. Different values of cloud-base updraft velocities are given from the minimum to the maximum values with a fixed interval. The minimum and maximum values are set to 0.1 and 1.4 ms^{-1}, with an interval of 0.1 ms^{-1}.

Then, the updraft properties are calculated upward with Eqs. (2), (4), (5), (6), and (7). This upward calculation continues even if the buoyancy is negative as long as the updraft velocity is positive. If the velocity becomes negative at some level, the air parcel detrains at the neutral buoyancy level which is below and closest to the level. That is, the scheme automatically judges whether the rising parcel can penetrate the negative buoyancy layers when there is a positive buoyancy layer above. The effect of the convective inhibition (CIN) near cloud base is also represented by this method. Note, however, that an effect of overshooting above cloud top is not represented for simplicity (i.e., detrainment never occurs above cloud top).

1.6.7 Cloud-base mass flux

The cloud-base mass flux is determined with the prognostic convective kinetic energy closure proposed by Arakawa and Xu (1990). That is, the cloud kinetic energy for each of the updraft types is explicitly predicted by

$$\frac{\partial K}{\partial t} = AM_B - \frac{K}{\tau_p}\,, \tag{261}$$

where K and A are the cloud kinetic energy and cloud work function respectively, and τ_p denotes a time scale of dissipation. The cloud work function A is defined as

$$A \equiv \int_{z_B}^{z_T} B\eta\, dz\,. \tag{262}$$

The cloud kinetic energy is linked with M_B by

$$K = \alpha M_B^2. \tag{263}$$

The cloud-base mass flux is then solved for each of the updraft types.

1.6.8 Microphysics

The method to obtain temperature and specific humidity of in-cloud air from moist static energy is identical to that in Arakawa and Schubert (1974). The ratio of precipitation to the total amount of condensates generated from cloud base to a given height z is formulated as

$$F_p(z) = 1 - e^{-(z-z_B-z_0)/z_p}, \tag{264}$$

where z_0 and z_p are tuning parameters.

The ratio of cloud ice to cloud condensate is determined simply by a linear function of temperature,

$$F_i(T) = \begin{cases} 1 & T \leq T_1 \\ (T_2 - T)/(T_2 - T_1) & T_1 < T < T_2 \\ 0 & T \geq T_2 \end{cases} \tag{265}$$

where T_1 and T_2 are set to 258.15 and 273.15 K. The ratio of snowfall to precipitation is also determined by this function.

From the conservation of condensate static energy, $C_pT + gz + L_vq - L_iq_i$ where L_i is the latent heat of fusion, for a cloud parcel, Q_i in Eq. (5) is written as

$$Q_i = L_i \left(\frac{\partial \eta \hat{q}_i}{\partial z} - \epsilon \eta \bar{q}_i \right) \tag{266}$$

and discretized as

$$Q_{ik} = L_i \left(\frac{\eta_{k+1/2}\hat{q}_{i,k+1/2} - \eta_{k-1/2}\hat{q}_{i,k-1/2}}{\Delta z_k} - E_k \bar{q}_{i,k} \right) \tag{267}$$

Strictly, the ratio of the cloud ice to the cloud condensate should be recalculated after the modification of temperature by Q_i and the iterations of the calculation are required; however, it is omitted for simplicity.

Melting and freezing of precipitation occurs depending on wet-bulb temperature of large-scale environment and cumulus mass flux.

1.6.9 Evaporation, sublimation and downdraft

A part of precipitation is evaporated at each level as

$$E_v = a_e(\bar{q}_w - \bar{q}) \left(\frac{P}{V_T} \right), \tag{268}$$

where E_v, q_w and V_T are the mass of evaporation per a unit volume and time, wet-bulb saturated specific humidity and terminal velocity of precipitation respectively a_e is a constant. Downdraft mass flux M_d is generated as

$$\frac{\partial M_d}{\partial z} = -b_e \bar{\rho}(\bar{T}_w - \bar{T})P, \tag{269}$$

where ρ and T_w are density and wet-bulb temperature, respectively; b_e is a constant. Properties of downdraft air are determined by budget equations and the detrainment occurs at neutral buoyancy level and below cloud base.

If the precipitation is composed of both rain and snow, the rain (snow) is evaporated (sublimated) in the same ratio as the ratio of rain (snow) to the total precipitation when the precipitation evaporates to produce downdrafts.

1.6.10 Cloudiness

Fractional cloudiness of the updrafts C_u used in the radiation scheme is diagnosed by

$$C_u = \frac{C_{\max} - C_{\min}}{\ln M_{\max} - \ln M_{\min}} (\ln \sum_j M_{u,j} - \ln M_{\min}) + C_{\min}, \tag{270}$$

where $C_{\max}$, $C_{\min}$, $M_{\max}$, $M_{\min}$ are the maximum and minimum values of the cloudiness and cumulus mass flux respectively.

The grid mean liquid cloud mixing ratio in the updrafts is given by

$$l_c = \frac{\beta C_u}{M} \sum_j \hat{q}_{l,j} M_{u,j}, \tag{271}$$

where β is a dimensionless constant. The grid mean ice cloud mixing ratio is determined similarly.

1.6.11 Cumulus Momentum Transport

Following Gregory et al. (1997), the zonal and meridional velocities of the updrafts are calculated as

$$\frac{\partial \eta \hat{u}}{\partial z} = \epsilon \eta \bar{u} + C_m \eta \frac{\partial \bar{u}}{\partial z}, \tag{272}$$

where C_m is a constant from 0 to 1 representing the effect of pressure. This equation can be rewitten as

$$\frac{\partial \eta \hat{u}}{\partial z} = (1 - C_m) \epsilon \eta \bar{u} + C_m \frac{\partial \eta \bar{u}}{\partial z}, \tag{273}$$

and is discretized as

$$\frac{\eta_{k+1/2} \hat{u}_{k+1/2} - \eta_{k-1/2} \hat{u}_{k-1/2}}{\Delta z_k} = (1 - C_m) E_k \bar{u}_k + C_m \frac{\eta_{k+1/2} \bar{u}_{k+1/2} - \eta_{k-1/2} \bar{u}_{k-1/2}}{\Delta z_k}. \tag{274}$$

The horizontal velocities of the downdrafts are calculated similarly. The tendencies of zonal and meridional velocities by the cumulus momentum transport (CMT) are calculated as

$$\left(\frac{\partial u}{\partial t} \right)_{\mathrm{CMT},k} = -g \frac{(\rho \overline{u'w'})_{k+1/2} - (\rho \overline{u'w'})_{k-1/2}}{\Delta p_k}, \tag{275}$$

$$\left(\frac{\partial v}{\partial t} \right)_{\mathrm{CMT},k} = -g \frac{(\rho \overline{v'w'})_{k+1/2} - (\rho \overline{v'w'})_{k-1/2}}{\Delta p_k} \tag{276}$$

respectively, where $\rho \overline{u'w'}$ and $\rho \overline{v'w'}$ are total zonal and meridional momentum fluxes respectively and $\Delta p_k = p_k - p_{k+1}$.

- 1. ??
- 2. ??
- 3. ??
  - 3.1. ??
  - 3.2. ??
  - 3.3. ??
  - 3.4. ??
- 4. ??
  - 4.1. ??
- 5. ??

2　浅い積雲対流のパラメタリゼーション

2.1　1. 浅い積雲の概要

浅い積雲は熱帯や亜熱帯で対流雲の中では最も頻度が多く，大気放射によるエネルギー収支を介して気候に与える影響が重要視されている。浅い積雲は境界層の大気を自由大気へ輸送する役割を担っており，降水を伴わないことが多く，深い対流のように降水性の下降流が地表まで到達しないことが特徴である．

浅い積雲対流が発生する境界層の鉛直構造について簡単に説明する．地表面が太陽光によって温められた，または上方から冷たい空気が流れ込んだとき，大気の最下層では対流不安定のエネルギーが乱流によって散逸し，海面からおよそ 600m から 800m の厚さで温度や水がほぼ鉛直一様に分布する混合層を形成する．混合層の上端には弱い安定成層の遷移層があり，ここに対流不安定による上昇流が凝結を始める高度 (lifting condensation level, LCL) が位置する．これより上では温度は湿潤断熱減率に従って変化し，上昇流は雲として観察される．さらに上昇して上向きの浮力を受けるようになる高度 (level of free convection, LFC) より上まで達する雲は周囲の空気と混合しながら成長を続ける．この対流雲の成長は自由大気下端の温度逆転層で制限され，地表から 2km 程度に雲頂を持つことが多い．

浅い積雲のパラメタリゼーションは気候の再現性や将来予測へ及ぼす影響の評価のため MIROC5 から導入された．当該のパッケージ pshcn.F は PSHCN と DISTANCE のサブルーチンから成る．PSHCN の主な入力変数は気温，水蒸気量，雲水量，雲氷量である．浅い積雲対流の鉛直輸送に応じた液水温位，総水量，雲氷量，水平風速を予報し，さらに雲量および降水量を診断する．DISTANCE は PSHCN 内部で実行され，浅い対流の浮力上昇および環境場との混合の程度を計算するものである．様々な物理過程の中で浅い積雲が発生する条件の判定には深い対流のパラメタリゼーション (CUMULUS) で診断された変数の値を参照するため，PSHCN および DISTANCE は CUMULUS の後に雲量の診断を経て実行される．また，降水を陸面や海洋のモデルで参照するため，地表面過程 (SURFCE) よりも前に実行する必要がある．

2.2 2. 雲モデルの基本

格子内の雲は主に Bretherton et al. (2004) や Park and Bretherton (2009) で考案された枠組みを元にモデル化する．このスキームではシンプルな雲のプルームモデルを採用し上昇流による保存量の鉛直輸送および降水を計算する．一つの水平格子内の浅い積雲の集団を単一の上昇流プルームで表現し，これが周囲の環境と水平方向の混合 (エントレインメント・デトレインメント) を起こすものとする．この上昇流の鉛直輸送のフラックスを以下の形で仮定する．

$$\rho\overline{w'\psi'} \approx M_u(\psi_u - \overline{\psi}) \tag{277}$$

ただし $M_u = \rho_u \sigma_u w_u$ は上昇流のマスフラックス，ψ_u は積雲対流で運ばれる何らかの保存量の上昇流内の代表値，$\overline{\psi}$ は同じ保存量の環境場での代表値を表す．質量と保存量それぞれのフラックスの診断式は

$$\frac{\partial M_u}{\partial z} = E - D \tag{278}$$

$$\frac{\partial}{\partial z}(\psi_u M_u) = X_\psi + S_\psi M_u \tag{279}$$

のように書ける．ただし X_ψ は環境場との水平方向の混合，S_ψ はソース項，E および D はエントレインメント割合で,

$$E = \tilde{E} M_u \tag{280}$$

$$D = \tilde{D} M_u \tag{281}$$

として質量フラックスに対する比の形で記述する．$\overline{\psi}$ を格子平均値で代表させ，水平混合の項を $X_\psi = E\overline{\psi} - D\psi_u$ でパラメタライズすることで，上記のフラックス診断式は

$$\frac{\partial M_u}{\partial z} = M_u(\tilde{E} - \tilde{D}) \tag{282}$$

$$\frac{\partial \psi_u}{\partial z} = \tilde{E}(\overline{\psi} - \psi_u) + S_\psi \tag{283}$$

となり ε と δ の二つのパラメーターについてのクロージャー問題に帰着する．これを雲底のでの境界条件とともに解くことで M_u と ψ_u の鉛直プロファイルを求める．

2.3 3. PSHCN での計算

計算手順の概略は以下の通り． - 温度 T，比湿 q，雲水量 l，雲氷量 q_i の入力から液滴温位 θ_l と総水量 q_t を診断する- 雲底における上昇流のマスフラックス M_u を診断する - 雲底高度を診断する - 浅い積雲の有無を診断する - 上昇流内での M_u，θ_l，q_t、水平風速 u、v の鉛直プロファイルを診断する- θ_l，q_t，q_i，u，v，液滴温度 T_l を予報する- T_l と q_t から T，q，l を診断する

2.3.1 3.1. 下部境界条件：雲底での質量フラックスの診断

雲底での質量フラックスは，境界層内部の乱流運動エネルギーと境界層上部の対流抑制（convective inhibition, CIN）に依存するように定式化する．まず浅い積雲が存在する層全体で上昇流速の鉛直分布について

$$\frac{1}{2}\frac{\partial}{\partial z}w_u^2 = aB_u - b\tilde{E}w_u^2 \tag{284}$$

が成り立つものとする．B_u は浮力，a, b は経験的な定数であり，右辺第一項は浮力による加速，第二項はエントレインメントによるドラッグを意味する．LFC より下ではエントレインメントは起こらないものと仮定し，上の式を雲底から LFC まで積分することにより，上昇プルームが混合層から LFC まで達するための雲底での上昇流速の臨界値 w_c が次のように求められる

$$w_c = \sqrt{2a(CIN)}. \tag{285}$$

この臨界値 w_c を超えた上昇流が雲底から入ってくることになる．CIN の導出は Bretherton et al. (2004) Appendix C にならい，

$$CIN = [B_u(p_{base}) + B_u(p_{LCL})]\frac{p_{LCL} - p_{base}}{g(\rho_{LCL} + \rho_{base})} + B_u(p_{LCL})\frac{p_{LFC} - p_{LCL}}{g(\rho_{LFC} + \rho_{LCL})} \tag{286}$$

とする．

次に雲底での鉛直流についての情報を得るため，w の分布は $k_f e_{avg}$ に等しい分散を持つガウス分布

$$f(w) = \frac{1}{2\pi k_f e_{avg}} \exp\left[-\frac{w^2}{2k_f e_{avg}}\right] \tag{287}$$

であると仮定する．e_{avg} は MIROC の乱流・鉛直拡散スキームで診断された平均の乱流運動エネルギー，k_f は乱流運動エネルギーが鉛直と水平の各方向に分配される比率で，ここでは経験的に 0.5 に固定されている．

臨界値 w_c を超える全ての範囲で上記の分布に従う上昇流速の期待値を取ることで，雲底における質量フラックス $M_{u,base}$ を次のように診断する

$$M_{u,base} = \overline{\rho_{base}} \int_{w_c}^{\infty} w f(w) dw \tag{288}$$

$$= \overline{\rho_{base}} \sqrt{\frac{k_f e_{avg}}{2\pi}} \exp\left[-\frac{w_c^2}{2k_f e_{avg}}\right]. \tag{289}$$

ここで $\overline{\rho_{base}}$ は自由対流高度での大気の密度である．この質量フラックスは境界層の乱流運動エネルギーが大きいほど大きく，CIN が大きいほど小さくなるようになっている．

2.3.2 3.2. 雲底高度の診断

雲底高度は境界層上端と LCL の間に設定することになっており，CIN が大きいほど雲底が低くなる形を取る．境界層の上端は相対湿度の鉛直勾配が最大になる高度として診断し，これと LCL とのうち高い方を z_{Hi}，低い方を z_{Lo} とすれば，雲底高度 z_{base} は

$$z_{base} = z_{Hi} - (z_{Hi} - z_{Lo})\frac{CIN - CIN_{Lo}}{CIN_{Hi} - CIN_{Lo}} \tag{290}$$

とする．ただし CIN_{Hi}，CIN_{Lo} はそれぞれ CIN の典型的な値に対して $CIN_{Lo} \leq CIN \leq CIN_{Hi}$ となるような定数である．

2.3.3 3.3. 浅い積雲の有無の判定

各水平格子について，以下の条件によって浅い積雲対流が発生するかどうかを判定する．- 推定逆転層強度 (estimated nversion strength, EIS) がある閾値を超える場合は，層積雲が卓越する環境場であると判断し，浅い積雲は発生させない．この基準は，気候モデルの鉛直解像度では境界層の上にできる薄く強い逆転層を十分に表現できず，CIN の過小評価により浅い積雲が過大に表現される問題があるため導入されている．EIS は

$$EIS = \theta_{700} - \theta_0 - \Gamma_m^{850}(z_{700} - LCL) \tag{291}$$

で求める．ただし θ_{700}，θ_0 はそれぞれ 700hPa と地表面での温位，Γ_m^{850} は 850hPa 高度の湿潤断熱減率，z_{700} は 700hPa 高度．- 深い積雲のスキームで診断された積雲対流の深さが特定の閾値を超えた場合，深い対流卓越する環境場であるとし，浅い積雲は発生させない．- 浅い積雲に伴う上昇流の面積が或る閾値を越えない場合浅い積雲の計算を省略する．

2.3.4 3.4. 上昇流フラックスの鉛直プロファイルの診断

浅い積雲が発生すると判定された雲底と判断された格子では，上述の雲底高度に輸送される量 ψ_u の境界層格子平均値と雲底の質量フラックス $M_{u,base}$ を与え，エントレインメントとデトレインメントを計算していく．

エントレインメントとデトレインメントの比率 $\tilde{E}$, $\tilde{D}$ を決定するプロセスは Kain and Fritsch (1990) などでも用いられている浮力ソートの考え方を利用する．厚さ δz の層内で，環境場の空気 δM_e と上昇流内の空気 δM_u が等しく $\tilde{E}_0 M_u \delta z$ ずつ水平混合に関与して様々な混合状態のスペクトルを成す状況を考える．混合に関与する全質量フラックスは $2\tilde{E}_0 M_u \delta z$ である．混合空気内では，環境場からの空気が比率 χ を占めるような混合状態が確率密度 $q(\chi)$ で存在しており，ここでは計算を簡単にするため $\chi = 0$ の純粋な湿潤空気から $\chi = 1$ の純粋な環境場の空気までの混合状態が一様な確率で分布していると考える（Kain-Fritsch スキームではガウス分布を仮定している）．この混合空気のうちエントレインされる環境場の空気とデトレインされる上昇流の空気それぞれの量は混合状態ごとの浮力に基づいて計算され，この過程で PSHCN の内部でサブルーチン DISTANCE が呼び出される．上昇流の液水温位 (THETLU) とエントレインメント・デトレインメントの判定のブール値 (JUDGE) が出力変数である．

エントレインメントの条件は以下のように判定される．まず上昇流が飽和しているかを判断し，飽和していなければエントレインメントは起こらない．次にパーセルに働く浮力を環境場の仮温位 $\overline{\theta_v}$，上昇流内の仮温位 θ_{vu} を用いて

$$B_u = g\frac{\theta_{vu} - \overline{\theta_v}}{\overline{\theta_v}} \tag{292}$$

で計算し，正の浮力を持つ場合にはエントレインメントが起こるとする．さらに，浮力が負の場合でも慣性によってある渦混合距離 l_c を超えて上昇し続けることができる場合にはエントレインメントが起こるものとする．混合距離は $l_c \equiv c_1 H$ で定義する．ただし H は対流層の厚さで，定数 $c_1 = 0.1$ は貿易風帯のケースに最適化した値を使用している．上昇流内の浮力 B_u が臨界値

$$B_c = -\frac{1}{2}\frac{w_u^2}{l_c} \tag{293}$$

を超えていればエントレインメントが起こると判定される．浮力が負で l_c だけ上昇できるような最初の混合状態の臨界値 χ_c が求まれば，エントレインメントによって上昇流内に取り込まれる環境場の空気

$$M_t \int_0^{\chi_c} \chi q(\chi) d\chi = \tilde{E}_0 M_u \chi_c^2 \tag{294}$$

とデトレインメントによって環境場へ放出される上昇流内の空気

$$M_t \int_{\chi_c}^{1} (1-\chi) q(\chi) d\chi = \tilde{E}_0 M_u (1-\chi_c)^2 \tag{295}$$

が計算でき，

$$\tilde{E} = \tilde{E}_0 \chi_c^2 \tag{296}$$

$$\tilde{D} = \tilde{E}_0 (1-\chi_c)^2 \tag{297}$$

$$\frac{1}{M}\frac{\partial M_u}{\partial z} = \tilde{E} - \tilde{D} = \tilde{E}_0 (2\chi - 1) \tag{298}$$

となる．χ_c は混合空気の仮温位

$$\theta_v(\chi) = \theta_{vu} + \chi \left[\beta(\overline{\theta_l} - \theta_{l,u}) - \left(\frac{\beta L}{c_p \Pi} - \theta_u \right) (\overline{q_t} - q_{l,u}) \right] \tag{299}$$

(Randall,1980) をもとに導出する．

ψ_u の中の液水温位と総水量から雲水量 l と比湿 q を診断し，閾値を上回った雲水は雨水 q_r として落下させる．q_r の生成量に応じて液水温位を更新し，w_u および $M_{u,base}$ と整合するように上昇流の面積を診断する．これを離散化した支配方程式で上方に積分していくことで上昇流の鉛直プロファイルを求めていき，w_u または上昇流面積が下限値の定数を下回る高さを雲頂高度とする．

2.4 4. 実装に際しての補足

2.4.1 4.1. 質量フラックスのリミッター

本パラメタリゼーションでの保存量の鉛直フラックスの定式化は，講師の下端から流入する上昇流は時間ステップ Δt で格子内の大気を全て入れ替えるほど大きくないと仮定しているに等しい．よって上昇流の質量フラックスを求める際には次のような上限を課している．

$$M_u = min. \left(M_u, \frac{\rho \Delta z}{\Delta t} \right) \tag{300}$$

このリミッターは数値不安定を防ぐ効果を持っている．

2.5 5. 参考文献

- Bretherton, C. S., J. R. McCaa, and H. Grenier 2004: A new parameterization for shallow cumulus convection and its application to marine subtropical cloud-topped boundary layers. Part I: description and 1D results, *Mon. Wea. Rev.*, 132, 864-882.
- Park, S. and C. S. Bretherton 2009: The University of Washington shallow convection and moist turbulence schemes and their impact on climate simulations with the Community Atmosphere Model, *J. Clim*, 22, 3449-3469.
- Kain, J. S., and J. M. Fritsch 1990: A one-dimensional entraining/detraining plume model and its application in convective parameterization, *J. Atmos. Sci.*, 47, 2784-2802.
- Randall, D. A. 1980: Conditional instability of the first kind upside-down. *J. Atmos. Sci.*, 37, 125–130.

3 pmlsc: Large Scale Condensation

The module is written in the 'pmlsc' file and called in 'padmn', 'pcumc', 'pshcn', 'pcldphys' and 'pvdfm' files.

3.1 Physical basis for statistical PDF scheme

General Circulation Models (GCMs) typically adopt fractional cloud cover (the volume of cloudy air per total air volume in a grid box) assumption to realistically represent clouds because of their coarse horizontal resolution ($O(100km)$). Statistical cloud schemes assume a subgrid - scale probability density function (PDF) of humidity within the grid. Integration of the specific PDFs will give the cloud fraction and the amount of water condensate consistently.

By means of the "fast condensation" assumption, the cloud water amount in a local area in the grid is

$$q_c = (q_t - q_s)\,\delta\,(q_t - q_s) \tag{301}$$

where q_s denotes the saturation mixing ratio and q_c does the cloud water ratio. q_t is sum of water vapor and cloud water mixing ratio. $\delta(x)$ denotes the Heviside function of x.

The majority of statistical cloud schemes use the so-called "s-distribution" following Sommeria and Deardorff (1977). A single variable s, which considers the subgrid-scale perturbations of liquid temperature T_l and total water mixing ratio q_t, is employed. s is defined as

$$s = a_L\,(q_t - \alpha_L T_l) \tag{302}$$

where

$$a_L = 1/\,(1 + L\alpha_L/c_p)\,, \alpha_L = \partial q_s/\,\partial T|_{T=\bar{T}_l}\,. \tag{303}$$

For any choice of the PDF of s, denoted as $G(s)$, the grid-mean cloud fraction, C, and cloud water content, q_c, are obtained by integrating $G(s)$ and $(Qc + s)G(s)$,

$$C = \int_{-Q_c}^{\infty} G(s)ds \tag{304}$$

$$\bar{q}_c = \int_{-Q_c}^{\infty} (Q_c + s)\,G(s)ds, \tag{305}$$

where Qc denotes the grid-scale saturation deficit defined as

$$Q_c \equiv a_L\left\{\bar{q}_t - q_s\left(\bar{T}_l, \bar{p}\right)\right\}. \tag{306}$$

3.2 Hybrid Prognostic Cloud (HPC) scheme

The statistical scheme implemented in MIROC6 is called Hybrid Prognostic Cloud (HPC) scheme (Watanabe et al. 2009). The HPC scheme proposes two types of shape for the PDF $G(s)$, Double-uniform PDF and Skewed-triangular PDF. Here we focus on Skewed-triangular scheme because MIROC6 adoptes the shape. The physical basics of the scheme are in common with Double-uniform PDF.

Example of the basis PDF for HPC: skewed-triangular functions. Copied from Fig.1 in Watanabe et al. 2009.

The scheme preicts variance (V) and skewness (S) of the PDF. V, S, the second moment μ_2, and the third moment μ_3 are defined as follows.

$$\mu_2 \equiv V = \int_{-\infty}^{\infty} s^2 G(s) ds \tag{307}$$

$$\mu_3 \equiv \mu_2^{3/2} S = \int_{-\infty}^{\infty} s^3 G(s) ds \tag{308}$$

V and S are affected by cumulus convection, cloud microphysics, turbulent mixing, and advection.

The integrals to obtain C and q_c is symbolically expressed as

$$C = I_C \left(\bar{p}, \bar{T}_l, \bar{q}_t, \mathcal{V}, \mathcal{S} \right) \tag{309}$$

$$\bar{q}_c = I_q \left(\bar{p}, \bar{T}_l, \bar{q}_t, \mathcal{V}, \mathcal{S} \right) \tag{310}$$

where $\bar{p}$ denotes the pressure. The overbars denote the grid-mean quantity.

If the PDF is not too complicated, (1, 2) can be analytically solved for V and S by defining integrand functions $\tilde{I}$ as

$$\mathcal{V} = \tilde{I}_{\mathcal{V}} \left(\bar{p}, \bar{T}_l, \bar{q}_v, \bar{q}_c, C \right) \tag{311}$$

$$\mathcal{S} = \tilde{I}_{\mathcal{S}} \left(\bar{p}, \bar{T}_l, \bar{q}_v, \bar{q}_c, C \right) \tag{312}$$

The relationship between (1, 2) and (4, 5) is quasireversible. The double-uniform function and skewed-triangular function PDFs are selected for $G(s)$ because of their feasibility in analytically nalderiving $\tilde{I}$.

3.3 PDF change through processes

The HPC cloud scheme is composed using prognostic equations for four variables determining I, namely, T_l, q_t, V, and S. The prognostic variables can be T_l, q_t, C, and q_c that determine $\tilde{I}$.

Prognostic equations for the PDF variance and skewness are expressed as

$$\frac{D\mathcal{V}}{Dt} = \left.\frac{\Delta\mathcal{V}}{\Delta t}\right|_{\text{conv.}} + \left.\frac{\Delta\mathcal{V}}{\Delta t}\right|_{\text{micro.}} + \left.\frac{\Delta\mathcal{V}}{\Delta t}\right|_{\text{turb.}} + \left.\frac{\Delta\mathcal{V}}{\Delta t}\right|_{\text{others}} - \varepsilon\mathcal{V} \tag{313}$$

$$\frac{D\mathcal{S}}{Dt} = \left.\frac{\Delta\mathcal{S}}{\Delta t}\right|_{\text{conv.}} + \left.\frac{\Delta\mathcal{S}}{\Delta t}\right|_{\text{micro.}} + \left.\frac{\Delta\mathcal{S}}{\Delta t}\right|_{\text{turb.}} + \left.\frac{\Delta\mathcal{S}}{\Delta t}\right|_{\text{others}} - \varepsilon_{\mathcal{S}} \tag{314}$$

where subscripts 'conv.', 'micro.' and 'turb.' indicate cumulus convection, cloud microphysics and turbulent mixing processes, which all affect the PDF shape. The last terms represent dissipation due to subgrid-scale horizontal motions. The specific formulations for each term are described below.

The HPC scheme is referred to as and $G(s)$ is updated every after the process that affects cloud water PDF. $G(s)$ is thus modified several times within a single time step.

3.3.1 Cumulus convection

The total effect of cumulus convection to the PDF moments is written as

$$\left.\frac{\Delta\mathcal{V}}{\Delta t}\right|_{\text{conv.}} = M_c\frac{\partial\mathcal{V}}{\partial z} + \frac{\Delta\tilde{I}_{\mathcal{V}}}{\Delta t} \tag{315}$$

$$\left.\frac{\Delta\mathcal{S}}{\Delta t}\right|_{\text{conv.}} = M_c\frac{\partial\mathcal{S}}{\partial z} + \frac{\Delta\tilde{I}_{\mathcal{S}}}{\Delta t} \tag{316}$$

M_c is the cumulus mass-flux including updraft in the convection tower and downdraft in the environment. The vertical transport of the PDF moments is represented by the first terms on the right side hand of (14, 15).

Cumulus convections modify the grid-mean T_l, q_t, and q_c by upward transportation of grid-mean moist static energy, q_v, and q_c. Detrainment also affects these variables. The detrainment of the cloudy air mass is considered, as in Bushell et al. (2003),

$$\left.\frac{\partial C}{\partial t}\right|_{\text{conv.}} = D(1-C) \tag{317}$$

The second terms on the right hand side of (14, 15) indicates that the changes in the PDF moments is calculated consistent with the changes in the grid-scale temperature, humidity, cloud water, and cloud fraction.

$$\Delta\tilde{I}_{\mathcal{X}} = \tilde{I}_{\mathcal{X}}\left(\bar{p}, \bar{T}_l + \Delta\bar{T}_l, \bar{q}_v + \Delta\bar{q}_v, \bar{q}_c + \Delta\bar{q}_c, C + \Delta C\right) - \tilde{I}_{\mathcal{X}}\left(\bar{p}, \bar{T}_l, \bar{q}_v, \bar{q}_c, C\right) \tag{318}$$

(319)

where $\mathcal{X}$ is either $\mathcal{V}$ or $\mathcal{S}$.

3.3.2 Cloud Microphysics

The tendency due to microphysical processes can be written in a similar manner to the cumulus convection effect.

$$\left.\frac{\Delta\mathcal{V}}{\Delta t}\right|_{\text{micro.}} = \frac{\Delta\tilde{I}_{\mathcal{V}}}{\Delta t} \tag{320}$$

$$\left.\frac{\Delta\mathcal{S}}{\Delta t}\right|_{\text{micro.}} = \frac{\Delta\tilde{I}_{\mathcal{S}}}{\Delta t} \tag{321}$$

Changes in $\bar{T}_l, \bar{q}_v,$ and$\bar{q}_c$ are derived from microphysical tendency terms including precipitation, evaporation, melting/freezing.

3.3.3 Turbulent mixing

From the definition of s, the PDF variance $\mathcal{V}$ becomes

$$\mathcal{V} = a_L^2\left(\overline{q_t'^2} + \alpha_L^2\Pi\overline{\theta_l'^2} - 2\alpha_L\Pi\overline{q_t'\theta_l'}\right), \tag{322}$$

where Π is the Exner function. Assuming the level-2 closure in Nakanishi and Niino (2004), the time evolution of V can be derived as

$$\begin{aligned}\left.\frac{\Delta\mathcal{V}}{\Delta t}\right|_{\text{turb.}} =& 2a_L^2\left[\left(\alpha_L\Pi\right)^2 K_H\left(\frac{\partial\bar{\theta}_l}{\partial z}\right)^2 + K_q\left(\frac{\partial\bar{q}_t}{\partial z}\right)^2\right.\\ &\left.-\alpha_L\Pi\left(K_H+K_q\right)\frac{\partial\bar{\theta}_l}{\partial z}\frac{\partial\bar{q}_t}{\partial z}\right] - \frac{2q}{\Lambda_2}\mathcal{V},\end{aligned} \tag{323}$$

where K_H and K_q are the mixing coefficients for sensible heat and moisture, respectively. $q^2 = \overline{u'^2 + v'^2 + w'^2}$ denotes the turbulent kinetic energy. The other symbols follow the original notation.

Since the turbulence production does not affect the PDF shape parameter defined by the third moment (cf. Tompkins 2002), the skewness change $\Delta\mathcal{S}/\ \Delta t|_{\text{turb.}}$ is simply calculated due to the variance change in (28).

3.3.4 Subgrid-scale horizontal eddy

In the planetary boundary layer, the subgrid-scale inhomogeneity is dissipated due to the turbulent mixing. In free atmosphere, the grid box will be homogenized mainly due to mesoscale motions, which are expressed by the Newtonian damping as in (Tompkins 2002): $\varepsilon_{\mathcal{V}} = \frac{\mathcal{V}}{\tau_h}, \varepsilon_{\mathcal{S}} = \frac{\mathcal{S}}{\tau_h}$, where the relaxation timescale is parameterized by the horizontal wind shear as

$$\tau_h^{-1} = C_s^2 \left\{ \left(\frac{\partial \bar{u}}{\partial x} \right)^2 + \left(\frac{\partial \bar{v}}{\partial y} \right)^2 \right\}^{1/2} \tag{324}$$

The coefficient C_s is set to 0.23 following Tompkins 2002.

3.3.5 Other processes

Dynamics, shallow convection, radiation, mass source, and dissipation heating processes change the grid-mean temperature and humidity. Such effects on the shape of PDF are included following (16).

3.4 Solving procedures

The shape of the Skewed-triangular PDF is represented as follows. The widths defined by positions of the left and right edges on the s-coordinate are denoted as a and b, respectively. The position of the top, denoted as q, is constrained by $a + b + q = 0$. By definition, $q \leq b$ and $a \leq q$ must be satisfied. The PDF is then expressed as

$$G(s) = \begin{cases} -\frac{2(s-b)}{(b-q)(b-a)} & \text{for } q < s \leq b \\ \frac{2(s-a)}{(q-a)(b-a)} & \text{for } a < s \leq q \end{cases} \tag{325}$$

The pmlsc module includes two main subroutines, PDF2CLD and CLD2PDF. The subroutine PDF2CLD calculates C and $\bar{q}_c$ given $\bar{p}, T_l, \bar{q}_t, \mathcal{V}, \mathcal{S}$. The subroutine CLD2PDF calculates $\mathcal{V}$ and $\mathcal{S}$ given $\bar{p}, T_l, \bar{q}_t, \bar{q}_c, C$. We will derive the concrete calculation processes in this subsection.

3.4.1 PDF2CLD

From μ_1, μ_2, μ_3 To a, b, q The first, second, and third moments of the PDF is calculated as follows.

$$\mu_1 = \int_{q-a}^{q+b} sG(s)ds = q + \frac{b-a}{3} \tag{326}$$

$$\mu_2 = \int_{q-a}^{q+b} (s-\mu_1)^2 G(s)ds = \frac{a^2 + ab + b^2}{18} \tag{327}$$

$$\mu_3 = \int_{q-a}^{q+b} (s-\mu_1)^3 G(s) ds = \frac{(b-a)\left(2a^2+5ab+2b^2\right)}{270} \tag{328}$$

From (7,8,9), we will derive the solution for a, b, q given μ_1, μ_2, μ_3.
We define $\delta \equiv b-a, \beta \equiv ab$. (8,9) are

$$\delta^2 + 3\beta = 18\mu_2 \tag{329}$$

$$\delta\left(\beta + 12\mu_2\right) = 90\mu_3 \tag{330}$$

Eliminate β or δ from these equations, you will get the equations.

$$\delta^3 - 54\mu_2\delta + 270\mu_3 = 0 \tag{331}$$

$$\beta = 6\mu_2 - \frac{1}{3}\delta^2 \tag{332}$$

We apply the formula for the solution of a cubic equation to (10) to obtain δ.

$$\delta = 2\sqrt{18\mu_2}\cos\left(\frac{1}{3}\cos^{-1}\left(\frac{-135\mu_3}{\sqrt{(18\mu_2)^3}}\right) + \frac{4}{3}\pi\right) \tag{333}$$

β is obtained from (11). We define $\alpha \equiv \sqrt{\delta^2+4\beta}$ for simplicity. Finally, a, b, q is calculated as follows.

$$a = (\alpha - \delta)/2 \tag{334}$$

$$b = (\alpha + \delta)/2 \tag{335}$$

$$q = \mu_1 - \delta/3 \tag{336}$$

From PDF to C and qc Once the PDF $G(s)$ is determined by the parameters a, b, q, the cloud fraction C and grid-mean cloud water mixing ratio $\bar{q_c}$ are derived as follows.

$$C = \begin{cases} 0 & \text{if } b < -Q_c \\ \frac{(Q_c+b)^2}{(b-q)(b-a)} & \text{if } q \leq -Q_c \leq b \\ \frac{(Q_c+a)^2}{(q-a)(b-a)} & \text{if } a \leq -Q_c \leq q \\ 1 & \text{if } -Q_c < a \end{cases} \tag{337}$$

$$\bar{q_c} = \begin{cases} 0 & \text{if } b < -Q_c \\ \frac{1}{3}C\left(Q_c + b\right) & \text{if } q \leq -Q_c \leq b \\ Q_c - \frac{1}{3}(1-C)\left(Q_c + a\right) & \text{if } a \leq -Q_c \leq q \\ Q_c & \text{if } -Q_c < a \end{cases} \tag{338}$$

3.4.2 CLD2PDF

From $\bar{q_c}, C$ To a, b, q We can not determine the position of Q_c in the triangle at the beginning of the calculation. Thus we calculate a, b assuming that $a \leq -Q_c \leq q$ at first. If the calculated parameters are physically consistent with the PDF ($a+b \geq 0$), a, b, q are determined. Otherwise, we regard $q \leq -Q_c \leq b$ and then a, b, q are derived.

1. $a \leq -Q_c \leq q$

From (16), a is derived as follows.

$$a = \frac{3\left(Q_c - q_c\right)}{1-C} - Q_c \tag{339}$$

We eliminate q from (15) using $q = -a - b$. The quadratic equation for b is obtained.

$$b^2 + ab - 2a^2 + \left(Q_c + a\right)^2/(1-C) = 0 \tag{340}$$

The physically meaningful solution for b is

$$b = \left(-a\sqrt{9a^2 - 4\left(Q_c + a\right)^2/(1-C)}\right)/2 \tag{341}$$

2. $q \leq -Q_c \leq b$

From (16), b is

$$b = \frac{3q_c}{C} - Q_c \tag{342}$$

We eliminate q from (15) using $q = -a - b$. The quadratic equation of a is obtained.

$$a^2 + ab - 2b^2 + \left(Q_c + b\right)^2/C = 0 \tag{343}$$

The physically meaningful solution for a is

$$a = \left(-b - \sqrt{9b^2 - 4\left(Q_c + b\right)^2/C}\right)/2 \tag{344}$$

Adjustment of Cloud Fraction When there is no physically meaningful solution for (18), C is adjusted so that a reasonable solution is obtained. The critical conditions for the existence of real solutions for (18) are as follows.

$$\begin{array}{ll} 9a^2 - 4\left(Q_c + a\right)^2/(1-C) = 0 & (a \le -Q_c \le q) \\ 9b^2 - 4\left(Q_c + b\right)^2/C = 0 & (q \le -Q_c \le b) \end{array} \tag{345}$$

Eliminate a and b uging (17), we get the relationship between C and q_c,

$$\begin{array}{ll} 9\left(\frac{3(Q_c - q_c)}{1-C} - Q_c\right)^2 = \frac{4}{1-C}\left(\frac{3(Q_c - q_c)}{1-C}\right)^2 & (a \le -Q_c \le q) \\ 9\left(\frac{3q_c}{C} - Q_c\right)^2 = \frac{4}{C}\left(\frac{3q_c}{C}\right)^2 & (q \le -Q_c \le b) \end{array} \tag{346}$$

We take the square root of the both sides of the equations and define $\gamma_1 \equiv \sqrt{1-C}$ and $\gamma_2 \equiv \sqrt{C}$. The cubic equations for γ is obtained.

$$\begin{array}{ll} \gamma_1^3 - 3\left(1 - \frac{q_c}{Q_c}\right)\gamma_1 \pm 2\left(1 - \frac{q_c}{Q_c}\right) = 0 & (a \le -Q_c \le q) \\ \gamma_2^3 - 3\frac{q_c}{Q_c}\gamma_2 \pm 2\frac{q_c}{Q_c} = 0 & (q \le -Q_c \le b) \end{array} \tag{347}$$

We define $R_1 = 1 - \frac{q_c}{Q_c}, R_2 = \frac{q_c}{Q_c}$.

$$\gamma^2 = \begin{cases} -4R\sinh^2\left(\frac{1}{3}\sinh^{-1}\left(\frac{1}{\sqrt{-R}}\right)\right) & (R < 0) \\ 4R\cos^2\left(\frac{1}{3}\cos^{-1}\left(\frac{1}{\sqrt{R}}\right) + \frac{4}{3}\pi\right) & (R > 1) \end{cases} \tag{348}$$

Note that, $\gamma = \gamma_1, R = R_1\,(a \le -Q_c \le q)$ or $\gamma = \gamma_2, R = R_2\,(q \le -Q_c \le b)$.

The actual calculation procedure is as follows. If the solution for (18) is not a real number, C is adjusted using (26). Then we solve (18) again.

From a, b, q To μ_2, μ_3 By definition, the PDF moments are expressed in terms of a and b.

$$\mu_2 = \frac{a^2 + ab + b^2}{6} \tag{349}$$

$$\mu_3 = \frac{-(a+b)ab}{10} \tag{350}$$

3.4.3 Treatment of cloud ice and in-cloud water vapor

Because the original HPC scheme by Watanabe et al. (2009) does not consider the cloud ice, it is modified when coupled with the Wilson and Ballard (1999) ice microphysics. Since the statistical PDF scheme employs a 'fast condensation' assumption that is no more valid for ice, the ice mixing ratio is assumed to be conserved in the large scale condensation process.

Here we assume that - the water vapor mixing ratio within the cloudy area in a grid is constant - cloud ice preferentially exists in areas with large total water content

Based on these assumptions, the cloud fraction and each condensate mixing ratios are diagnosed. The notations for the mixing ratios (q_l, q_i, q_v, q_{vi}) of liquid water (subscript l), ice (subscript i), vapor (subscript v), in-cloud vapor (subscript vi) are employed.

At first the total condensate mixing ratio $q_c = q_l + q_i$ is diagnosed from q_t and T_l assuming that ice does not exist in the grid. The saturation mixing ratio is set for liquid (q_{satl}).

Mixed-phase cloud is generated when the condensate amount is more than the ice content ($q_c > q_i$), whereas the cloud fraction and vapor amount are adjusted in the case of a pure ice cloud when the condensate amount is less than the ice content ($q_c < q_i$). Specifically, q_c, C and q_{vi} are calculated as follows.

1. $q_c > q_i$

Liquid-phase clouds and ice clouds coexist.

$$q_l = q_c - q_i \tag{351}$$

$$q_{vi} = q_{\mathrm{satl}} \tag{352}$$

2. $q_c < q_i$

Only ice clouds exist ($q_l = 0$). In this case, C and q_{vi} are rediagnosed. We eliminate Q_c in (15,16) assuming that $q_c = q_i$. Equations for C are given as

$$C^3 = \frac{9q_i^2}{(b-q)(b-q)} \, (q \le -Q_c \le b) \tag{353}$$

$$C^3 + 3C^2 = 4 - \frac{9\,(q_i + a)^2}{(q-a)(b-a)} \, (a \le -Q_c < q) \tag{354}$$

From these equations, C is obtained as follows.

$$C = \begin{cases} \sqrt[3]{\frac{9q_i^2}{(b-q)(b-a)}} & \left(0 \le q_i \le \frac{(b-q)^2}{3(b-a)}\right) \\ 2\cos\left(\frac{1}{3}\cos^{-1}\left(1 - \frac{9(q_i+a)^2}{2(q-a)(b-a)}\right)\right) - 1 & \left(\frac{(b-q)^2}{3(b-a)} < q_i \le -a\right) \\ 1 & (-a < q_i) \end{cases} \tag{355}$$

,where

$$Q_c = \frac{3q_i}{C} - b = \sqrt[3]{3q_i(b-q)(b-a)} - b. \tag{356}$$

Given Q_c, $q_{vi} = q_t - Q_c$ is calculated as follows.

$$q_{vi} = \begin{cases} q_t - \frac{3q_i}{C} + b & \left(0 \le q_i \le \frac{(b-q)^2}{3(b-a)}\right) \\ q_t - \frac{3(q_i+a)}{2+C} + a & \left(\frac{(b-q)^2}{3(b-a)} < q_i \le -a\right) \\ q_t - q_i & (-a < q_i) \end{cases} \tag{357}$$

4 pcldphys: Cloud Microphysics

The code is written in the 'pcldphys' file.

4.1 Overview of Cloud Microphysics

Cloud microphysics control the conversion from water condensate to precipitate. The condensate parameterization closely links to the lifetime of and radiative properties of the clouds.

The stratiform (non-convective) cloud microphysics in MIROC6 (Tetebe et al. 2019) are basically the same as those used in MIROC5 (Watanabe et al. 2010). MIROC5 implemented a physically based bulk microphysical scheme. The previous version of the scheme in MIROC3.2 diagnoses the fraction of liquid-phase condensate to total condensate simply as a function of the local temperature. In contrast, the explicit treatment of ice cloud processes allows flexible representation of the cloud liquid/ice partitioning in MIROC5 and MIROC6 (Watanabe et al. 2010; Cesana et al. 2015).

The MIROC6 cloud microphysics scheme uses four quantities to describe water in the atmosphere: vapour; liquid-phase cloud droplets; raindrops; and frozen water. Only one quantity, which we will refer to as 'ice', is used to describe all frozen water in large-scale clouds, including aggregated snow, pristine ice crystals and rimed particles. Physically based transfer terms link the four water quantities. The scheme treats two prognostic condansate variables: ice water mixing ratio q_i and cloud water mixing ratio q_c. Water vapor mixing ratio q_v affects the rate of microphysical processes and q_v itself is also modified via microphysical processes. Ice number concentration N_i is diagnosed as a function of q_i and air temperature T in K. Cloud number concentration N_c is predicted by the online aerosol module implemented. Rain water mixing ratio q_r is treated as a diagnostic variable: q_r falls out to the surface within the time step. Cloud fraction is predicted as described in the section 'pmlsc: Large Scale Condensation'.

The cold rain parameterization following Wilson and Ballard (1999) predicts q_i using physically based tendency terms, which represent homogeneous nucleation, heterogeneous nucleation, deposition/sublimation between vapor and ice, riming (cloud liquid water collection by falling ice), and ice melting. The warm rain processes produce rain as the sum of autoconversion and accretion processes. Specific formulations of each process are described in the following "Microphysical Processes" subsection.

The scheme utilizes a "dry" mixing ratio (kg kg^{-1}) to define the amount of water condensate. For example, q_c is the mass of cloud water per mass of dry air in the layer. The dry air density ρ kg m^{-3} is calculated as $\rho = P/(R_{air}T)$, where P is the pressure in Pa, and the gas constant of air $R_{air} = 287.04$ J kg^{-1} K^{-1}. A condensate mass is obtained by multiplying the mixing ratio by the air density. (e.g., the mass of ice $m_i = \rho q_i$). A number concentraion is in units m^{-3}.

Hereafter, unless stated otherwise, the cloud variables $q_c, q_i, N_c,$ and $N_i$represent grid-averaged values; prime variables represent mean in-cloud quantities (e.g., such that $q_c = Cq_c^{'}$, where C is cloud fraction). Note that $q_v{}' \neq q_v$. $q_v{}'$ for ice clouds is determined as described in pmlsc section. The sub-grid scale variability of water content within the cloudy area is not considered at present.

4.2 Microphysical Processes

The time evolution of q_i by microphysical processes is written in symbolic form as follows.

$$\left(\frac{\partial q_i}{\partial t}\right)_{\text{micro}} = \left(\frac{\partial q_i}{\partial t}\right)_{\text{esnw}} + \left(\frac{\partial q_i}{\partial t}\right)_{\text{fallin}} + \left(\frac{\partial q_i}{\partial t}\right)_{\text{fallout}} + \left(\frac{\partial q_i}{\partial t}\right)_{\text{hom}} + \left(\frac{\partial q_i}{\partial t}\right)_{\text{het}} + \left(\frac{\partial q_i}{\partial t}\right)_{\text{dep}} + \left(\frac{\partial q_i}{\partial t}\right)_{\text{rim}} + \left(\frac{\partial}{\partial}\right.$$

where t is time. The terms of the right hand side denote evaporation of snow (sunscript esnw), ice fall in from above layers (subscript fallin), ice fall out to below layers (subscript fallout), homogeneous nucleation (subscript hom), heterogeneous nucleation (subscript het), deposition/sublimation (subscript dep), riming (subscript rim), and melting (subscript mlt). Similarly, the time evolution of q_c by microphysical processes is

$$\left(\frac{\partial q_c}{\partial t}\right)_{\text{micro}} = \left(\frac{\partial q_c}{\partial t}\right)_{\text{hom}} + \left(\frac{\partial q_c}{\partial t}\right)_{\text{het}} + \left(\frac{\partial q_c}{\partial t}\right)_{\text{rim}} + \left(\frac{\partial q_c}{\partial t}\right)_{\text{evap}} + \left(\frac{\partial q_c}{\partial t}\right)_{\text{auto}} + \left(\frac{\partial q_c}{\partial t}\right)_{\text{accr}} \quad (359)$$

where the terms on the right hand side are homogeneous nucleation, heterogeneous nucleation, riming, evaporation (subscript evap), autoconversion (subscript auto), and accretion (subscript accr). The formulations of these processes are detailed in the following subsections.

The conversion terms of all processes are calculated at every layer downward from the top layer (k=kmax) to the bottom layer of the column (k=1). k is the vertical level increasing with height, i.e., k+1 is the next vertical level above k.

The changes in the temperature of a layer is treated consistent with the phase-change of water.

$$\left(\frac{\partial T}{\partial t}\right)_{phase\ change} = \left(\frac{\partial T}{\partial t}\right)_{vapor\leftrightarrow liquid} + \left(\frac{\partial T}{\partial t}\right)_{vapor\leftrightarrow solid} + \left(\frac{\partial T}{\partial t}\right)_{liquid\leftrightarrow solid} \quad (360)$$

with

$$\left(\frac{\partial T}{\partial t}\right)_{vapor\leftrightarrow liquid} = \frac{L_v}{c_p}\left(\left(\frac{\partial q_c}{\partial t}\right)_{evap} + \left(\frac{\partial q_r}{\partial t}\right)_{erain}\right) \quad (361)$$

$$\left(\frac{\partial T}{\partial t}\right)_{vapor\leftrightarrow solid} = \frac{L_s}{c_p}\left(\left(\frac{\partial q_i}{\partial t}\right)_{esnw} + \left(\frac{\partial q_i}{\partial t}\right)_{dep}\right) \quad (362)$$

$$\left(\frac{\partial T}{\partial t}\right)_{liquid\leftrightarrow solid} = \frac{L_f}{c_p}\left(\left(\frac{\partial q_i}{\partial t}\right)_{hom} + \left(\frac{\partial q_i}{\partial t}\right)_{het} + \left(\frac{\partial q_i}{\partial t}\right)_{rim} + \left(\frac{\partial q_i}{\partial t}\right)_{mlt}\right), \quad (363)$$

where L_v, L_s, and L_f is the latent heat of vaporization, sublimation, and fusion, respectively. C_p is the specific heat of moist air at constant pressure.

4.2.1 Ice Properties

The formulation of the ice conversion terms requires parametrization of the mass, fall speed and particle size distributions of ice. These are described first and then subsequently used to derive the conversion terms.

The ice particle size distribution is parametrized as

$$N_i(D) = N_{i0} \exp(-0.1222(T - T_0)) \exp\left(-\Lambda_i D\right), \tag{364}$$

where D is the equivolume diameter of the particle in m, $N_{i0} = 2.0 \times 10^6$ m^{-4}, T is the temperature in K, and $T_0 = 273.15$ K. Λ_i represents the slope of the exponential distribution. The temperature function $\exp(-0.1222(T - T_0))$ represents the fact that ice particles tend to be smaller at lower temperatures, and is an implicit way of parametrizing aggregation.

The mass of an ice particle is parametrized as a function of D

$$m_{\mathrm{i}}(D) = aD^b \tag{365}$$

where $a = 0.069$ kg m^{-2}and $b = 2.0$.

The fall-speed of an ice particle at an air density of $\rho_0 = 1$ kg m^{-3} is

$$v_{\mathrm{i}}(D, \rho_0) = cD^d \tag{366}$$

where $c = 25.2m^{0.473}$ s^{-1} and $d = 0.527$.

At low air densities a particle will fall faster than at high air densities. Considering such ventilation effect, the fall-speed of a particle at arbitrary air density ρ is

$$v_{\mathrm{i}}(D, \rho) = (\rho_0/\rho)^{0.4}\, v_{\mathrm{i}}\left(D, \rho_0\right) \tag{367}$$

The combination of the size distribution, mass and velocity relationships yields a fall-speed and ice water content relationship.

For a given ice content and temperature, Λ_{i} can be calculated by integrating (A.2) across the particle size distribution (A.1). This gives the result that, for a given temperature, Λ_{i} is proportional to the inverse cube root of the ice water content.

$$\Lambda_{\mathrm{i}} = \left(\frac{2aN_{i0} \exp(-0.1222(T - T_0))}{m_i}\right)^{\frac{1}{3}} \tag{368}$$

4.2.2 Evaporation of Rain and Snow

The evaporation rate of rain $\left(\frac{\partial q_r}{\partial t}\right)_{\mathrm{erain}}$ is expressed as

$$\left(\frac{\partial q_r}{\partial t}\right)_{\mathrm{erain}} = \frac{1}{\rho \Delta z} k_E \left(q^w - q_v\right) \frac{F_r}{V_{Tr}}, \tag{369}$$

where F_r denotes the net accumulation of rain water at the layer in kg m^{-2} s^{-1}, V_{Tr} the terminal velocity, and k_E the evaporation factor ($V_{Tr} = 5$ m s^{-1}and $k_E = 0.5$). q^w correcponds to the saturation water vapor mixing ratio at the wet-bulb temperature. The evaporation occurs only when $q^w - q_v > 0$.

Similary to this, the evaporation rate of falling ice $\left(\frac{\partial q_i}{\partial t}\right)_{\text{esnw}}$ is expressed as

$$\left(\frac{\partial q_i}{\partial t}\right)_{\text{esnw}} = k_E \left(q^w - q_v\right) \frac{F_i}{V_{Tr}} \tag{370}$$

where F_i denotes sedimentation of cloud ice from above layers. V_{Ts} is set to 5 m s^{-1}.

4.2.3 Ice Fall

The total ice flux from the layer 'k' is

$$F_i|_k = \int_0^\infty N_{\text{i}}(D) m_{\text{i}}(D) v_{\text{i}}(D) dD. \tag{371}$$

The fraction of ice flux from level the 'k' to the below level 'kk' (1 <= kk < k) iceweight$|_{k,kk}$, is given as

$$\frac{\int_0^{f(\text{zm(k)}-\text{zm(kk)})} N_{\text{i}}(D) m_{\text{i}}(D) v_{\text{i}}(D) dD - \int_0^{f(\text{zm(k)}-\text{zm(kk+1)})} N_{\text{i}}(D) m_{\text{i}}(D) v_{\text{i}}(D) dD}{\int_0^\infty N_{\text{i}}(D) m_{\text{i}}(D) v_{\text{i}}(D) dD}, \tag{372}$$

where zm(k) is the middle of the height of the layer k, and f(dz) is the ice size which falls the distance dz in a single time step.

The net ice fall out from the layer is

$$\left(\frac{\partial q_i}{\partial t}\right)_{\text{fallout}} = -\frac{\Delta t}{\rho \Delta z} F_i. \tag{373}$$

.

The net ice fall in to the layer 'k' is

$$\left(\frac{\partial q_i}{\partial t}\right)_{\text{fallin}} = \frac{\Delta t}{\rho \Delta z} \sum_{l=k+1}^{l=kmax} F_i|_{k=l} \times \text{iceweight}|_{l,k} \tag{374}$$

4.2.4 Homogeneous nucleation

This term simply converts all liquid cloud water to ice if the temperature is less than a given threshold of 233.15 K.

$$\left(\frac{\partial q_i}{\partial t}\right)_{\text{hom}} = -\left(\frac{\partial q_c}{\partial t}\right)_{\text{hom}} = \frac{q_c}{\Delta t} \tag{375}$$

4.2.5 Heterogeneous nucleation

A Spectral Radiation-Transport Model for Aerosol Species (SPRINTARS; Takemura et al. 2000, 2002, 2005, 2009) coupled with MIROC6 explicitly predicts the masses and number concentrations for aerosol species. Heterogeneous freezing of cloud droplets takes place through contact and immersion freezing on ice cucleating particles (INPs), which are parameterized according to Lohmann and Diehl (2006) and Diehl et al. (2006). Soil dust and black carbon are assumed to act as INPs. Ratios of activated INPs to the total number concentration of soil dust and black carbon for the contact freezing and the immersion/condensation freezing are based on Fig. 1 in Lohmann and Diehl (2006). Using the number of INPs (N_{nuc}) predicted in SPRINTARS, the rate of heterogeneous freezing is diagnosed as follows.

$$\left(\frac{\partial q_i}{\partial t}\right)_{\rm het} = -\left(\frac{\partial q_c}{\partial t}\right)_{\rm het} = \max\{N_{nuc}W_{nuc0}, \frac{q_c}{\Delta t}\} \tag{376}$$

The weight of nucleated drop, W_{nuc0}, is set to 1.0×10^{-12}.

4.2.6 Deposition/Sublimation

A single ice particle grows or disappears by water vapor diffusion according to the following equation:

$$\frac{\partial m_i(D)}{\partial t} = \{4\pi C\,(S_{\rm i} - 1)\,F\} \,/\, [\{L_{\rm s}/(R_v T) - 1\}\, L_{\rm s}/\,(k_{\rm a} T) + R_v T/\,(X P_{\rm sati}\,)] \tag{377}$$

where $\frac{\partial m_i(D)}{\partial t}$ is the rate of change of the particle mass; $(S_i - 1)$ is the supersaturation of the atmosphere with respect to ice; R_v is the gas constant for water vapour; k_a is the thermal conductivity of air at temperature T, X is the diffusivity of water vapour; $P_{\rm sati}$ is the saturated vapour pressure over ice; $L_{\rm s}$ is the latent heat of sublimation of ice; C is a capacitance term and F is a ventilation coefficient. C is assumed to appropriate to spheres, so is equal to $D/2$. F is given by Pruppacher and Klett (1978) as $F = 0.65 + 0.44Sc^{1/3}Re^{1/2}$, where Sc is the Schmidt number, equal to 0.6, and Re is the Reynolds number, $v(D)\rho D/\mu$, where μ is the dynamic viscosity of air.

Integrating ice size distribution, $\left(\frac{\partial q_i}{\partial t}\right)_{\rm dep}$ is obtained as

$$\left(\frac{\partial q_i}{\partial t}\right)_{\rm dep} = \frac{1}{\rho}\int \frac{\partial m_i(D)}{\partial t} N(D) dD \tag{378}$$

The ice grows or disappears depending on the sign of $(S_i - 1)$.

1. $(S_i - 1) > 0$

The ice grows (deposition). If q_c exists in the same grid, q_c is evaporated as fast as the deposition process (Wegener–Bergeron–Findeisen process).

$$\left(\frac{\partial q_c}{\partial t}\right)_{\text{evap}} = -\left(\frac{\partial q_i}{\partial t}\right)_{\text{dep}} \tag{379}$$

The basis of this theory is the fact that the saturation vapor pressure of water vapor with respect to ice is less than that with respect to liquid water at the same temperature. Thus, within a mixture of these particles, the ice would gain mass by vapor deposition at the expense of the liquid drops that would lose mass by evaporation.

1. $(S_i - 1) < 0$

The ice disappears (sublimation).

4.2.7 Cloud water collection by ice (riming)

Riming process (the ice crystals settling through a population of supercooled cloud droplets, freezing them upon collision) is based on the geometric sweep-out integrated over all ice sizes (Lohmann 2004):

$$\left(\frac{\partial q_i}{\partial t}\right)_{\text{rim}} = -\left(\frac{\partial q_c}{\partial t}\right)_{\text{rim}} = \frac{\pi E_{\text{SW}} n_{0S} a q_c \Gamma(3+b)}{4\lambda_S^{(3+b)}} \left(\frac{\rho_0}{\rho}\right)^{0.5} \tag{380}$$

where $n_{0S} = 3 \times 10^6$ m^{-4} is the intercept parameter, λ_S is the slope of the exponential Marshall-Palmer ice crystal size distribution, $a = 4.84, b = 0.25$, and $\rho_0 = 1.3$ kg m^{-3} is the reference density. Γ is the gamma fanction. The collection efficiency E_{sw} is highly dependent on the cloud droplet and snow crystal size (Pruppacher and Klett 1997). The size-dependent collection efficiency for aggregates is introduced as obtained from laboratory results by Lew et al. (1986) (simulation ESWagg).

$$E_{\text{SW}}^{\text{agg}} = 0.939\text{St}^{2.657} \tag{381}$$

The Stokes number (St) is given by

$$\text{St} = \frac{2\,(V_t - v_t)\,v_t}{Dg}. \tag{382}$$

V_t is the snow crystal terminal velocity, and D is the maximum dimension of the snow crystal. v_t is the cloud droplet terminal velocity. g is the acceleration due to gravity.

4.2.8 Ice melt

Since this term is essentially a diffusion term, although of heat instead of moisture, its form is very similar to that of the deposition and evaporation of ice term. The rate of change of ice mass of a melting particle is given by:

$$\left(\frac{\partial q_r}{\partial t}\right)_{\rm mlt} = -\left(\frac{\partial q_i}{\partial t}\right)_{\rm mlt} = 4\pi CF\left\{k_{\rm a}/L_{\rm m}\left(T^{\rm w}-T_0\right)\right\}, \tag{383}$$

where $L_{\rm m}$ is the latent heat of melting of ice, $T^{\rm w}$ is the wet-bulb temperature of the air and $T_0 = 273.15$K is the freezing point of ice. Ice melt occurs when $T^{\rm w} - T_0 > 0$. The capacitance term, C, is considered to be that for spherical particles. Hence $C = D/2$. The ventilation factor, F is considered to be the same as in the deposition/sublimation process.

4.2.9 Warm rain cloud microphysics

We assume N_c is the number of aerosols activated as droplets. The nucleation of cloud droplets is predicted in the aerosol module SPRINTARS (Takemura et al. 2000; 2002; 2005; 2009) based on the parameterization by Abdul-Razzak and Ghan (2000), which depends on the aerosol particle number concentrations, size distributions and chemical properties of of each aerosol species, and the updraft velocity.

The autoconversion term following Berry (1967) is a function of q_c and N_c.

$$\left(\frac{\partial q_r}{\partial t}\right)_{\rm auto} = -\left(\frac{\partial q_c}{\partial t}\right)_{\rm auto} = \frac{1}{\rho}\frac{b_1 \times m_c'^2}{b_2 + b_3\frac{N_c}{m_c'}} \tag{384}$$

The parameters are set as $b_1 = 0.035$, $b_2 = 0.12$, $b_3 = 1.0 \times 10^{-12}$. The effect of aerosol-cloud interaction on cloud lifetime is taken into account by the dependency on N_c.

The accretion term is given as

$$\left(\frac{\partial q_r}{\partial t}\right)_{\rm auto} = -\left(\frac{\partial q_c}{\partial t}\right)_{\rm auto} = \frac{1}{\rho} q_c q_r \tag{385}$$

Rain water q_r into the layer is from above the layer. q_r is treated as a diagnostic variables: q_r falls out to surface within the time step.

4.2.10 Total precipitation

The total amount of precipitation at a certain pressure level, p, is obtained by integrating the relevant processes from the top of the model ($p = 0$) to the respective pressure level. The fluxes of rain and ice kgm^{-2} s^{-1} are then expressed as

$$P_{\rm rain}(p) = \frac{1}{g}\int_0^p \left(\left(\frac{\partial q_r}{\partial t}\right)_{\rm auto} + \left(\frac{\partial q_r}{\partial t}\right)_{\rm accr} + \left(\frac{\partial q_r}{\partial t}\right)_{\rm mlt} - \left(\frac{\partial q_r}{\partial t}\right)_{\rm revap}\right) dp \tag{386}$$

$$P_{\rm ice}(p) = \frac{1}{g}\int_0^p \left(\left(\frac{\partial q_i}{\partial t}\right)_{\rm fallin} - \left(\frac{\partial q_i}{\partial t}\right)_{\rm fallout} + \left(\frac{\partial q_i}{\partial t}\right)_{\rm rim} - \left(\frac{\partial q_r}{\partial t}\right)_{\rm mlt} - \left(\frac{\partial q_r}{\partial t}\right)_{\rm esnw}\right) dp \tag{387}$$

4.3 Radiant Flux.

4.3.1 Summary of Radiation Flux Calculations

The CCSR/NIES AGCM radiation scheme was created based on the Discrete Ordinate Method and the k-Distribution Method. The scheme calculate the value of the radiation flux at each level by taking into acount solar radiatin by gases and clouds/aerosols and the absorption, emission, and scattering processes of terrestrial radiation. The main input data are temperature T, specific humidity q, cloud cover l, and cloud cover C. The output data are upward and downward radiation fluxes F^-, F^+ and the differential coefficient of upward radiation flux with respect to surface temperature dF^-/dT_g.

The calculation is separated for several wavelengths.It is further divided into several subchannels, based on the k-distribution method. As for gaseous absorption, line absorption bands in H_2O, CO_2, O_3, N_2O, CH_4 and continuous absorption bans of H_2O, O_2, O_3 and CFC absorption is incorporated. As for scattering, Rayleigh scattering of gases and scattering by cloud and aerosol particles is incorporated.

The outline of the calculation procedure is as follows (subroutine names in parentheses).

1. Calculate the Planck function from atmospheric temperature `[PLANKS]`.
2. Calculates the optical thickness due to gas in each subchannel absorption `[PTFIT]`.
3. Calculate the optical thickness by continuous absorption and CFC absorption `[CNTCFC]`.
4. Calculate the optical thickness of Rayleigh scattering and particle scattering and scattering moment `[SCATMM]`.
5. Seeking sea-level albedo from the optical thickness and solar zenith angle of the scattering `[SSRFC]`.
6. Expand the Planck function by optical thickness for each sub-channel `[PLKEXP]`.
7. Calculate the transmission coefficient, reflection coefficient and source function for each layer for each sub-channel `[TWST]`
8. Calculate the radiation flux by adding method `[ADDING]`

To account for the partial coverage of clouds, the transmission coefficients, reflection coefficients and source functions for each layer are calculated separately for cloud cover and cloud-free conditions at weighted average of the cloud cover. The cloud cover of the cumulus is also consider the cloud cover of the cumulus clouds. In addition, it also performs several additing and calculates the clear-sky radiation flux.

4.3.2 Wavelengths and Subchannels

The basics of radiative flux calculations are represented by Beer-Lambert's Law.

$$F^\lambda(z) = F^\lambda(0) exp(-k^\lambda z) \tag{388}$$

F^λ is the radiant flux density at the wavelength of λ and k^λ is the absorption coefficient. In order to calculate the radiative fluxes related to the heating rate,theintegration operation with respect to the wavelength is required.

$$F(z) = \int F^\lambda(z)d\lambda = \int F^\lambda(0)exp(-k^\lambda z)d\lambda \tag{389}$$

$$\tag{390}$$

However, it is not easy to evaluate this integration precisely because the absorption and emission of radiation by gas molecules have the complicated wavelength dependence of the absorption line attributed to the structure of the molecule. The k-distribution method is a method designed to make the relatively precise calculation easier.Within a certain wavelength range, considering the density function $F(k)$ for λ, and of the absorption coefficient of k, (389) is approximated as follows,

$$\int F^\lambda(0)exp(-k^\lambda z)d\lambda \simeq \int \bar{F}^k(0)exp(-kz)F(k)dk \tag{391}$$

, by where $\bar{F}^k(0)$ is the absorption coefficient in this wavelength k the flux averaged over a wavelength having the absorption coefficient in this wavelength $k$in the $z = 0$.

if $\bar{F}_k, F(k)$ are a relatively smooth functions of the k, this expression

$$\int F^\lambda(0)exp(-k^\lambda z)d\lambda \simeq \sum \bar{F}^i(0)exp(-k^i z)F^i \tag{392}$$

, as such above, can be relatively precisely calculated by the addition of a finite number (subchannels) of exponential terms. This method has furthermore the advantage easy to consider the absorption and scattering at the same time.

In the CCSR/NIES AGCM, By changing the radiation parameter data, the calculations can be performed at various wavelengths. In the version currently used as a standard, the wavelength range is divided into 18 parts. In addition, each wavelength range is divided into 1 to 6 subchannels (corresponding to the i in the above formula), There are 40 channels in total. The wavelength range is divided by a wavenumber (cm^{-1}), 10, 250, 530, 610, 670, 980, 1175, 1225, 2000, 2500, 3300, 6000, 10000, 23000, 30000, 33500, 36000, 43500, and 50000. A global warming version with 29 bands and 111 chanels has been developed. Additionally, a chemical version is also with 37 bands and 126 chanels for chemical transport model. The boundary of the SW region is also changed to 54000 cm^{-1}.

4.3.3 Calculating the Planck function [PLANKS]

The Planck function $\overline{B}^w(T)$ integrated in each wavelength range is, evaluate by the following formula.

$$\overline{B}^w(T) = \lambda^{-2} T \exp\left\{\sum_{n=0} 4B_n^w (\bar{\lambda}^w T)^{-n}\right\} \tag{393}$$

$\bar{\lambda}^w$ is the average wavelength of the wavelength range, B_n^w is the parameter determined by function fitting. This is caluculated to the atmospheric temperature of each layer, T_l, and the boundary atmospheric temperature of each layer, $T_{l+1/2}$ and surface temperature T_g.

In the following, the index w is basically abbreviated for the wavelength range.

4.3.4 Calculating the optical thickness by gas absorption [PTFIT]

The optical thickness of the gas absorption is expressed as follows by using the index m as the type of molecule.

$$\tau^g = \sum_{m=1} N_m k^{(m)} C^{(m)} \tag{394}$$

where $k^{(m)}$ is the absorption coefficient of the molecule m, which is different for each subchannel and determined as a function of temperature T(K) and atmospheric pressure p(hPa).

$$k^{(m)} = \exp\left\{\sum_{i=0} N_i \sum_{j=0} N_j A_{ij}^{(m)} (\ln p)^i (T - T_{STD})^j\right\} \tag{395}$$

$C^{(m)}$ is the amount of gas in the layer represented by mol cm^{-2}. Based on the Volume Mixing Ratio r (in ppmv),

$$C = 1 \times 10^{-5} \frac{p}{R_u T} \Delta z \cdot r \tag{396}$$

it can be calculated. Note that R_u is the gas constant per mole (8.31 J mol$_{-1}$ K^{-1}), The unit of air layer thickness Δz is in km. The volume mixing ratio r at ppmv, from Mass Mixture Ratio q,

$$r = 10^6 R^{(m)}/R^{(air)} q = 10^6 M^{(air)}/M^{(m)} \tag{397}$$

can be converted. $R^{(m)}, R^{(air)}$ are gas constant per targetted molecule and atmospheric mass, and respectively, $M^{(m)}, M^{(air)}$ is the average molecular weight of the target molecule and the atmosphere.

This calculation is done for each sub-channel and each layer.

4.3.5 Optical Thickness by Continuous Absorption and CFC Absorption [CNTCFC]

The optical thickness of the H_2O continuous absorption τ^{H_2O} is , in consideration of a dimer, Basically, evaluated in proportion to the square of the volume mixing ratio of water vapor.

$$\tau^{H_2O} = (A^{H_2O} + f(T)\hat{A}^{H_2O})(r^{H_2O})^2 \rho \Delta z \tag{398}$$

The $f(T)$ for the $\hat{A}$ section is , the temperature dependence of the absorption of the dimer. Furthermore, in the wavelength range where normal gas absorption is ignored, a contribution proportional to the square of the volume mixing ratio of water vapor is incorporated.

The continuous absorption of O_2 is assumed to be constant in the mixing ratio.

$$\tau^{O_2} = A^{O_2} \rho \Delta z \tag{399}$$

The continuous absorption of O_3 is based on the mixing ratio r^{O_3} and incorporates a temperature dependence.

$$\tau^{O_3} = \sum_{n=0} 2A_n^{O_3} r^{O_3} \frac{T}{T_{STD}}^n \rho \Delta z \tag{400}$$

Absorption of CFCs is considered for N_m types of CFCs.

$$\tau^{CFC} = \sum_{m=1} N_m A_m^{CFC} r^{(m)} \rho \Delta z \tag{401}$$

The sum of these optical thicknesses is τ^{CON}.

$$\tau^{CON} = \tau^{H_2O} + \tau^{O_2} + \tau^{O_3} + \tau^{CFC} \tag{402}$$

This calculation is performed for each wavelength range and each layer.

4.3.6 Scattering optical thickness and scattering moments [SCATMM]

The optical thicknesses of Rayleigh scattering and particle dissipation (including scattering and absorption) are

$$\tau^s = \left(e^R + \sum_{p=1} N_p e_m^{(p)} r^{(p)} \right) \rho \Delta z \tag{403}$$

where e^R is the dissipation coefficient of Rayleigh scattering, the $e^{(p)}$ is the dissipation factor of the particle p, the $r^{(p)}$ is the volume mixing ratio of the particle p converted to standard conditions.

Here, The conversion from the mass mixing ratio of cloud water l to cloud grains of standard state-conversion volume mixing ratios (ppmv) is as follows.

$$r = 10^6 \frac{p_{STD}}{RT_{STD}} / \rho_w \tag{404}$$

ρ_w is the density of cloud particles.

On the other hand, the scattering-induced part of the optical thickness, τ_s^s is

$$\tau_s^s = \left(s^R + \sum_{p=1} N_p s_m^{(p)} r^{(p)} \right) \rho \Delta z \tag{405}$$

where s^R is the scattering coefficient of Rayleigh scattering, $s^{(p)}$ is the scattering coefficient for the particle p.

Also, the standardized scattering moments g (asymmetry factor) and f (forward scattering factor) are

$$g = \frac{1}{\tau_s} \left[\left(g^R + \sum_{p=1} N_p g_m^{(p)} r^{(p)} \right) \rho \Delta z \right] \tag{406}$$

$$f = \frac{1}{\tau_s} \left[\left(f^R + \sum_{p=1} N_p f_m^{(p)} r^{(p)} \right) \rho \Delta z \right] \tag{407}$$

Here, g^R, f^R are the scattering moments of Rayleigh scattering, $g^{(p)}, f^{(p)}$ is the scattering moment of the particle p.

This calculation is performed for each wavelength range and each layer.

4.3.7 Albedo at Sea Level [SSRFC]

Albedo α_s at sea level is expressed as follows by using the vertical addition of the optical thickness of the scattering $< \tau^s >$ and the solar incidence angle factor μ_0.

$$\alpha_s = \exp \left\{ \sum_{i,j} C_{ij} \mathcal{T}^j {\mu_0}^j \right\} \tag{408}$$

However,

$$\mathcal{T} = (4 < \tau^s > / \mu)^{-1} \tag{409}$$

This calculation is done for each wavelength.

4.3.8 Total Optical Thickness.

All optical thickness including gaseous band absorption, continuous absorption, Rayleigh scattering, particle scattering and absorption is,

$$\tau = \tau^g + \tau^{CON} + \tau^s \tag{410}$$

where because τ^g is different for each subchanne, the calculation is done for each sub-channel and each layer.

4.3.9 Planck function expansion [PLKEXP]

In each layer, the Planck function B is expanded as follows and the expansion coefficients $b_0, b_1, b, 2$ is obtained.

$$B(\tau') = b_0 + b_1\tau' + b_2\left(\tau'\right)^2 \tag{411}$$

Here, as $B(0)$ B at the top of each layer (bordering the top layer) is used, and as $B(\tau)$, B at the bottom edge of each layer (the boundary with the layer below), and as $B(\tau/2)$, the B at the representative level of each layer.

$$\begin{aligned} b_0 &= B(0) \\ b_1 &= (4B(\tau/2) - B(\tau) - 3B(0))/\tau \\ b_2 &= 2(B(\tau) + B(0) - 2B(\tau/2))/\tau^2 \end{aligned} \tag{412}$$

This calculation is done for each sub-channel and each layer.

4.3.10 Transmission and reflection coefficients of each layer, the source function [TWST]

Using the So far obtained, optical thickness τ, optical thickness of scattering τ^s, scattering Moments g, f, expansion Coefficient for Planck Function b_0, b_1, b_2, and solar incidence angle factor μ_0, assuming a uniform layer, and using the two-stream approximation, transmission Coefficient R, reflection Coefficient T, downward Radiation Source Function ϵ^+, and the upward radiation source function ϵ^- are founded.

The single-scattering albedo ω is,

$$\omega = \tau_s^s/\tau \tag{413}$$

The optical thickness τ^* corrected by the contribution from the forward scattering factor f and the single-scattering albedo ω^*, and asymmetric factor g^* are,

$$\tau^* = \frac{\tau}{1-\omega f} \tag{414}$$

$$\omega^* = \frac{(1-f)\omega}{1-\omega f} \tag{415}$$

$$g^* = \frac{g-f}{1-f} \tag{416}$$

As a phase function of the normalized scattering,

$$\hat{P}^{\pm} = \omega^* W^{-2} \left(1 \pm 3g^*\mu\right)/2 \tag{417}$$

$$\hat{S}_s^{\pm} = \omega^* W^{-} \left(1 \pm 3g^*\mu\mu_0\right)/2 \tag{418}$$

However, μ is a two-stream directional cosine, and

$$\mu \equiv \begin{cases} 1/\sqrt{3} & visible/near-infraredregion \\ 1/1.66 & infraredregion \end{cases} \tag{419}$$

$$W^{-} \equiv \mu^{-1/2} \tag{420}$$

Furthermore,

$$X = \mu^{-1} - (\hat{P}^{+} - \hat{P}^{-}) \tag{421}$$

$$Y = \mu^{-1} - (\hat{P}^{+} + \hat{P}^{-}) \tag{422}$$

$$\hat{\sigma}_s^{\pm} = \hat{S}_s^{+} \pm \hat{S}_s^{-} \tag{423}$$

$$\lambda = \sqrt{XY} \tag{424}$$

using the above formula, the reflectance R and transmission T become

$$\frac{A^{+}\tau^*}{A^{-}\tau^*} = \frac{X(1+e^{-\lambda\tau^*}) - \lambda(1-e^{-\lambda\tau^*})}{X(1+e^{-\lambda\tau^*}) + \lambda(1-e^{-\lambda\tau^*})} \tag{425}$$

$$\frac{B^{+}\tau^*}{B^{-}\tau^*} = \frac{X(1-e^{-\lambda\tau^*}) - \lambda(1+e^{-\lambda\tau^*})}{X(1-e^{-\lambda\tau^*}) + \lambda(1+e^{-\lambda\tau^*})} \tag{426}$$

$$R = \frac{1}{2}\left(\frac{A^{+}\tau^*}{A^{-}\tau^*} + \frac{B^{+}\tau^*}{B^{-}\tau^*}\right) \tag{427}$$

$$T = \frac{1}{2}\left(\frac{A^{+}\tau^*}{A^{-}\tau^*} - \frac{B^{+}\tau^*}{B^{-}\tau^*}\right) \tag{428}$$

Next, we find the source function from which the Planck function is derived.

$$\hat{b}_n = 2\pi(1-\omega^*)W^{-}b_n \quad n = 0, 1, 2 \tag{429}$$

The expansion coefficients of the radiant function can be found from the above formulathe.

$$D_2^{\pm} = \frac{\hat{b}_2}{Y} \tag{430}$$

$$D_1^{\pm} = \frac{\hat{b}_1}{Y} \mp \frac{2\hat{b}_2}{XY} \tag{431}$$

$$D_0^{\pm} = \frac{\hat{b}_0}{Y} + \frac{2\hat{b}_2}{XY^2} \mp \frac{\hat{b}_1}{XY} \tag{432}$$

$$\tag{433}$$

$$D^{\pm}(0) = D_0^p m \tag{434}$$

$$D^{\pm}(\tau^*) = D_0^p m + D_1^p m\tau^* + D_2^p m{\tau^*}^2 \tag{435}$$

The source function $\hat{\epsilon}_A^{\pm}$, which is derived from the Planck function, is

$$\hat{\epsilon}_A^- = D^-(0) - RD^+(0) - TD^-(\tau^*) \tag{436}$$

$$\hat{\epsilon}_A^+ = D^+(0) - TD^+(0) - RD^-(\tau^*) \tag{437}$$

On the other hand, the source function of the solar-induced radiation is

$$Q\gamma = \frac{X\hat{\sigma}_s^+ + \mu_0^{-1}\hat{\sigma}_s^-}{\lambda^2 - \mu_0^{-2}} \tag{438}$$

than, by using

$$V_s^{\pm} = \frac{1}{2}\left[Q\gamma \pm \left(\frac{Q\gamma}{\mu X} + \frac{\hat{\sigma}_s^-}{X}\right)\right] \tag{439}$$

we obtain the following.

$$\hat{\epsilon}_S^- = V_s^- - RV_s^+ - TV_s^- e^{-\tau^*/\mu_0} \tag{440}$$

$$\hat{\epsilon}_S^+ = V_s^+ - TV_s^+ - RV_s^- e^{-\tau^*/\mu_0} \tag{441}$$

This calculation is done for each sub-channel and each layer.

4.3.11 Combinations of source functions for each layer

The source function combined between the Planck function origin and solar-induced origin is

$$\epsilon^{\pm} = \epsilon_A^{\pm} + \hat{\epsilon}_S^{\pm} e^{-<\tau^*>/\mu_0} F_0 \tag{442}$$

$$\tag{443}$$

,where the $< \tau^* >$ is the total optical thickness adding the τ^* to the top of the considered layer and F_0 is the incident flux in the wavelength range under consideration. Thus, $e^{-<\tau^*>/\mu_0} F_0$ is the incident flux at the top of the layer under consideration. This calculation is actually done as follows.

$$e^{-<\tau^*>/\mu_0} = \Pi' e^{-\tau^*/\mu_0} \tag{444}$$

Π' will be taken from the uppermost layer of the atmosphere by Represents the product up to one layer above the layer considering now.

Π' represents the product from the uppermost layer of the atmosphere to one layer above the layer considering now.

4.3.12 Radiation flux at each layer boundary [ADDING]

By using transmission coefficient R_l, reflection coefficient T_l, and radiation source function $\epsilon_l^{\pm}$ in all layers l, the radiation fluxes at each layer boundary can be obtained by using the adding method. This means that the when two layers of R, T, ϵ are known, the R, T, ϵ of the whole combined layer of the two layers can be easily calculated. In a homogeneous layer, the reflectance of the incident light and transmission coefficient from above are the same as those from below. On the other hands, because it is different in heterogeneous layers composed of multiple layers, the reflectance and transmittance of the incident light from above (R^+, T^+, R^+, T^+) is distinguished with those from below (R^-, T^-). If $R_1^{\pm}, T\pm_1, \epsilon_1^{\pm}, R_2^{\pm}, T\pm_2, \epsilon_2^{\pm}$ are known in above layer 1and below layer 2, the Value in the composite layer $R_{1,2}^{\pm}, T\pm_{1,2}, \epsilon_{1,2}^{\pm}$ are as folllows.

$$\begin{aligned}
R_{1,2}^+ &= R_1^+ + T_1^-(1 - R_2^+ R_1^-)^{-1} R_2^+ T_1^+ && (445)\\
R_{1,2}^- &= R_2^- + T_2^+(1 - R_1^+ R_2^-)^{-1} R_1^- T_2^- && (446)\\
T_{1,2}^+ &= T_2^+(1 - R_1^+ R_2^-)^{-1} T_1^+ && (447)\\
T_{1,2}^- &= T_1^-(1 - R_1^+ R_2^-)^{-1} T_2^- && (448)\\
\epsilon_{1,2}^+ &= \epsilon_2^+ + T_2^+(1 - R_2^+ R_1^-)^{-1}(R_1^- \epsilon_2^- + \epsilon_1^+) && (449)\\
\epsilon_{1,2}^- &= \epsilon_1^- + T_1^-(1 - R_2^+ R_1^-)^{-1}(R_2^+ \epsilon_1^+ + \epsilon_2^-) && (450)
\end{aligned}$$

There are layers 1, 2, ... N from the top and the surface is considered to be a single layer and the N layer.Given the reflectance and source function of the layers from the n to the N layer as a single layer $R_{n,N}^+, \epsilon_{n,N}^-$,

$$\begin{aligned}
R_{n,N}^+ &= R_n^+ + T_n^-(1 - R_{n+1,N}^+ R_n^-)^{-1} R_{n+1,N}^+ T_n^+ && (451)\\
\epsilon_{n,N}^- &= \epsilon_n^- + T_n^-(1 - R_{n,N}^+ R_n^-)^{-1}(R_{n,N}^+ \epsilon_n^+ + \epsilon_{n,N}^-) && (452)
\end{aligned}$$

This can be solved by $n = N-1, \ldots 1$ in sequence, starting from the value at the surface

$$\begin{aligned}
R_{N,N}^+ &= R_N^+ = 2W^{+2}\alpha_s && (453)\\
\epsilon_{N,N}^- &= \epsilon_N^- = W^+\left(2\alpha_s \mu_0 e^{-<\tau^*>/\mu_0} F_0 + 2\pi(1-\alpha_s) B_N\right) && (454)
\end{aligned}$$

However,

$$W^+ \equiv \mu^{1/2} \tag{455}$$

Given the reflectance and source function regarded from the first to the n layers as a single layer $R^-_{1,n}, \epsilon^+_{1,n}$, $R^-_{1,n}, \epsilon^+_{1,n}$,

$$\begin{aligned} R^-_{1,n} &= R^-_n + T^+_n(1 - R^+_{1,n-1}R^-_n)^{-1}R^-_{1,n-1}T^-_n & (456)\\ \epsilon^+_{1,n} &= \epsilon^+_n + T^+_n(1 - R^+_{1,n-1}R^-_n)^{-1}(R^-_{1,n-1}\epsilon^-_n + \epsilon^+_{1,n-1}) & (457) \end{aligned}$$

and this is also $R^-_{1,1} = R^-_1, \epsilon^+_{1,1} = \epsilon^+_1$ It can be solved by $n = 2, \ldots N$, starting from $R^-_{1,1} = R^-_1, \epsilon^+_{1,1} = \epsilon^+_1$.

With these, downward flux at the boundary between layers n and $n+1$ $u^+_{n,n+1}$ and upward flux $u^-_{n,n+1}$ are came back to a problem between two layers of combined layer, the combinations of layers $1 \sim n$ and $n+1 \sim N$.

$$\begin{aligned} u^+_{n+1/2} &= (1 - R^-_{1,n}R^+_{n+1,N})^{-1}(\epsilon^+_{1,n} + R^-_{1,n}\epsilon^-_{n+1,N}) & (458)\\ u^-_{n+1/2} &= R^+_{n+1,N}u^+_{n,n+1} + \epsilon^-_{n+1,N} & (459) \end{aligned}$$

can be written as above. However, the flux at the top of the atmosphere is

$$\begin{aligned} u^+_{1/2} &= 0 & (460)\\ u^-_{1/2} &= \epsilon^-_{1,N} & (461) \end{aligned}$$

Finally, since this flux is scaled , We rescaled and added direct solar incidence to the find the radiation flux.

$$\begin{aligned} F^+_{n+1/2} &= \frac{W^+}{\bar{W}}u^+_{n+1/2} + \mu_0 e^{-<\tau^*>_{1,n}/\mu_0}F_0 & (462)\\ & & (463)\\ F^-_{n+1/2} &= \frac{W^+}{\bar{W}}u^-_{n+1/2} & (464)\\ & & (465) \end{aligned}$$

This calculation is done for each sub-channel.

4.3.13 Add in the flux

If the radiation flux $F^\pm_c$ is found for each subchannel in each layer, the wavelength-integrated flux is found by applying it a weight (w_c) correspondingly to a wavelength representative of the subchannel and adding them together.

$$\bar{F}^{\pm} = \sum_{c} w_c F^{\pm} \tag{466}$$

In practice, it is divided into the short wavelength range (solar region) and long wavelengths (earth's radiation region) and added together. In addition, the downward flux of a part of the short wavelength region (shorter than the wavelength of 0.7μ) at the surface is obtained as PAR (photosynthetically active radiation).

4.3.14 The temperature derivative of the flux

To implicitly solve for surface temperature, calculate differential term of upward flux with respect to surface temperature dF^{-}/dT_g.

Therefore, we obtained the value for temperatures 1K higher than T_g $\overline{B}^{w}(T_g + 1)$ and used it to redo the flux calculation using the addition method, and the difference from the original value is set to dF^{-}/dT_g.

This is a meaningful value only in the long-wavelength region (Earth's radiation region).

4.3.15 Treatment of cloud cover

In the CCSR/NIES AGCM, the horizontal coverage of clouds in a single grid is considered. There are two types of clouds as follows.

1. Stratus cloud. Diagnosed by the large scale condensation scheme `[LSCOND]`. For each layer (n), the lattice-averaged cloud water content l_n^l and the horizontal coverage factor (cloud cover) C_n^l are defined.

2. Cumulus cloud. Diagnosed by the cumulus convection scheme `[CUMLUS]`. For each layer (n) the lattice-averaged cloud water content l_n^c is defined, but horizontal coverage (cloud cover) C^c is constant in the vertical direction.

In these treatments, we assume that the stratocumulus clouds overlap randomly in a vertical direction and the cumulus cloud always occupies the same area in the upper and lower layers (the cloud cover is 0 or 1 if it is confined to that region). In order to do that, we perform the following calculations.

1. Calculate for optical thickness of Rayleigh and particle scattering/absorption, etc. τ^s, τ_s^s, g, f,

    1. when cloud water of the l_n^l/C_n^l exists (stratocumulus)
    2. when there are no clouds at all
    3. when cloud water in the cloud cover of l_n^c/C^c is present (cumulus clouds)

2. Reflection, transmission coefficients for each layer, and radiant source function (Planck function origin, insolation origin) for each layer are calculated for each of the three cases above. The values for no clouds R°, in the case of stratus clouds R^l, in the case of cumulus clouds R^c and so on.

3. Reflection, transmission coefficients for each layer, and source function for each layer are averaged with the weight of the cloud cover of the stratocumulus, C^l. The averages are represented by $\bar{}$,

$$\begin{aligned}
\bar{R} &= (1-C^l)R^\circ + C^l R^l && (467)\\
\bar{T} &= (1-C^l)T^\circ + C^l T^l && (468)\\
\bar{\epsilon} &= (1-C^l)\epsilon_A^\circ + C^l \epsilon_A^l && (469)\\
&+ \left[(1-C^l)\epsilon_S^\circ + C^l\epsilon_S^l\right] e^{-\overline{<\tau^*>}/\mu_0} F_0 && (470)
\end{aligned}$$

However,

$$e^{-\overline{<\tau^*>}/\mu_0} = \Pi' \left[(1-C^l)e^{-\tau^{*\circ}/\mu_0} + C_l e^{-\tau^{*l}/\mu_0}\right] \quad (471)$$

Also, we seek

$$\begin{aligned}
\epsilon^\circ &= \epsilon_A^\circ + \epsilon_S^\circ e^{-<\tau^{*\circ}>/\mu_0} F_0 && (472)\\
\epsilon^c &= \epsilon_A^c + \epsilon_S^c e^{-<\tau^{*c}>/\mu_0} F_0 && (473)
\end{aligned}$$

4. When the characteristic values of the average (e.g., $\bar{R}$) are used, when using a characteristic value without clouds (e.g., R°) and when the characteristic values of cumulus clouds (e.g., R^c), fluxes $\bar{F}, F^\circ, F^c$ are found, fluxes by adding, respectively.

5. The final flux we seek is

$$F = (1-C^c)\bar{F} + C^c F^c \quad (474)$$

(F$^\circ is calculated to estimate cloud radiative forcing$)

4.3.16 Incidence flux and angle of incidence [SHTINS]

Incident Flux F_0 is represented as follows

$$F_0 = F_0 0 r_s^- 2 \quad (475)$$

where F_{00} is the solar constant and r_s is the ratio of the ratio to the time of the distance between the sun and the earth. Also, r_s asks for the following.

$$M \equiv 2\pi(d - d_0) \quad (476)$$

$$r_s = a_0 - a_1 \cos M - a_2 \cos 2M - a_3 \cos 3M \tag{477}$$

Note that d is the time in days since the beginning of the year.
Also, the angle of incidence is obtained as follows. Solar angle position ω_s is

$$\omega_s = M + b_1 \sin M + b_2 \sin 2M + b_3 \sin 3M \tag{478}$$

If the solar declination δ_s is

$$\sin \delta_s = \sin \epsilon \sin(\omega_s - \omega_0) \tag{479}$$

the angle of incidence factor $\mu = \cos \zeta$ (where ζ is the zenith angle) is

$$\mu = \cos \zeta = \cos \varphi \cos \delta_s \cos h + \sin \varphi \sin \delta_s \tag{480}$$

where φ is a latitude and h is the time angle (local time minus π).
Assuming that the eccentricity of the Earth's orbit is e (Katayama, 1974),

$$\begin{aligned}
a_0 &= 1 + e^2 && (481)\\
a_1 &= e - 3/8e^3 - 5/32e^5 && (482)\\
a_2 &= 1/2e^2 - 1/3e^4 && (483)\\
a_3 &= 3/8e^3 - 135/64^5 && (484)\\
b_1 &= 2e - 1/4e^3 + 5/96e^5 && (485)\\
b_2 &= 5/4e^2 - 11/24e^4 && (486)\\
b_3 &= 13/12e^3 - 645/940e^5 && (487)\\
& && (488)
\end{aligned}$$

It is also possible to give average annual insolation. In this case, the annual mean incidence and the annual mean angle of incidence are approximated as follows.

$$\overline{F} = F_{00}/\pi \tag{489}$$

$$\overline{\mu} \simeq 0.410 + 0.590 \cos^2 \varphi. \tag{490}$$

4.3.17 Other Notes.

The calculation of the radiation is usually not done at every step. Thus, the radiation flux is saved, and it is used if the time is not used for radiation calculation.

As for the shortwave radiation, using the percentage of time (time is that $\mu_0 > 0$) between next calculation time (f) and the solar incidence angle factor averaged over the daylight hours ($\bar{\mu_0}$), seek the Flux $\bar{F}$,

$$F = f\frac{\mu_0}{\bar{\mu_0}}\bar{F} \tag{491}$$

2. Cloud water is dependent on the temperature, and treated as water and ice cloud particles. Percentage treated as ice clouds f_I is,

$$f_I = \frac{T_0 - T}{T_0 - T_1} \tag{492}$$

4.4 Turbulence scheme

The turbulence scheme represents the effect of subgrid-scale turbulence on the grid-averaged quantities. The turbulence scheme accounts for the vertical diffusion of momentum, heat, water and other tracers. The Mellor-Yamada-Nakanishi-Niino scheme (the MYNN scheme; Nakanishi 2001; Nakanishi and Niino 2004), an improved version of the Mellor-Yamada scheme (Mellor 1973; Mellor and Yamada 1974; Mellor and Yamada 1982), has been used as the turbulence scheme in MIROC since version 5. Closure level is 2.5. Level 3 is also available, but it is a non-standard option because it does not provide a performance gain worth the increase in computation.

In the MYNN scheme, liquid water potential temperature θ_l and total water q_w are used as thermodynamic variables and are defined as follows, respectively. These are conserved quantities that do not depend on the phase change of water.

$$\theta_l \equiv \left(T - \frac{L_v}{C_p} q_l - \frac{L_v + L_f}{C_p} q_i \right) \left(\frac{p_s}{p} \right)^{\frac{R_d}{C_p}} \tag{493}$$

$$q_w \equiv q_v + q_l + q_i \tag{494}$$

where T and p are temperature and pressure; q_v, q_l, and q_i are specific humidity, cloud water, and cloud ice; C_p and R_d are specific heat at constant pressure and gas constant of dry air; and L_v and L_f are latent heat of vaporization and per unit mass, respectively. p_s is 1000 hPa.

In Level 2.5, the amount of kinetic energy of turbulence multiplied by two is a forecast variable, and its time evolution is also calculated within this scheme. This value is defined by

$$q^2 \equiv \langle u^2 + v^2 + w^2 \rangle \tag{495}$$

where u, v, and w are velocities in the zonal, meridional, and vertical directions, respectively. Hereafter in this chapter, uppercase variables will represent grid mean quantities, and the lowercase variables will represent the deviation from them. $\langle\ \rangle$ denotes an ensemble mean. For Level 3, $\langle {\theta_l}^2 \rangle$, $\langle {q_w}^2 \rangle$, $\langle \theta_l q_w \rangle$ are also forecast variables, but the details are not explained here.

The outline of the calculation procedure is given as follows along with the names of the subroutines.

1. calculation of the friction velocity and the Monin-Obukhov length
2. calculation of the buoyancy coefficients in consideration of partial condensation [`VDFCND`]
3. calculation of the stability functions in Level 2 [`VDFLEV2`]
4. calculation of the depth of the planetary boundary layer [`PBLHGT`]
5. calculation of the master turbulent length scale [`VDFMLS`]
6. calculation of the diffusion coefficients, and the vertical fluxes and their derivatives [`VDFLEV3`]
7. calculation of the generation and dissipation terms of turbulent flow [`VDFLEV3`]
8. computation of implicit time integration of prognostic variables

4.4.1 Surface boundary layer

The friction velocity u_* and the Monin-Obukhov length L_M are given as follows.

$$u_* = \left(\langle uw \rangle_g{}^2 + \langle vw \rangle_g{}^2 \right)^{\frac{1}{4}} \tag{496}$$

$$L_M = -\frac{\Theta_{v,g} {u_*}^3}{kg\langle w\theta_v \rangle_g} \tag{497}$$

where the subscript g indicates that the value is near the surface of the earth, and the value of the lowest layer of the model is used. Θ_v and θ_v denote virtual potential temperature, k the Von Karman constant, and g the gravitational acceleration.

4.4.2 Diagnosis of the buoyancy coefficients

The calculation of the buoyancy term appearing in the turbulence equation requires the value of $\langle w\theta_v \rangle$. Following Mellor (1982), this term can be written as

$$\langle w\theta_v \rangle = \beta_\theta \langle w\theta_l \rangle + \beta_q \langle wq_w \rangle \tag{498}$$

by assuming a probability distribution in the grid of θ_l, q_w. However, unlike Mellor (1982) and Nakanishi and Niino (2004), the probability distribution is not Gaussian, but triangular in shape as given by the PDF-based prognostic large-scale condensation scheme (Watanabe et al. 2008). The buoyancy coefficients β_θ, β_q are written as follows.

$$\beta_\theta = 1 + \epsilon Q_w - (1+\epsilon) Q_l - Q_i - \tilde{R} abc \tag{499}$$

$$\beta_q = \epsilon \Theta + \tilde{R} ac \tag{500}$$

where $\epsilon = R_v/R_d - 1$. R_d and R_v are the gas constants for dry air and water vapor, respectively. Also,

$$a = \left(1 + \frac{L_v}{C_p} \left. \frac{\partial Q_s}{\partial T} \right|_{T=T_l} \right)^{-1} \tag{501}$$

$$b = \frac{T}{\Theta} \left. \frac{\partial Q_s}{\partial T} \right|_{T=T_l} \tag{502}$$

$$c = \frac{\Theta}{T} \frac{L_v}{C_p} \left[1 + \epsilon Q_w - (1+\epsilon) Q_l - Q_i \right] - (1+\epsilon)\Theta \tag{503}$$

$$\tilde{R} = R\left\{1 - a\left[Q_w - Q_s(T_l)\right]\frac{Q_l}{2{\sigma_s}}\right\} - \frac{{Q_l}^2}{4{\sigma_s}^2} \tag{504}$$

$${\sigma_s}^2 = \langle {q_w}^2 \rangle - 2b\langle \theta_l q_w \rangle + b^2 \langle {\theta_l}^2 \rangle \tag{505}$$

where R, Q_l are the amount of cloud and liquid water diagnosed from the probability distribution in the grid, respectively, and Q_s is the amount of saturated water vapor.

4.4.3 Stability functions in the Level 2

It is known that the Mellor-Yamada Level 2.5 scheme fails to capture the behavior of growing turbulence realistically (Helfand and Labraga 1988). Therefore, the MYNN scheme first calculates the kinetic energy of turbulence at Level2, ${q_2}^2/2$, where the local equilibrium is assumed, and then applies a correction when $q < q_2$, i.e., the turbulence is in the growth phase. The stability functions S_{H2}, S_{M2} of Level 2, which are required for the calculation of q_2, can be obtained as follows.

$$S_{H2} = S_{HC}\frac{Rf_c - Rf}{1 - Rf} \tag{506}$$

$$S_{M2} = S_{MC}\frac{R_{f1} - Rf}{R_{f2} - Rf}S_{H2} \tag{507}$$

where Rf denotes the flux Richardson number which is given as follows.

$$Rf = R_{i1}\left(Ri + R_{i2} - \sqrt{Ri^2 - R_{i3}Ri + R_{i4}}\right) \tag{508}$$

Ri is the gradient Richardson number calculated as follows.

$$Ri = \frac{g}{\Theta}\left(\beta_\theta \frac{\partial \Theta_l}{\partial z} + \beta_q \frac{\partial Q_w}{\partial z}\right) \Bigg/ \left[\left(\frac{\partial U}{\partial z}\right)^2 + \left(\frac{\partial V}{\partial z}\right)^2\right] \tag{509}$$

The other symbols are quantities that are independent of the environmental field and are given as follows.

$$S_{HC} = 3A_2(\gamma_1 + \gamma_2) \tag{510}$$

$$S_{MC} = \frac{A_1}{A_2}\frac{F_1}{F_2} \tag{511}$$

$$Rf_c = \frac{\gamma_1}{\gamma_1 + \gamma_2} \tag{512}$$

$$R_{f1} = B_1 \frac{\gamma_1 - C_1}{F_1} \tag{513}$$

$$R_{f2} = B_1 \frac{\gamma_1}{F_2} \tag{514}$$

$$R_{i1} = \frac{1}{2S_{Mc}} \tag{515}$$

$$R_{i2} = R_{f1} S_{MC} \tag{516}$$

$$R_{i3} = 4R_{f2} S_{MC} - 2R_{i2} \tag{517}$$

$$R_{i4} = {R_{i2}}^2 \tag{518}$$

where

$$A_1 = B_1 \frac{1 - 3\gamma_1}{6} \tag{519}$$

$$A_2 = A_1 \frac{\gamma_1 - C_1}{\gamma_1 Pr} \tag{520}$$

$$C_1 = \gamma_1 - \frac{1}{3A_1 {B_1}^{\frac{1}{3}}} \tag{521}$$

$$F_1 = B_1(\gamma_1 - C_1) + 2A_1(3 - 2C_2) + 3A_2(1 - C_2)(1 - C_5) \tag{522}$$

$$F_2 = B_1(\gamma_1 + \gamma_2) - 3A_1(1 - C_2) \tag{523}$$

$$\gamma_2 = \frac{B_2}{B_1}(1 - C_3) + \frac{2A_1}{B_1}(3 - 2C_2) \tag{524}$$

and

$$(Pr, \gamma_1, B_1, B_2, C_2, C_3, C_4, C_5) = (0.74, 0.235, 24.0, 15.0, 0.7, 0.323, 0.0, 0.2) \tag{525}$$

4.4.4 Master turbulent length scale

Formulation by Nakanishi (2001) Nakanishi (2001) proposed the following formula as the master length scale L.

$$\frac{1}{L} = \frac{1}{L_S} + \frac{1}{L_T} + \frac{1}{L_B} \tag{526}$$

L_S, L_T, L_B represent the length scales in the surface layer, convective boundary layer, and stably stratified layer, respectively, and are formulated as follows.

$$L_S = \begin{cases} kz/3.7, & \zeta \geq 1 \\ kz/(2.7+\zeta), & 0 \leq \zeta < 1 \\ kz(1-\alpha_4\zeta)^{0.2}, & \zeta < 0 \end{cases} \tag{527}$$

$$L_T = \alpha_1 \frac{\displaystyle\int_0^\infty qz\, dz}{\displaystyle\int_0^\infty q\, dz} \tag{528}$$

$$L_B = \begin{cases} \alpha_2 q/N, & \partial\Theta_v/\partial z > 0 \quad \text{and} \quad \zeta \geq 0 \\ \left[\alpha_2 + \alpha_3\sqrt{q_c/L_T N}\right] q/N, & \partial\Theta_v/\partial z > 0 \quad \text{and} \quad \zeta < 0 \\ \infty, & \partial\Theta_v/\partial z \leq 0 \end{cases} \tag{529}$$

where $\zeta \equiv z/L_M$ is the height normalized by the Monin-Obukhov length L_M, $N \equiv [(g/\Theta)(\partial\Theta_v/\partial z)]^{1/2}$ is the Brunt-Väisälä frequency, and $q_c \equiv [(g/\Theta)\langle w\theta_v\rangle_g L_T]^{1/3}$ is the velocity scale in the convective boundary layer.

Modifications in the implementation for MIROC The above formulation in Nakanishi (2001) is appropriate when the domain of the model is limited to the atmospheric boundary layer and its peripheral region. However, when the model includes the upper troposphere, problems such as follows may arise depending on the conditions: L_T, the length scale of the convective boundary layer, is used in the free atmosphere, and the turbulent energy in the free atmosphere is included as q in the calculation of L_T.

Therefore, for implementation in MIROC, the top height of the convective boundary layer H_{PBL} is estimated and the region below $h = \sqrt{(F_H H_{PBL})^2 + H_0^2}$ is considered as the region where boundary-layer turbulence is dominant. Here, $F_H = 1.5$ and $H_0 = 500$m.

Below the altitude h, equation (1) is used as the master length scale, but in L_T, the range of integration is modified as follows.

$$\frac{1}{L} = \frac{1}{L_S} + \frac{1}{L_A} + \frac{1}{L_{max}} \tag{530}$$

where $L_A = \alpha_5\, q/N$ is the length scale when an air mass moves vertically due to turbulence in stable stratification. α_5 represents the effect of dissipation and $\alpha_5 = 0.53$. $L_{max} = 500$m gives the upper limit of L.

Estimation of the top height of the convection boundary layer Based on Holtslag and Boville (1993), the estimate of H_{PBL} is calculated using the bulk Richardson number Ri_B given as follows.

$$Ri_B = \frac{[g/\Theta_v(z_1)][\Theta_v(z_k) - \Theta_{v,g}](z_k - z_g)}{[U(z_k) - U(z_1)]^2 + [V(z_k) - V(z_1)]^2 + F_u {u_*}^2} \tag{531}$$

where z_k is the full level altitude of the kth layer from the bottom, z_1 is the full level altitude of the lowest layer of the model, and z_g is the surface altitude. F_u is a dimensionless tuning parameter. Also,

$$\Theta_{v,g} = \Theta_v(z_1) + F_b \frac{\langle w\theta_v \rangle_g}{w_m} \tag{532}$$

$$w_m = u_*/\phi_m \tag{533}$$

$$\phi_m = \left(1 - 15\frac{z_s}{L_M}\right)^{-\frac{1}{3}} \tag{534}$$

where z_s is the altitude of the surface layer, and $z_s = 0.1 H_{PBL}$. F_b is a dimensionless tuning parameter.

Ri_B is calculated in turn from $k = 2$ upward, and is linearly interpolated between the layer where $Ri_B > 0.5$ for the first time and the layer immediately below it. The height where $Ri_B = 0.5$ exactly is used as H_{PBL}. Since H_{PBL} is required for the calculation of z_s, H_{PBL} is first calculated using z_s with the temporary value $H_{PBL} = z_1 - z_g$ substituted, and then the true H_{PBL} is recalculated using z_s with this H_{PBL} substituted.

4.4.5 Calculation of diffusion coefficients

Turbulent kinetic energy in the Level 2 The turbulent kinetic energy of level 2, ${q_2}^2/2$, is calculated from the following equation, which neglects the time derivative, advection, and diffusion terms in the time evolution equation of the turbulent kinetic energy.

$$P_s + P_b - \varepsilon = 0 \tag{535}$$

where P_s, P_b, ε denote the generation term by shear, the generation term by buoyancy, and the dissipation term, respectively. P_s, P_b are represented as follows.

$$P_s = -\langle wu \rangle \frac{\partial U}{\partial z} - \langle wv \rangle \frac{\partial V}{\partial z} \tag{536}$$

$$P_b = \frac{g}{\Theta} \langle w\theta_v \rangle \tag{537}$$

In the Level 2 of the MYNN scheme, they are written as follows.

$$P_s = LqS_{M2}\left[\left(\frac{\partial U}{\partial z}\right)^2 + \left(\frac{\partial V}{\partial z}\right)^2\right] \tag{538}$$

$$P_b = LqS_{H2}\frac{g}{\Theta}\left[\beta_\theta \frac{\partial \Theta_l}{\partial z} + \beta_q \frac{\partial Q_w}{\partial z}\right] \tag{539}$$

$$\varepsilon = \frac{q^3}{B_1 L} \tag{540}$$

From (2), (3), (4), and (5), ${q_2}^2$ is calculated as follows.

$${q_2}^2 = B_1 L^2 \left\{ S_{M2}\left[\left(\frac{\partial U}{\partial z}\right)^2 + \left(\frac{\partial V}{\partial z}\right)^2\right] + S_{H2}\frac{g}{\Theta}\left(\beta_\theta \frac{\partial \Theta_l}{\partial z} + \beta_q \frac{\partial Q_w}{\partial z}\right)\right\} \tag{541}$$

Stability functions in the Level 2.5 When $q < q_2$, i.e., the turbulence is in the growth phase, the stability functions of level 2.5, S_M and S_H, are calculated as follows using the coefficient $\alpha = q/q_2$ introduced by Helfand and Labraga (1998).

$$S_M = \alpha S_{M2}, \quad S_H = \alpha S_{H2} \tag{542}$$

On the other hand, when $q \geq q_2$, S_M and S_H are calculated as follows. The following equations differ from those in Nakanishi (2001) in the description method, but gives equivalent results with less computation.

$$S_M = A_1 \frac{E_3 - 3C_1 E_4}{E_2 E_4 + E_5 E_3} \tag{543}$$

$$S_H = A_2 \frac{E_2 + 3C_1 E_5}{E_2 E_4 + E_5 E_3} \tag{544}$$

where

$$E_1 = 1 - 3A_2 B_2 (1 - C_3) G_H \tag{545}$$

$$E_2 = 1 - 9A_1 A_2 (1 - C_2) G_H \tag{546}$$

$$E_3 = E_1 + 9{A_2}^2 (1 - C_2)(1 - C_5) G_H \tag{547}$$

$$E_4 = E_1 - 12A_1A_2(1 - C_2)G_H \tag{548}$$

$$E_5 = 6{A_1}^2 G_M \tag{549}$$

$$G_M = \frac{L^2}{q^2}\left[\left(\frac{\partial U}{\partial z}\right)^2 + \left(\frac{\partial V}{\partial z}\right)^2\right] \tag{550}$$

$$G_H = -\frac{L^2}{q^2}\frac{g}{\Theta}\left(\beta_\theta \frac{\partial \Theta_l}{\partial z} + \beta_q \frac{\partial Q_w}{\partial z}\right) \tag{551}$$

Calculation of diffusion coefficients The diffusion coefficients K_M, K_q, K_H, and K_w for wind speed, turbulent energy, heat, and water are calculated as follows from S_M, S_H.

$$K_M = LqS_M \tag{552}$$

$$K_q = 3LqS_M \tag{553}$$

$$K_H = LqS_H \tag{554}$$

$$K_w = LqS_H \tag{555}$$

Calculation of fluxes The vertical flux F of each physical quantity is calculated as follows.

$$F_{u,k-1/2} = -\rho_{k-1/2}K_{M,k-1/2}\frac{U_k - U_{k-1}}{\Delta z_{k-1/2}} \tag{556}$$

$$F_{v,k-1/2} = -\rho_{k-1/2}K_{M,k-1/2}\frac{V_k - V_{k-1}}{\Delta z_{k-1/2}} \tag{557}$$

$$F_{q,k-1/2} = -\rho_{k-1/2}K_{q,k-1/2}\frac{{q^2}_k - {q^2}_{k-1}}{\Delta z_{k-1/2}} \tag{558}$$

$$F_{T,k-1/2} = -\rho_{k-1/2}K_{H,k-1/2}\, C_p \Pi_{k-1/2}\frac{\Theta_{l,k} - \Theta_{l,k-1}}{\Delta z_{k-1/2}} \tag{559}$$

$$F_{w,k-1/2} = -\rho_{k-1/2} K_{w,k-1/2} \frac{Q_{w,k} - Q_{w,k-1}}{\Delta z_{k-1/2}} \tag{560}$$

where ρ is density and Π is the Exner function. In order to perform time integration with implicit scheme, the derivative of each vertical flux is also obtained as follows.

$$\frac{\partial F_{u,k-1/2}}{\partial U_{k-1}} = \frac{\partial F_{v,k-1/2}}{\partial V_{k-1}} = -\frac{\partial F_{u,k-1/2}}{\partial U_k} = -\frac{\partial F_{v,k-1/2}}{\partial V_k} = \rho_{k-1/2} K_{M,k-1/2} \frac{1}{\Delta z_{k-1/2}} \tag{561}$$

$$\frac{\partial F_{q,k-1/2}}{\partial {q^2}_{k-1}} = -\frac{\partial F_{q,k-1/2}}{\partial {q^2}_k} = \rho_{k-1/2} K_{q,k-1/2} \frac{1}{\Delta z_{k-1/2}} \tag{562}$$

$$\frac{\partial F_{T,k-1/2}}{\partial T_{k-1}} = \rho_{k-1/2} K_{H,k-1/2} C_p \frac{\Pi_{k-1/2}}{\Pi_{k-1}} \frac{1}{\Delta z_{k-1/2}} \tag{563}$$

$$\frac{\partial F_{T,k-1/2}}{\partial T_k} = -\rho_{k-1/2} K_{H,k-1/2} C_p \frac{\Pi_{k-1/2}}{\Pi_k} \frac{1}{\Delta z_{k-1/2}} \tag{564}$$

$$\frac{\partial F_{w,k-1/2}}{\partial Q_{w,k-1}} = -\frac{\partial F_{w,k-1/2}}{\partial Q_{w,k}} = \rho_{k-1/2} K_{w,k-1/2} \frac{1}{\Delta z_{k-1/2}} \tag{565}$$

where $\Delta z_{k-1/2} = z_k - z_{k-1}$. The fluxes for other tracers are also calculated in the same way using K_w.

4.4.6 Calculation of turbulent variables

Calculation of turbulent kinetic energy The prognostic equation for q^2 is expressed as follows.

$$\frac{dq^2}{dt} = -\frac{1}{\rho}\frac{\partial F_q}{\partial z} + 2\left(P_s + P_b - \varepsilon\right) \tag{566}$$

In the Level 2.5, P_s, P_b, ε are written as follows.

$$P_s = LqS_M \left[\left(\frac{\partial U}{\partial z} \right)^2 + \left(\frac{\partial V}{\partial z} \right)^2 \right] \tag{567}$$

$$P_b = LqS_H \frac{g}{\Theta} \left(\beta_\theta \frac{\partial \Theta_l}{\partial z} + \beta_q \frac{\partial Q_w}{\partial z} \right) \tag{568}$$

$$\varepsilon = \frac{q^3}{B_1 L} \tag{569}$$

Advection terms are calculated using tracer transport routines in the dynamics scheme. In the turbulence scheme, the time evolution by diffusion, generation and dissipation terms of q^2 is calculated by the implicit scheme.

Diagnosis of variance and covariance The prognostic equations for $\langle {\theta_l}^2 \rangle, \langle {q_w}^2 \rangle, \langle \theta_l q_w \rangle$ are expressed as follows.

$$\frac{d\left\langle {\theta_l}^2 \right\rangle}{dt} = -\frac{\partial}{\partial z}\left\langle w\theta_l^2 \right\rangle - 2\left\langle w\theta_l \right\rangle \frac{\partial \Theta_l}{\partial z} - 2\varepsilon_{\theta l} \tag{570}$$

$$\frac{d\left\langle {q_w}^2 \right\rangle}{dt} = -\frac{\partial}{\partial z}\left\langle wq_w^2 \right\rangle - 2\left\langle wq_w \right\rangle \frac{\partial Q_w}{\partial z} - 2\varepsilon_{qw} \tag{571}$$

$$\frac{d\left\langle \theta_l q_w \right\rangle}{dt} = -\frac{\partial}{\partial z}\left\langle w\theta_l q_w \right\rangle - \left\langle wq_w \right\rangle \frac{\partial \Theta_l}{\partial z} - \left\langle w\theta_l \right\rangle \frac{\partial Q_w}{\partial z} - 2\varepsilon_{\theta q} \tag{572}$$

In the Level 2.5, the time derivative, advection, and diffusion terms in these equations are ignored, and the following balances are assumed locally.

$$-\left\langle w\theta_l \right\rangle \frac{\partial \Theta_l}{\partial z} - \varepsilon_{\theta l} = 0 \tag{573}$$

$$-\left\langle wq_w \right\rangle \frac{\partial Q_w}{\partial z} - \varepsilon_{qw} = 0 \tag{574}$$

$$-\left\langle wq_w \right\rangle \frac{\partial \Theta_l}{\partial z} - \left\langle w\theta_l \right\rangle \frac{\partial Q_w}{\partial z} - 2\varepsilon_{\theta q} = 0 \tag{575}$$

In the Level 2.5 of MYNN scheme, $-\left\langle w\theta_l \right\rangle$, $-\left\langle wq_w \right\rangle$, $\varepsilon_{\theta l}$, ε_{qw}, $\varepsilon_{\theta q}$ are represented as follows.

$$-\left\langle w\theta_l \right\rangle = LqS_H \frac{\partial \Theta_l}{\partial z} \tag{576}$$

$$-\left\langle wq_w \right\rangle = LqS_H \frac{\partial Q_w}{\partial z} \tag{577}$$

$$\varepsilon_{\theta l} = \frac{q}{B_2 L}\left\langle \theta_l^2 \right\rangle \tag{578}$$

$$\varepsilon_{qw} = \frac{q}{B_2 L}\left\langle q_w^2 \right\rangle \tag{579}$$

$$\varepsilon_{\theta q} = \frac{q}{B_2 L}\left\langle \theta_l q_w \right\rangle \tag{580}$$

from (6)-(13), $\langle {\theta_l}^2 \rangle$, $\langle {q_w}^2 \rangle$, $\langle \theta_l q_w \rangle$ can be diagnosed as follows.

$$\langle {\theta_l}^2 \rangle = B_2 L^2 S_H \left(\frac{\partial \Theta_l}{\partial z} \right)^2 \tag{581}$$

$$\langle {q_w}^2 \rangle = B_2 L^2 S_H \left(\frac{\partial Q_w}{\partial z} \right)^2 \tag{582}$$

$$\langle \theta_l q_w \rangle = B_2 L^2 S_H \frac{\partial \Theta_l}{\partial z} \frac{\partial Q_w}{\partial z} \tag{583}$$

Treatment in the bottom layer Since the lowest layer of the model corresponds to the ground layer where the vertical gradient of geophysical quantities change rapidly, the following Monin-Obukhov similarity theory is used to evaluate the vertical gradient accurately.

$$\frac{\partial M}{\partial z} = \frac{u_*}{kz} \phi_m \tag{584}$$

$$\frac{\partial \Theta}{\partial z} = \frac{\theta_*}{kz} \phi_h \tag{585}$$

$$\frac{\partial Q_v}{\partial z} = \frac{q_{v*}}{kz} \phi_h \tag{586}$$

where M is the wind speed when the horizontal axis is in the direction of the horizontal wind in the surface layer. ϕ_m and ϕ_h are the dimensionless gradient functions for momentum and heat, respectively. θ_*, q_{v*} are the scales of potential temperature and water vapor in the surface layer, respectively, and satisfy the following relationships.

$$\langle wm \rangle_g = -u_*^2 \tag{587}$$

$$\langle w\theta \rangle_g = -u_* \theta_* \tag{588}$$

$$\langle wq_v \rangle_g = -u_* q_{v*} \tag{589}$$

m is the deviation of M from the grid average. Using M and m, the generation term of turbulence kinetic energy can be written as

$$P_s + P_b = \langle wm \rangle \frac{\partial M}{\partial z} + \frac{g}{\Theta} \langle w\theta_v \rangle \tag{590}$$

Using (14), (17) and the defining equation of the Monin-Obukhov length, this can be calculated as follows.

$$P_s + P_b = \frac{u_*^3}{kz_1} \left[\phi_m \left(\zeta_1 \right) - \zeta_1 \right] \tag{591}$$

Here, ζ_1 is ζ at the full level of the lowest layer of the model.

By assuming that there are no cloud particles in the surface layer, $\langle {\theta_l}^2 \rangle$, $\langle {q_w}^2 \rangle$, $\langle \theta_l q_w \rangle$ can be calculated diagnostically from (6)-(8), (11)-(13), (15), (16), (18), and (19) as follows.

$$\langle {\theta_l}^2 \rangle = \frac{\phi_h \left(\zeta_1 \right)}{u_* k z_1} \langle w\theta \rangle_g{}^2 \Big/ \frac{q}{B_2 L} \tag{592}$$

$$\langle {q_w}^2 \rangle = \frac{\phi_h \left(\zeta_1 \right)}{u_* k z_1} \langle w q_v \rangle_g{}^2 \Big/ \frac{q}{B_2 L} \tag{593}$$

$$\langle \theta_l q_w \rangle = \frac{\phi_h \left(\zeta_1 \right)}{u_* k z_1} \langle w\theta \rangle_g \langle w q_v \rangle_g \Big/ \frac{q}{B_2 L} \tag{594}$$

ϕ_m, ϕ_h are formulated as follows based on Businger et al. (1971).

$$\phi_m(\zeta) = \begin{cases} 1 + \beta_1 \zeta, & \zeta \geq 0 \\ \left(1 - \gamma_1 \zeta \right)^{-1/4}, & \zeta < 0 \end{cases} \tag{595}$$

$$\phi_h(\zeta) = \begin{cases} \beta_2 + \beta_1 \zeta, & \zeta \geq 0 \\ \beta_2 \left(1 - \gamma_2 \zeta \right)^{-1/2}, & \zeta < 0 \end{cases} \tag{596}$$

$$(\beta_1, \beta_2, \gamma_1, \gamma_2) = (4.7, 0.74, 15.0, 9.0) \tag{597}$$

4.4.7 Time integration with implicit scheme

- ??
- ??
  - ??
    - ??
    - ??
  - ??
    - ??
  - ??
  - ??

5 1 Surface Flux

Until CCSR/NIES AGCM, both land surface and sea surface were treated as one of the atmospheric physical processes, but after MIROC3 (Hasumi and Emori, 2004), land surface processes became independent as MATSIRO. However, since MIROC3 (Hasumi and Emori, 2004), land surface processes have been separated into MATSIRO. In `SUBROUTINE:[SURFCE]` in pgsfc.F, `ENTRY:[OCNFLX]` (in `SUBROUTINE:[OCEAN]` of pgocn.F) is called for the sea surface, and `ENTRY:[LNDFLX]` (in `SUBROUTINE:[MATSIRO]` of matdrv.F) is called for the land surface, respectively. This chapter describes sea surface processes, which are still treated within the framework of atmospheric physical processes (MIROC6). For the land surface processes, please refer to Description of ILS.

カップラーのセクションと merge 予定。

- Outputs

Meaning	Presentation	Variable	dimension	unit
upward long wave		RFLXLG	IJLSDIM	
upward short wave		RFLXSG	IJLSDIM	

- Inputs

Meaning	Presentation	Variable	dimension	unit
surface downward radiation		RFSFCD	IJSDIM, NRALB	
cos(solar zenith)	$cos(\theta)$	RCOSZ	IJSDIM	[-]
rainfall (cumulus convection scheme)		GPRCC	IJSDIM, NTR	
rainfall (Large scale condensation scheme)		GPRCL	IJSDIM, NTR	
snowfall (cumulus convection scheme)		GSNWC	IJSDIM, NTR	

Meaning	Presentation	Variable	dimension	unit
snowfall (cLarge scale condensation scheme)		GSNWL	IJSDIM, NTR	
u wind	u	GDU	IJSDIM, KMAX	[m/s]
v wind	v	GDV	IJSDIM, KMAX	[m/s]
temperature	T	GDT	IJSDIM, KMAX	[K]
humidity	q	GDQ	IJSDIM, KMAX, NTR	[kg/kg]
pressure	P	GDP	IJSDIM, KMAX+1	
pressure (half level)		GDPM	IJSDIM, KMAX+1	
altitude (half level)		GDZM	IJSDIM, KMAX+1	
time		TIME		
dt for implicit		DELTP		
time step (interval)		DELTI		

The only 1st layer is practically handed to the surface schemes.

6 1.1 Sea surface flux [OCNFLX]

Sea surface processes provide the boundary conditions at the lower end of the atmosphere through the exchange of momentum, heat, and water fluxes between the atmosphere and the surface. In ENTRY:[OCNFLX], the following procedure is used to deal with sea surface processes.

1. prepare variables for sea ice extent and no ice extent, respectively, using sea ice concentration.
2. Determine the surface boundary conditions.
3. Calculate the flux balance.
4. Calculate the radiation budget at the sea surface.
5. Calculate the deposition by CHASER.
6. solve the heat balance at the sea surface and update the surface temperature and each flux value.

Meaning	Presentation	Variable	dimension	unit
u wind of the 1st layer of the atmosphere	u_a	GAUA	IJOSDM	[m/s]
v wind of the 1st layer of the atmosphere	v_a	GAVA	IJOSDM	[m/s]
temperature of the 1st layer of the atmosphere	T_a	GATA	IJOSDM	[K]
humidity of the 1st layer of the atmosphere	q_a	GAQA	IJOSDM	[kg/kg]
pressure of the 1st layer of the atmosphere	P_a	GAPA	IJOSDM	
surface pressure Ps	P_s	GAPS	IJOSDM	
surface height		GAZS	IJOSDM	
surface radiation fluxes		RSFCD	IJOSDM	
cos(solar zenith)	$cos(\theta)$	RCOSZ	IJOSDM	[-]

If use CHASER, variables below are also needed.

Meaning	Presentation	Variable	dimension	unit
Henry const		EH	IJOSDM	
precipitation flux (cumulus convection scheme)	Pr_c	PFLXC	IJOSDM	
precipitation flux (large scale condensation scheme)	Pr_l	PFLXL	IJOSDM	
latitude		LLAT	IJOSDM	

Practically, precipitation flux from 2 schemes are treated together.

$$Pr = Pr_c + Pr_l \tag{598}$$

In the sea ice area ($L = 1$), the surface temperature T_s is the sea ice surface temperature T_{ice}. However, if T_{ice} is higher than $T_{melt} = 0$, then T_{melt} is used.

$$T_s = min(T_{ice}, T_{melt}) \tag{599}$$

The sea ice bottom temperature T_b is assumed to be the sea surface temperature $T_{o(1)}$.

$$T_b = T_{o(1)} \tag{600}$$

The amount of sea ice W_{ice} and the amount of snow on it W_{snow} are converted per unit area by considering R_{ice} and used in the calculation. However, a limiter ϵ is provided to prevent the values from becoming too small.

$$R_{ice} = \max(R_{ice,orginal}, \epsilon) \tag{601}$$

In the ice-free region ($L = 2$), the surface temperature T_s and sea ice bottom temperature T_b are assumed to be the sea temperature temperature $T_{o(1)}$.

$$T_s = T_b = T_{o(1)} \tag{602}$$

The evaporation efficiency ise set to 1 for both $L = 1, 2$.

If the sea ice concentration R_{ice} is not given, it can be diagnosed simply from the sea ice volume W_{ice} in `ENTRY:[OCNICR]`.

$$R_{ice} = \min\Big(\sqrt{\frac{\max(W_{ice}, 0)}{W_{ice,c}}}, 1.0\Big) \tag{603}$$

The standard gives the amount of sea ice per area as $W_{ice,c} = 300[\mathrm{kg/m^2}]$.

6.1 1.2 Sea Surface Conditions `[OCNBCS]`

- Output variables

Meaning	Presentation	Variable	dimension	unit
surface albedo	α	GRALB	IJLODM, NRDIR, NRBND	–
surface roughness	r_0	GRZ0	IJLODM, NTYZ0	–
heat flux	G	FOGFLX	IJLODM	–
heat diffusion coefficient	$\frac{\partial G}{\partial T}$	DGFDS	IJLODM	–

- Input variables

Meaning	Presentation	Variable	dimension	unit
surface temperature	T_s	GRTS	IJLODM	[K]
ice base temperature	T_b	GRTB	IJLODM	[K]
lake ice amount	Ic	GRICE	IJLODM	[kg/m^2]
snow amount	Sn	GRSNW	IJLODM	
ice concentration	R_{ice}	GRICR	IJLODM	[-]
u wind of the 1st layer of the atmosphere	u_a	GDUA	IJLODM	[m/s]
v wind of the 1st layer of the atmosphere	v_a	GDVA	IJLODM	[m/s]
cos(solar zenith)	$\cos(\theta)$	RCOSZ	IJLODM	[-]

In `ENTRY[OCNBCS]` in `SUBROUTINE:[OCNSUB]`, surface albedo and roughness are calculated. They are calculated supposing ice-free conditions, then modified.

First, let us consider the sea albedo. The sea level $\alpha_{(d,b)}$, $b = 1, 2, 3$ represent the visible, near-infrared, and infrared wavelength bands, respectively. Also, $d = 1, 2$ represents direct and scattered light, respectively. The albedo for the visible bands are calculated in `SUBROUTINE [SEAALB]`, supposing ice-free conditions. The albedo for near-infrared is set to same as the visible one. The albedo for infrared is uniformly set to a constant value.

The grid-averaged albedo, taking into account the sea ice concentration R_{ice}, is

$$\alpha = \alpha - R_{ice}\alpha_{ice} \tag{604}$$

α_{ice} is given by the standard as $\alpha_{ice,1} = 0.5, \alpha_{ice,2} = 0.5, \alpha_{ice,3} = 0.05$. 4.

In addition, we want to consider the effect of snow cover. Here, we consider the albedo modification by temperature. The standard threshold values for snow temperature are $T_{al,2} = 258.15$[K] and $T_{al,1} = 273.15$[K]. The snow albedo changes linearly with temperature change from $\alpha_{snow,1} = 0.75$ to $\alpha_{snow,2}$. Let the coefficient τ_{snow}, which is $0 \leq \tau \leq 1$.

$$\tau_{snow} = \frac{T_s - T_{al,1}}{T_{al,2} - T_{al,1}} \tag{605}$$

Update the snow albedo α_{snow} as

$$\alpha_{snow} = \alpha_{snow,0} + \tau_{snow}(\alpha_{snow,2} - \alpha_{snow,1}) \tag{606}$$

Second, let us consider the sea surface roughness. The roughnesses of for momentum, heat and vapor are calculated in `[SEAZOF]`, supposing the ice-free conditions.

When the sea ice exists ($L = 1$), each roughness is modified to take into account the sea concentration R_{ice}.

$$z_{0,M} = z_{0,M} + (z_{0,ice,M} - z_{0,M})\alpha_{ice} \tag{607}$$

$$z_{0,H} = z_{0,H} + (z_{0,ice,H} - z_{0,H})\alpha_{ice} \tag{608}$$

$$z_{0,E} = z_{0,E} + (z_{0,ice,E} - z_{0,E})\alpha_{ice} \tag{609}$$

Here, $r_{0,ice,*}$ is roughness of sea ice, α_{ice} is the sea ice concentration.

When the snow even exists,

$$z_{0,M} = z_{0,M} + (z_{0,snow,M} - z_{0,M})\alpha_{snow} \tag{610}$$

$$z_{0,H} = z_{0,H} + (z_{0,snow,H} - z_{0,H})\alpha_{snow} \tag{611}$$

$$z_{0,E} = z_{0,E} + (z_{0,snow,E} - z_{0,E})\alpha_{snow} \tag{612}$$

Here, $r_{0,snow,*}$ is roughness of sea ice, α_{snow} is the sea ice concentration.

Third, let us consider the conductivity of ice.

When sea ice exists ($L = 1$), the thermal conductivity $k^{\star}_{ice}$ of sea ice is obtained by using $D_{f,ice}$ (thermal diffusivity of sea ice) and sea ice density σ_{ice}.

$$k^{\star}_{ice} = \frac{D_{f,ice}}{\max(R_{ice}/\sigma_{ice}, \epsilon)} \tag{613}$$

The calculated thermal conductivity is modified to k_{ice} to take into account that it varies with snow cover.

$$h_{snow} = \min(\max(R_{snow}/\sigma_{snow}), \epsilon), h_{snow,max}) \tag{614}$$

$$k_{ice} = k^{\star}_{ice}(1 - R_{ice}) + \frac{D_{ice}}{1 + \|D_{ice}/D_{snow} \cdot h_{snow}\|} R_{ice} \tag{615}$$

where h_{snow} is the snow depth, R_{snow} is the snow area fraction, σ_{snow} is the snow density, $h_{snow,max}$ is the maximum snow depth, and D_{snow} is the thermal diffusivity of snow.

Therefore, the heat conduction flux and its derivative are

$$G = k_{ice}(T_b - T_s) \tag{616}$$

$$\frac{\partial G}{\partial T} = k_{ice} \tag{617}$$

Note that in the ice-free region ($L = 2$)

$$G = k_{ocn} \tag{618}$$

where k_{ocn} is the heat flux in the sea temperature layer. Here, k_{ocn} is the heat flux in the sea temperature layer.

6.1.1 1.2.1 Sea Surface Albedo for Visible [SEAALB]

- Inputs

Meaning	Presentation	Variable	dimension	unit
cos(solar zenith)	$cos(\theta)$	COSZ	IJLODM	[-]

- Outputs

Meaning	Presentation	Variable	dimension	unit
sea surface albedo (direct, diffuse)	$\alpha_{L(d)}$	GALB	IJLODM ,2	[-]

For sea surface level albedo $\alpha_{L(d)}$, $d = 1, 2$ represents direct and scattered light, respectively. Using the solar zenith angle at latitude θ, the albedo for direct light is presented by

$$\alpha_{L(1)} = e^{(C_3 A^* + C_2)A^* + C_1} \tag{619}$$

where

$$A = \min(\max(\cos(\theta), 0.03459), 0.961) \tag{620}$$

On the other hand, the albedo for scattered light is uniformly set to a constant parameter.

$$\alpha_{L(2)} = 0.06 \tag{621}$$

6.1.2 1.2.2 Sea Surface Roughness [SEAZ0F]

- Outputs

Meaning	Presentation	Variable	dimension	unit
surface roughness for momentum	$r_{0,M}$	GRZ0M	IJLODM	–
surface roughness for heat	$r_{0,H}$	GRZ0H	IJLODM	–
surface roughness for vapor	$r_{0,E}$	GRZ0E	IJLSDIM	–

- Inputs

Meaning	Presentation	Variable	dimension	unit
u wind of the 1st layer of the atmosphere	u_a	GDUA	IJLODM	[m/s]
v wind of the 1st layer of the atmosphere	v_a	GDVA	IJLODM	[m/s]

The roughness variation of the sea surface is determined by the friction velocity $u^\star$

$$u^\star = \sqrt{C_{M_0}({u_a}^2 + {v_a}^2)} \tag{622}$$

We perform successive approximation calculation of C_{M_0}, because F_u, F_v, F_θ, F_q are required.

$$r_{0,M} = z_{0,M_0} + z_{0,M_R} + \frac{z_{0,M_R} {u^\star}^2}{g} + \frac{z_{0,M_S}\nu}{u^\star} \tag{623}$$

$$r_{0,H} = z_{0,H_0} + z_{0,H_R} + \frac{z_{0,H_R} {u^\star}^2}{g} + \frac{z_{0,H_S}\nu}{u^\star} \tag{624}$$

$$r_{0,E} = z_{0,E_0} + z_{0,E_R} + \frac{z_{0,E_R} {u^\star}^2}{g} + \frac{z_{0,E_S}\nu}{u^\star} \tag{625}$$

Here, $\nu = 1.5 \times 10^{-5}[\mathrm{m}^2/\mathrm{s}]$ is the kinetic viscosity of the atmosphere. $z_{0,M}, z_{0,H}$ and $z_{0,E}$ are surface roughness for momentum, heat, and vapor, respectively. z_{0,M_0}, z_{0,H_0} and z_{0,E_0} are base, and rough factor (z_{0,M_R}, z_{0,M_R} and z_{0,E_R}) and smooth factor (z_{0,M_S}, z_{0,M_S} and z_{0,E_S}) are taken into account.

6.2 1.3 Sea Surface Flux [SFCFLX]

The surface flux scheme evaluates the physical quantity fluxes between the atmospheric surfaces due to turbulent transport in the boundary layer. The main input are wind speed (u_a, v_a),

temperature (T_a), and specific humidity (q_s) from the 1st layer of the atmosphere. The output are the vertical fluxes and the differential values (for obtaining implicit solutions) of momentum, heat, and water vapor.

Surface fluxes (F_u, F_v, F_θ, F_q) are expressed using the bulk coefficients (C_M, C_H, C_E) as follows

$$F_u = -\rho C_M |\mathbf{v}| u \tag{626}$$

$$F_v = -\rho C_M |\mathbf{v}| v \tag{627}$$

$$F_\theta = \rho c_p C_H |\mathbf{v}| (\theta_g - \theta) \tag{628}$$

$$F_q^P = \rho C_E |\mathbf{v}| (q_g - q_a) \tag{629}$$

Note that F_q^P is the possible evaporation flux.

The turbulent fluxes at the sea surface are solved by bulk formulae as follows. Then, by solving the surface energy balance, the ground surface temperature (T_s) is updated, and the surface flux values with respect to those values are also updated. The solutions obtained here are temporary values. In order to solve the energy balance by linearizing with respect to T_s, the differential with respect to T_s of each flux is calculated beforehand.

- Momentum flux

$$\tau_x = -\rho C_M |V_a| u_a \tag{630}$$

$$\tau_y = -\rho C_M |V_a| v_a \tag{631}$$

where τ_x and τ_y are the momentum fluxes (surface stress) of the zonal and meridional directions, respectively.

- Sensible heat flux

$$H_s = c_p \rho C_{Hs} |V_a| (T_s - (P_s/P_a)^\kappa T_a) \tag{632}$$

where H_s is the sensible heat flux from the sea surface; $\kappa = R_{air}/c_p$ and $R_{air}$are the gas constants of air; and c_p is the specific heat of air.

- Bare sea surface evaporation flux

$$\hat{F} q_{1/2}^P = \rho_{1/2} C_E |\mathbf{v}_1| \left(q^\star(T_0) - q_1\right) \tag{633}$$

6.2.1 1.3.1 Bulk factor [BLKCOF]

The bulk Richardson number (R_{iB}), which is used as a benchmark for the stability between the atmospheric surfaces, is

$$R_{iB} = \frac{\frac{g}{\theta_s}(\theta_1 - \theta(z_0))/z_1}{(u_1/z_1)^2} = \frac{g}{\theta_s}\frac{T_1(p_s/p_1)^\kappa - T_0}{u_1^2/z_1} f_T \tag{634}$$

Here, g is the gravitational accerelation, θ_s (Θ_0 in MATSIRO description) is the basic potential temperature, T_1 is the atmospheric temperature of the 1st layer, T_0 is the surface surface temperature, p_s is the surface pressure, p_1 is the pressure of the 1st layer, $\$\kappa\$ is the Karman constant, and

$$f_T = (\theta_1 - \theta(z_0))/(\theta_1 - \theta_0) \tag{635}$$

The bulk coefficients of C_M, C_H, C_E are calculated according to Louis (1979) and Louis *et al.*(1982). However, corrections are made to take into account the difference between momentum and heat roughness. If the roughnesses for momentum, heat, and water vapor are set to $z_{0,M}, z_{0,H}, z_{0,E}$, respectively, the results are generally $z_{0,M} > z_{0,H}, z_{0,E}$, but the bulk coefficients for heat and water vapor for the fluxes from the height of $z_{0,M}$ are also set to $\widetilde{C_H}$, $\widetilde{C_E}$ first, and then corrected.

$$C_M = \begin{cases} C_{0,M}[1 + (b_M/e_M)R_{iB}]^{-e_M} & , R_{iB} \geq 0 \\ C_{0,M}\left[1 - b_M R_{iB}\left(1 + d_M b_M C_{0,M}\sqrt{\frac{z_1}{z_{0,M}}|R_{iB}|}\right)^{-1}\right] & , R_{iB} < 0 \end{cases} \tag{636}$$

$$\widetilde{C_H} = \begin{cases} \widetilde{C_{0,H}}[1 + (b_H/e_H)R_{iB}]^{-e_H} & , R_{iB} \geq 0 \\ \widetilde{C_{0,H}}\left[1 - b_H R_{iB}\left(1 + d_H b_H \widetilde{C_{0,H}}\sqrt{\frac{z_1}{z_{0,M}}|R_{iB}|}\right)^{-1}\right] & , R_{iB} < 0 \end{cases} \tag{637}$$

$$C_H = \widetilde{C_H} f_T \tag{638}$$

$$\widetilde{C_E} = \begin{cases} \widetilde{C_{0,E}}[1 + (b_E/e_E)R_{iB}]^{-e_E} & , R_{iB} \geq 0 \\ \widetilde{C_{0,E}}\left[1 - b_E R_{iB}\left(1 + d_E b_E \widetilde{C_{0,E}}\sqrt{\frac{z_1}{z_{0,M}}|R_{iB}|}\right)^{-1}\right] & , R_{iB} < 0 \end{cases} \tag{639}$$

$$C_E = \widetilde{C_E} f_q \tag{640}$$

$C_{0M}, \widetilde{C_{0H}}, \widetilde{C_{0E}}$ is the bulk coefficient (for fluxes from z_{0M}) at neutral,

$$C_{0M} = \widetilde{C_{0H}} = \widetilde{C_{0E}} = \frac{k^2}{\left[\ln\left(\frac{z_1}{z_{0M}}\right)\right]^2} \tag{641}$$

Correction Factor f_q is ,

$$f_q = (q_1 - q(z_0))/(q_1 - q^*(\theta_0)) \tag{642}$$

but the method of calculation is omitted. The coefficients of Louis factors are $(b_M, d_M, e_M) = (9.4, 7.4, 2.0)$, $(b_H, d_H, e_H) = (b_E, d_E, e_E) = (9.4, 5.3, 2.0)$.

is a correction factor, which is approximated from the uncorrected bulk Richardson number, but we abbreviate the calculation here.

6.3 1.4 Radiation Flux at Sea Surface [RADSFC]

For the ground surface albedo $\alpha_{(d,b)}$, $b = 1, 2$ represent the visible and near-infrared wavelength bands, respectively. Also, $d = 1, 2$ are direct and scattered, respectively. For the downward shortwave radiation $SW^{\downarrow}$ and upward shortwave radiation $SW^{\uparrow}$ incident on the earth's surface, the direct and scattered light together are

$$SW^{\downarrow} = SW^{\downarrow}_{(1,1)} + SW^{\downarrow}_{(1,2)} + SW^{\downarrow}_{(2,1)} + SW^{\downarrow}_{(2,2)} \tag{643}$$

$$SW^{\uparrow} = SW^{\downarrow}_{(1,1)} \cdot \alpha_{(1,1)} + SW^{\downarrow}_{(1,2)} \cdot \alpha_{(1,2)} + SW^{\downarrow}_{(2,1)} \cdot \alpha_{(2,1)} + SW^{\downarrow}_{(2,2)} \cdot \alpha_{(2,2)} \tag{644}$$

6.4 1.5 Sea Surface Heat Balance [OCNSLV]

The comments for some variables say "soil", but this is because the program was adapted from a land surface scheme, and has no particular meaning.

- Outputs

Meaning	Presentation	Variable	dimension	unit
surface water flux	$W_{free/ice}$	WFLUXS	IJLODM,2	–
upward long wave	$LW^{\uparrow}$	RFLXLU	IJLODM	–
flux balance	F	SFLXBL	IJLODM	–

- Inputs variables

Meaning	Presentation	Variable
sensible heat flux coefficent	$\frac{\partial H}{\partial T_s}$	DTFDS
latent heat flux coefficient	$\frac{\partial E}{\partial T_s}$	DQFDS
surface heat flux coefficient	$\frac{\partial G}{\partial T_s}$	DGFDS
downward SW radiation	$SW^{\downarrow}$	RFLXSD
upward SW radiation	$SW^{\uparrow}$	RFLXLU

Meaning	Presentation	Variable
downward LW radiation	$LW^{\downarrow}$	RFLXLD
sea surface albedo	α	GRALBL
sea ice concentration	R_{ice}	GRICR

- Modified in this subroutine

Meaning	Presentation	Variable	dimension	unit
surface temperature	T_s	GDTS	IJLODM	–
surface heat flux from `seaBC`	G	GFLUXS	IJLODM	–
sensible heat flux	H	TFLUXS	IJLODM	–
latent heat flux	E	QFLUXS	IJLDSM	–

- Others (appeared in texts)

Meaning	Presentation	Variable	dimension	unit
sea surface albedo for shortwave radiation (ice-free)	α_S	–	[-]	–
the Stefan-Boltzmann constant	σ	STB	–	–

Reference: Hasumi, 2015, Appendices A

Downward radiative fluxes are not directly dependent on the condition of the sea surface, and their observed values are simply specified to drive the model. Shotwave emission from the sea surface is negligible, so the upward part of the shortwave radiative flux is accounted for solely by reflection of the incoming downward flux. Let α_S be the sea surface albedo for shortwave radiation. The upward shortwave radiative flux is represented by

$$SW^{\uparrow} = -\alpha_S SW^{\downarrow} \tag{645}$$

On the other hand, the upward longwave radiative flux has both reflection of the incoming flux and emission from the sea surface. Let α be the sea surface albedo for longwave radiation and ϵ be emissivity of the sea surface relative to the black body radiation. The upward shortwave radiative flux is represented by

$$LW^{\uparrow} = -\alpha LW^{\downarrow} + \epsilon\sigma T_s^4 \tag{646}$$

where σ is the Stefan-Boltzmann constant and T_s is surface temperature. If sea ice exists, snow or sea ice temperature is considered by fractions. When radiative equilibrium is assumed, emissivity becomes identical to co-albedo:

$$\epsilon = 1 - \alpha \tag{647}$$

The net surface flux is presented by

$$F^* = H + (1-\alpha)\sigma T_s^4 + \alpha LW^{\uparrow} - LW^{\downarrow} + SW^{\uparrow} - SW^{\downarrow} \tag{648}$$

The heat flux into the sea surface is presented, with the surface heat flux calculated in `PSFCM`

$$G^* = G - F^* \tag{649}$$

Note that G^* is downward positive.
The temperature derivative term is

$$\frac{\partial G^*}{\partial T_s} = \frac{\partial G}{\partial T_s} + \frac{\partial H}{\partial T_s} + \frac{\partial R}{\partial T_s} \tag{650}$$

When the sea ice exists, the sublimation flux is considered

$$G_{ice} = G^* - l_s E \tag{651}$$

The temperature derivative term is

$$\frac{\partial G_{ice}}{\partial T_s} = \frac{\partial G^*}{\partial T_s} + l_s \frac{\partial E}{\partial T_s} \tag{652}$$

Finally, we can update the surface temperature with the sea ice concentration with $\Delta T_s = G_{ice}(\frac{\partial G_{ice}}{\partial T_s})^{-1}$

$$T_s = T_s + R_{ice}\Delta T_s \tag{653}$$

Then, the sensible and latent heat flux on the sea ice is updated.

$$E_{ice} = E + \frac{\partial E}{\partial T_s}\Delta T_s \tag{654}$$

$$H_{ice} = H + \frac{\partial H}{\partial T_s}\Delta T_s \tag{655}$$

When the sea ice does not existed, otherwise, the evaporation flux is added to the net flux.

$$G_{free} = F^* + l_c E \tag{656}$$

Finally each flux is updated.
For the sensible heat flux, the temperature change on the sea ice is considered.

$$H = H + R_{ice}H_{ice} \tag{657}$$

Then, the heat used for the temperature change is saved.

$$F = R_{ice}H_{ice} \tag{658}$$

For the upward longwave radiative flux, the temperature change on the sea ice is considered.

$$LW^{\uparrow} = LW^{\uparrow} + 4\frac{\sigma}{T_s}R_{ice}\Delta T_s \tag{659}$$

For the surface heat flux, the sea ice concentration is considered.

$$G = (1 - R_{ice})G_{free} + R_{ice}G_{ice} \tag{660}$$

For the latent heat flux, the sea ice concentration is considered.

$$E = (1 - R_{ice})E + R_{ice}E_{ice} \tag{661}$$

Each term above are saved as freshwater flux.

$$W_{free} = (1 - R_{ice})E \tag{662}$$

$$W_{ice} = R_{ice}E_{ice} \tag{663}$$

7 References (dynamics)

1. Arakawa, A., and C. S. Konor, 1996: Vertical Differencing of the Primitive Equations Based on the Charney–Phillips Grid in Hybrid &sigma– p Vertical Coordinates. Monthly Weather Review, 124, 511–528.

2. Asselin, R., 1972: Frequency Filter for Time Integrations. Monthly Weather Review, 100, 487–490.

3. Bourke, W., 1988: Spectral methods in global climate and prediction models. In "Physically-based modeling and simulation of climate and climatic change (Part 1)". M. E. Schlesinger, Ed., Kluwer Academic Publisher, 169-222.

4. Colella, P., and P. R. Woodward, 1984: The Piecewise Parabolic Method (PPM) for Gas-Dynamical Simulations. Journal Of Computational Physics, 54, 174-201.

5. Haltiner, G J and T Williams, 1980: Numerical Prediction and Dynamic Meteorology. Second Edition, John Wiley and Sons, 477pp.

6. Lin, S.-J., and R. B. Rood, 1996: Multidimensional flux-form semi-Lagrangian transport schemes. Monthly Weather Review, 124, 2046–2070.

7. Mesinger, F., and A. Arakawa, 1976: Numerical methods used in atmospheric models, GARP Publications Series 17, WMO-ICSU Joint Organising Committee, 64pp.

8. Williams, P. D., 2009: A proposed modification to the Robert–Asselin time filter. Monthly Weather Review, 137, 2538–2546.